P1826

ACTA PROTOZOOLOGICA

Instytut Biologii Doświadczalnej PAN Biblioteka

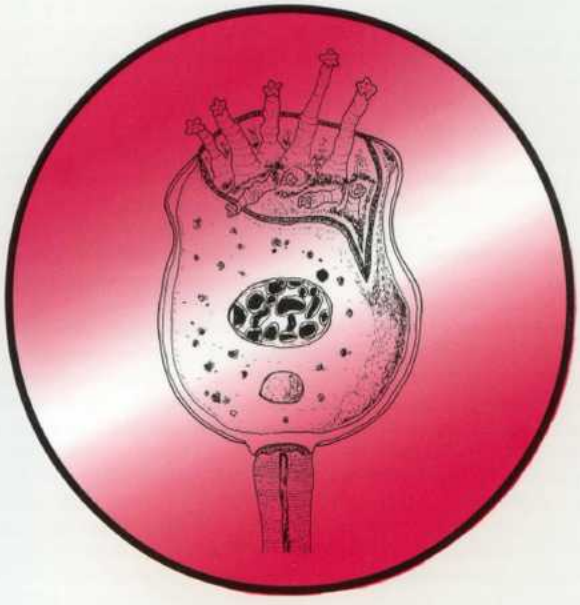

NENCKI INSTITUTE OF EXPERIMENTAL BIOLOGY
WARSAW, POLAND

2003

VOLUME 42 NUMBER 1
ISSN 0065-1583

Polish Academy of Sciences
Nencki Institute of Experimental Biology
and
Polish Society of Cell Biology

ACTA PROTOZOOLOGICA
International Journal on Protistology

Editor in Chief Jerzy SIKORA
Editors Hanna FABCZAK *and* Anna WASIK
Managing Editor Małgorzata WORONOWICZ-RYMASZEWSKA

Editorial Board

Christian F. BARDELE, Tübingen
Linda BASSON, Bloemfontein
Helmut BERGER, Salzburg
Jean COHEN, Gif-Sur-Yvette
John O. CORLISS, Albuquerque
György CSABA, Budapest
Johan F. De JONCKHEERE, Brussels
Isabelle DESPORTES-LIVAGE, Paris
Genoveva F. ESTEBAN, Ambleside
Tom FENCHEL, Helsingør
Wilhelm FOISSNER, Salzburg
Vassil GOLEMANSKY, Sofia
Andrzej GRĘBECKI, Warszawa, *Vice-Chairman*
Lucyna GRĘBECKA, Warszawa
Donat-Peter HÄDER, Erlangen
Janina KACZANOWSKA, Warszawa
Stanisław L. KAZUBSKI, Warszawa
Leszek KUŹNICKI, Warszawa, *Chairman*
J. I. Ronny LARSSON, Lund
John J. LEE, New York
Jiří LOM, České Budějovice
Pierangelo LUPORINI, Camerino
Kálmán MOLNÁR, Budapest
Yutaka NAITOH, Tsukuba
Jytte R. NILSSON, Copenhagen
Eduardo ORIAS, Santa Barbara
Sergei O. SKARLATO, St. Petersburg
Michael SLEIGH, Southampton
Jiří VÁVRA, Praha

ACTA PROTOZOOLOGICA appears quarterly.

The price (including Air Mail postage) of subscription to *Acta Protozoologica* at 2003 is: US $ 200.- by institutions and US $ 120.- by individual subscribers. Limited numbers of back volumes at reduced rate are available. Terms of payment: check, money order or payment to be made to the Nencki Institute of Experimental Biology account: 11101053-401050001074 at BPH PBK S. A. III O/Warszawa, Poland. For matters regarding *Acta Protozoologica*, contact Editor, Nencki Institute of Experimental Biology, ul. Pasteura 3, 02-093 Warszawa, Poland; Fax: (4822) 822 53 42; E-mail: jurek@ameba.nencki.gov.pl For more information see Web page **http://www.nencki.gov.pl/public.htm**

Front cover: Fernandez-Leborans G., Hanamura Y. and Nagasaki K. (2002) A new suctorian, *Flectacineta isopodensis* (Protozoa: Ciliophora) epibiont on marine isopods from Hokkaido (Northern Japan). *Acta Protozool.* **41:** 79-84

©Nencki Institute of Experimental Biology
Polish Academy of Sciences
This publication is supported by the State Committee for Scientific Research

Desktop processing: Justyna Osmulska, Information Technology Unit of the Nencki Institute
Printed at the MARBIS, ul. Poniatowskiego 1
05-070 Sulejówek, Poland

Acta Protozool. (2003) 42: 1 - 6

ACTA
PROTOZOOLOGICA

An Expanded Phylogeny of the Entodiniomorphida (Ciliophora: Litostomatea)

Stephen L. CAMERON[1], Andre-Denis G. WRIGHT[2] and Peter J. O'DONOGHUE[1]

[1]Department of Microbiology and Parasitology, The University of Queensland, Brisbane; [2]CSIRO Livestock Industries, Wembley, Australia

Summary. The Entodiniomorphida are a diverse and morphologically complex group of ciliates which are symbiotic within the digestive tracts of herbivorous mammals. Previous phylogenies of the group have exclusively considered members of one family, the Ophryoscolecidae, which are symbiotic within ruminants. We sought to improve understanding of evolution within the entodiniomorphs by expanding the range of ciliates examined to include the Cycloposthiidae and Macropodiniidae (symbionts of equids and macropodids respectively). The entire SSU-rRNA gene was sequenced for 3 species, *Cycloposthium edentatum*, *Macropodinium ennuensis* and *M. yalanbense*, and aligned against 14 litostome species and 2 postciliodesmatophoran outgroup species. *Cycloposthium* was consistently grouped as the sister-taxon to the Ophryoscolecidae although support for this relationship was low. This suggests that there is more evolutionary distance between the Cycloposthiidae and Ophryoscolecidae than previously inferred from studies of gross morphology, cell ontogeny or ultrastructure. In contrast, *Macropodinium* did not group with any of the entodiniomorphs, instead forming the sister group to the entire Trichostomatia (Entodiniomorphida + Vestibuliferida). This early diverging position for the macropodiniids is concordant with their morphology and ontogeny which failed to group the family with any of the entodiniomorph suborders. The currently accepted classification of the Trichostomatia is thus deficient and in need of review.

Key words: Ciliophora, Cycloposthiidae, Entodiniomorphida, evolution, Macropodiniidae, ribosomal RNA genes, Trichostomatia.

INTRODUCTION

The Entodiniomorphida are endosymbiotic ciliates which inhabit the fermentative digestive organs of most mammalian herbivores (Williams and Coleman 1991). Currently 3 suborders with the Entodiniomorphida are recognised: the Archistomatia, Blepharocorythina and Entodiniomorphina (Lynn and Small 1997). The archistomes include a single family, the Buetschliidae, which are characterised by the possession of simple conical vestibulum, a holotrichous covering of longitudinal somatic kineties and fully developed concretement vacuoles (Wolska 1964). The blepharocorythines are also monofamilial (Blepharocorythiidae) and possess a complicated oral apparatus consisting of a conical vestibulum, a dorsal overture, an external adoral ciliary band and triangular vestibular ciliary band (Wolska 1971). The Entodiniomorphina are the most diverse group characterised by reduced somatic ciliation, forming tufts or bands, semi-rigid pellicle covering extensive non-ciliated areas and an adoral band of cilia around the cytostome. Nine families are currently assigned to this suborder including the best studied entodiniomorphs, the

Address for correspondence: Stephen L. Cameron, Department of Microbiology and Parasitology, The University of Queensland, Brisbane 4072, Australia; Fax: (+617) 3365 4620; E-mail: s.cameron@mailbox.uq.edu.au

families Ophryoscolecidae and Cycloposthiidae, endosymbionts of ruminants and equids respectively (Williams and Coleman 1991).

The most recently described family of entodiniomorphs has been the most difficult to classify: the monogeneric Macropodiniidae, endosymbiotes of macropodid marsupials (kangaroos and allies). The family was originally described by Dehority (1996) who did not assign them to any entodiniomorph suborder as their distinctive morphology differed substantially from all previously described families. Cameron *et al*. (2001a) examined the affinities of the macropodiniids by comparing subcellular features to those of other entodiniomorphs but found that different features suggested affinities with different entodiniomorph suborders and no consensus could be found. Our subsequent study of stomatogenesis within *Macropodinium* (Cameron and O'Donoghue 2001) similarly suggested different affinities depending on which feature's ontogenic sequence was considered. It is thus most probable that structural and developmental homologies between the macropodiniids and other entodiniomorphs have been obscured by the long isolation of the former within Australian marsupials (all other entodiniomorphs inhabit eutherian mammals). To determine the relationship of the macropodiniids to the entodiniomorphs it is therefore necessary to study their genetic sequence evolution.

Previous molecular phylogenetic studies on the entodiniomorphs have been confined to members of a single family, the Ophryoscolecidae. Embley *et al.* (1995) was the first study to examine the small subunit (SSU) ribosomal RNA gene of ophryoscolecids (*Entodinium caudatum* misidentified as *Polyplastron multivesiculatum*) which supported the placement of the entodiniomorphs as the sister-group of the vestibuliferans within the Class Litostomatea. Subsequent studies by Wright and Lynn (1997a) and Wright *et al.* (1997) expanded the phylogeny of the ophryoscolecids by the addition of 5 extra genera (*Diplodinium*, *Eudiplodinium*, *Ophryoscolex*, *Epidinium* and *Polyplastron*) and confirmed the hypotheses of Lubinsky (1957a, b) regarding structural evolution within the Ophryoscolecidae (i.e. basal position of *Entodinium* and reversal of orientation of the adoral ciliation in other genera). Despite excellent coverage of the ophryoscolecids, phylogenetic studies of the remaining entodinimorph families are totally lacking. This study therefore sought to examine the phylogenetic relationships of 2 additional families, the Macropodiniidae and Cycloposthiidae, to the Ophyroscolecidae.

MATERIALS AND METHODS

Source of samples

Samples of stomach content were collected from macropodid hosts shot in the field or euthenased in zoos and preserved in 9 volumes of 100% ethanol. Individual ciliate species were harvested from mixed species communities under a dissecting microscope by micromanipulation using fine drawn soda glass pipettes. Monospecific pellets of approximately 10 µl volume were obtained for *Cycloposthium edentatum*, *Macropodinium yalanbense* and *Macropodinium ennuensis* from the hosts, *Macropus dorsalis*, *Macropus robustus* (captive animal) and *Macropus robustus* (wild animal) respectively. *Cycloposthium edentatum* is ordinarily a symbiote of horses however the samples used here were recovered from the black-striped wallaby, *M. dorsalis* as described previously (Cameron *et al*. 2000).

DNA extraction and nucleotide sequencing

DNA was extracted using the cetyltrimethylammonium bromide (CTAB) extraction technique of Wright *et al*. (1997). The pellet was air-dried, resuspended in 30 µl of Tris-EDTA (TE) buffer and stored frozen at -20°C. The SSU-rRNA gene was amplified by polymerase chain reaction (PCR) using the primers JB1 and R18A (Cameron *et al.* 2001b). Amplification was performed on a Corbett Research thermal sequencer using the following conditions: denaturation at 95°C (1 min); primer annealing at 50°C (30 s); and chain extension at 72°C (1 min) for 31 cycles. On the final cycle, chain extension was extended for 7 min. The size of PCR bands was estimated by comparison to a 100 bp standard ladder and DNA concentration by comparison to a Mass standard ladder. PCR products were purified to remove unincorporated nucleotides using the QIAquick PCR purification kit (Qiagen, Inc). The 18S region was sequenced using dye terminator automated sequencing (ABI Prism and Big Dye automated sequencing kits). Sequencing of the 18S gene was performed using 6 nested sequencing primers (18B, 18C, SB2, R18B, R18C, R18D, Cameron *et al*. 2001b). Sequence results were examined and ambiguous bases resolved in the Sequence Navigator and Sequencher 3.0 programs. Sequence fragments were reconstructed into whole gene sequences using the Sequencher 3.0 program.

Phylogenetic analysis

A phylogeny of the Litostomatea was reconstructed by alignment of the 3 novel SSU-rRNA gene sequences of entodiniomorph ciliates against 14 other trichostome ciliates and 2 postciliodesmatophorean outgroup taxa (*Eufolliculina uhligi* and *Loxodes striatus*). As the monophyly of the Litostomatea is virtually beyond question (Wright *et al.* 1997; Wright and Lynn 1997a, b; Cameron *et al.* 2001b) sequences from other ciliate orders were not included. Sequences were aligned by eye using the Se-Al program ver 1.0a1 (Rambaut 1996) and modified after reference to secondary structure (Wright 1998). The accession numbers of the additional taxa are: *Dasytricha ruminantium* U57769 (Wright and Lynn 1997b); *Didinium nasutum* U57771 (Wright and Lynn 1997b); *Diplodinium dentatum* U57764 (Wright and Lynn 1997a); *Enchelydon* sp. U80313 (Wright unpub. data); *Entodinium caudatum* U57765 (Wright *et al*. 1997); *Epidinium caudatum* U57763 (Wright *et al*. 1997); *Eudiplodinium maggii*

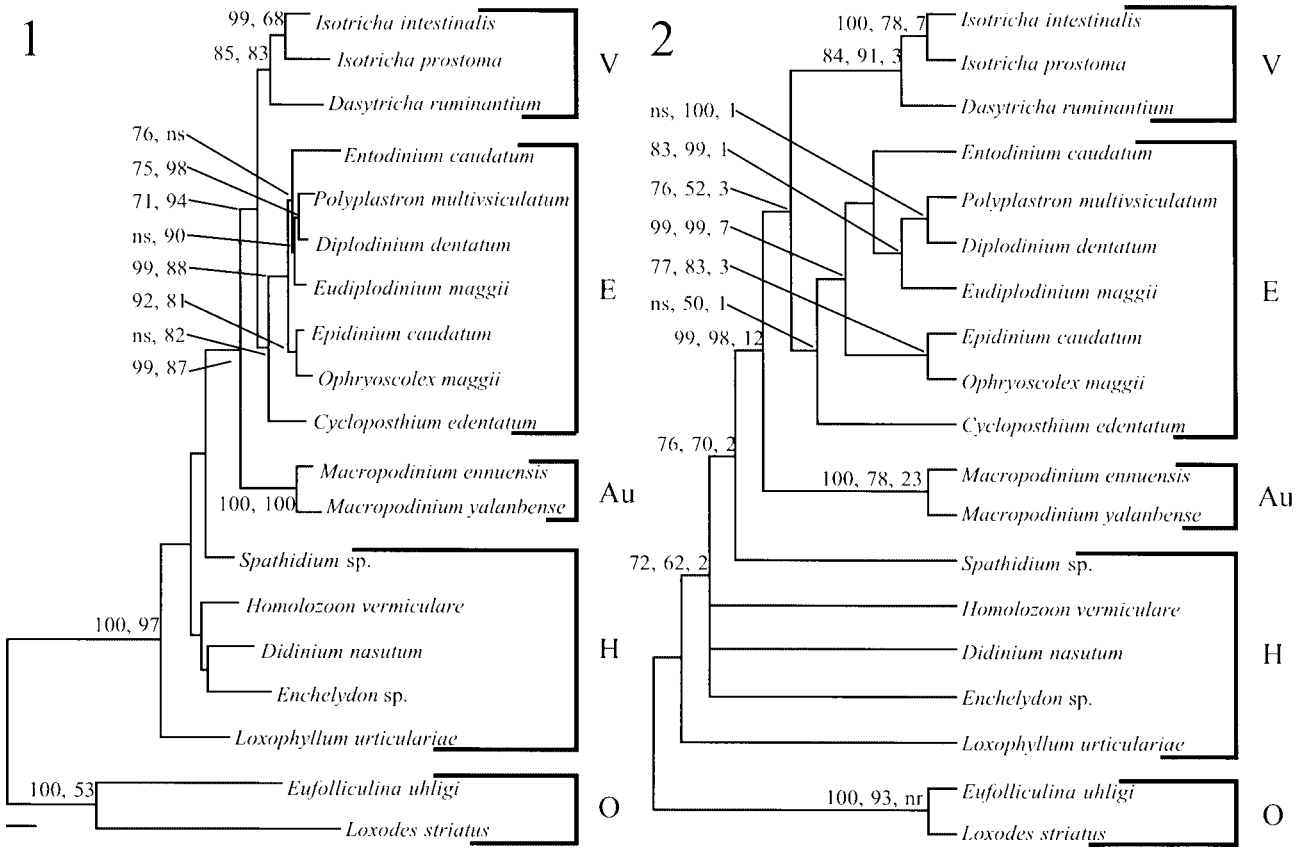

Figs 1-2. Phylogeny of the trichostome ciliates. **1** - maximum likelihood phylogram. Numbers on nodes indicate support: bootstrap and puzzle. **2** - maximum parsimony dendrogram. Numbers on nodes indicate support: bootstrap, puzzle and decay score. Higher taxonomic groups are bracketed: Au - Australian taxa, E - Entodiniomorphida, H - Haptoria, O - Outgroup, V - Vestibulifera. ns - not supported, nr - not reported.

U57766 (Wright and Lynn 1997a); *Eufolliculina uhligi* U47620 (Hammerschmidt *et al*. 1996); *Homolozoon vermiculare* L26447 (Leipe *et al*. 1994); *Isotricha intestinalis* U57770 (Wright and Lynn 1997b); *Isotricha prostoma* AF029762 (Wright and Lynn 1997b); *Loxodes striatus* U24248 (Hammerschmidt *et al*. 1996); *Loxophyllum utricullariae* L26448 (Leipe *et al*. 1994); *Ophryoscolex purkinjei* (Wright and Lynn 1997a); *Polyplastron multivesiculatum* U57767 (Wright *et al*. 1997) and *Spathidium* sp. Z22931 (Hirt *et al*. 1995). Regions with hypervariable sequences which could not be unambiguously aligned to the outgroup taxa were excluded. Eight regions totaling 369 bases were thus omitted; these regions correspond to 9a'→E10-1; loop within E10-1; loop within 11; loop within 17; 23b→23-2a; 29a→29a'; 43b→43b'; and 49g→49g' stem coordinates respectively. These omitted regions have previously been shown to produce misleading phylogenetic results in ciliates due to their arbitrary alignment (Cameron *et al*. 2001b).

Tree construction was performed using PAUP 4.0b8 (Swofford 1998). Two types of tree building algorithms were used: maximum likelihood (ML) and maximum parsimony (MP). Initial trees were constructed using heuristic search parameters. Three confidence indices were calculated: bootstraps (ML and MP); quartet puzzles (ML and MP); and Bremer support indices (MP only). Bootstrapping and quartet puzzling were performed using 1000 replicates in PAUP 4.0b8 (Swofford 1998). Bremer support indices were calculated using TreeRot ver. 2 (Sorenson 1999).

RESULTS

The entire SSU-rRNA gene was sequenced for the three entodiniomorph ciliates *Cycloposthium edentatum*, *Macropodinium ennuensis* and *M. yalanbense*. The SSU-rRNA gene was 1641 bp long in *C. edentatum*, 1639 bp in *M. ennuensisi* and 1639 bp in *M. yalanbense*. These sequences are lodged with Genbank under the accession numbers AF042485 (*C. edentatum*), AF298820 (*M. ennuensis*) and AF042486 (*M. yalanbense*).

Both parsimony and likelihood analyses supported the monophyly of the endosymbiotic litostomes, the

Trichostomatia (Figs 1, 2). In contrast their free-living sister group the Haptoria were paraphyletic in all analyses as *Spathidium* sp. consistently grouped with the trichostomes. Support for *Spathidium* + Trichostomatia was however not strong (unsupported in ML, low support MP). Within the Trichostomatia, support for the monophyly of the Vestibuiferida was consistent and strong. There was limited support for the monophyly of Entodiniomorphida as traditionally conceived. As in all previous, studies the Ophryoscolecidae are monophyletic with high levels of support for this node. Phylogenetic relationships within the Ophryoscolecidae are similar to those reported previously (Wright *et al*. 1997; Wright and Lynn 1997a, b) i.e. division of the family into 3 major clades: *Entodinium* (representing the subfamily Entodiniinae); *Polyplastron* + *Diplodinium* + *Eudiplodinium* (representing the Diplodiniinae); and *Epidinium* + *Ophryoscolex* (representing the remaining subfamilies). It differed with respect to the branching order of these clades; *Entodinium* has been traditionally considered the most basal member of the family (Crawley 1923, Lubinsky 1957a, Wright *et al*. 1997) however here the branching order of the ophryoscolecid clades is unresolved.

While *Cycloposthium* was consistently placed as the sister-taxon to the Ophryoscolecidae in the heuristic searches, there was little support for this relationship, unsupported by all analyses except MP quartet puzzling and then just 50%. The macropodiniids did not fall within the Entodiniomorphida in any of the analyses, rather forming the sister-group to the remainder of the Trichostomatia (Vestibuliferida *sensu* Lynn and Small 1997 + Entodiniomorphida *sensu* Lynn and Small 1997). *Macropodinium* is thus not an entodiniomorph.

DISCUSSION

The phylogeny of the Entodiniomorphida was examined by addition of sequences from the Cycloposthiidae (*C. edentatum*) and Macropodiniidae (*M. ennuensis* and *M. yalanbense*) to sequences of Ophryoscolecidae previously determined (Wright *et al*. 1997; Wright and Lynn 1997a, b). Neither group was found to be particularly closely related to the ophryoscolecids; the cycloposthids were shown to be a weakly supported sister group of the ophryoscolecids while the macropodiniids were much more distantly related forming the earliest diverging branch of the Trichostomatia.

The classification of *Macropodinium* has proven to be troublesome from its first description (Dehority 1996) to the present time. Dehority (1996) assigned the macropodiniids to the Entodiniomorphida primarily on the basis of its reduced somatic ciliation, even though more classical entodiniomorph characters such as retractable vestibula and somatic ciliary tufts were absent (Corliss 1979). Careful examination of the gross morphology of the group using silver staining and scanning electron microscopy (Cameron *et al.* 2001a) failed to resolve the affinities of the group; the vestibular characters were suggestive of blepharocorythiid affinities, the somatic kineties of vestibuliferan affinities and the pellicular folds of cycloposthiid or rhinozetid affinities. Subsequent studies of stomatogenesis in *Macropodinium yalanbense* again failed to unambiguously resolve the affinities of the group (Cameron and O'Donoghue 2001); the replication of the vestibular kineties was similar to that seen in the higher entodiniomorphs, the adoral kineties to that of haptorians and the somatic kineties to that of vestibuliferans. Indeed, rather than suggest which trichostome groups may be closely related to the macropodiniids, these studies highlighted the unique features of the group. The dorsoventral groove, pellicular plates and the ontogeny of the oral kineties *via* two separate processes are features without parallel amongst the ciliates (Cameron *et al*. 2001a, Cameron and O'Donoghue 2001). The current study places these findings into context, the macropodiniids form a distinct monophyletic assemblage which is not closely related to any other group within the Litostomatea. Those features which the macropodiniids share with other groups are therefore either probably convergences (e.g. most oral or pellicular features) or retained pleisomorphies (e.g. somatic ciliary characters).

In contrast, the Cycloposthiidae have been consistently grouped with the Ophryoscolecidae as members of the Entodiniomorphina (so-called higher entodiniomorphs) (Corliss 1979, Grain 1994). The two families share a large number of ultrastructural features in common (Grain 1966; Furness and Butler 1983, 1985a, b). The oral kineties are very similar, both are composed of polybrachykineties which form an adoral loop surrounding the anterior cytostome and a descending vestibular loop (Fernandez-Galiano 1959, Fernandez-Galiano *et al.* 1985). The somatic kineties differ substantially because they are primitively absent in the ophryoscolecids and secondarily derived in the higher genera from the oral kineties whereas they have several forms in the

cycloposthiids (Lubinsky 1957a, b; Corliss 1979). Cytoplasmic features shared include nuclear location, endoplasm/ectoplasm delimination and contractile vacuole structure and location (Ito and Imai 1998, 2000; Cameron *et al*. 2000). Given the number of similarities in cell structure and ultrastructure between the two families, our finding that *Cycloposthium* was only distantly related to the Ophryoscolecidae was surprising. While the heuristic analyses consistently placed *Cycloposthium* as the sister-group to the Ophyroscolecidae, only 1 of the 5 support indices (quartet puzzling of the ML trees) showed significant support for this relationship. It is unknown at this time whether this is due to restricted taxon sampling, lack of phylogenetic signal in the dataset or representative of the real phylogeny of the trichostomes. *Cycloposthium* is traditionally regarded as one of the more derived cycloposthiid genera (Corliss 1979) and the inclusion of more basal representatives of the family may break up the branch length between the two families and strengthen the analysis. Lack of phylogenetic signal from the SSU-rRNA gene has been found previously within the ciliates whereby traditional groups supported by considerable morphological, ultrastructural and developmental data were not recovered e.g. Oligohymenophora (Strüder-Kypke *et al*. 2000, Cameron *et al*. 2001b). Finally, it is possible that the similarities reported above are the result of convergence and are not indicative of phylogenetic relationship. While such convergences have been reported frequently amongst the ciliates (Embley *et al*. 1995, Hammerschmidt *et al*. 1996), it appears unlikely that this is the case in the present study as the relationship between *Cycloposthium* and the ophryoscolecids is simply not significantly supported rather than being contraindicated by any well supported relationships with other taxa.

The present study has significantly increased the taxonomic coverage of the trichostomes for the purposes of phylogenetic analysis. Our understanding of the evolution of the group is, however, still significantly hampered by the large number of taxa for which phylogenetically useful data, gene sequences or complete ultrastructural data, is available. Of the 14 families of trichostomes currently recognised (Corliss 1979, van Hoven *et al.* 1987, Dehority 1996), sequence data is available for only 4 families. More tellingly, some key families have yet to be examined at all; Wolska (1965) has proposed that the Buetschlidae are the most basal representative of the Entodiniomorphida and further that the Blepharocorythidae form a link between the basal buetschlids and the remaining families (Wolska 1971). No representatives of either family have been sequenced. Examination of such key taxa will be necessary before the major divisions within the Trichostomatia can be recovered. Recovery of these divisions is necessary before a robust classification of the trichostomes can be proposed to adequately classify taxa such as *Macropodinium* which do not fit into any of the presently proposed orders.

Acknowledgements. The authors would like to thank Dr. Vere Nicholson and Mr. Jason Round for assistance with field collections and Drs. Glenn Anderson, Nick Campbell and Jess Morgan for their technical assistance and advice. This research was supported by Australian Research Council small grants scheme and the Australian Biological Resources Study post-graduate scholarship initiative.

REFERENCES

Cameron S. L., O'Donoghue P. J. (2001) Stomatogenesis in the ciliate genus *Macropodinium*, Dehority 1996 (Litostomatea: Macropodiniidae). *Europ. J. Protistol.* **37:** 199-206

Cameron S. L., O'Donoghue P. J., Adlard R. D. (2000) The first record of *Cycloposthium edentatum* Strelkow, 1928 from the black-striped wallaby, *Macropus dorsalis*. *Parasitol. Res.* **86:** 158-162

Cameron S. L., O'Donoghue P. J., Adlard R. D. (2001a) Four new species of *Macropodinium* (Ciliophora: Litostomatea) from wallabies and pademelons. *J. Eukaryot. Microbiol.* **48:** 542-555

Cameron S. L., Adlard R. D., O'Donoghue P. J. (2001b) Molecular evidence for an independent radiation of holotrich trichostome ciliates in Australian marsupials. *Mol. Phylogenet. Evol.* **20:** 302-310

Corliss J. O. (1979) The Ciliated Protozoa, Characterisation, Classification and Guide to the Literature. 2 ed. Pergamon Press, Oxford

Crawley H. (1923) Evolution in the ciliate family Ophryoscolecidae. *Proc. Acad. Nat. Sci. Philadelphia* **75:** 393-412

Dehority B. A. (1996) A new family of entodiniomorph protozoa from the marsupial forestomach, with descriptions of a new genus and five new species. *J. Eukaryot. Microbiol.* **43:** 285-95

Embley T. M., Finlay B. J., Dyal P. L., Hirt R. P., Wilkinson M., Williams A. G. (1995) Multiple origins of anaerobic ciliates with hydrogenosomes within the radiation of aerobic ciliates. *Proc. Royal Soc. London B series* **262:** 87-93

Fernández-Galiano D. (1959) La infraciliación en *Cycloposthium edentatum* Strelkow. *Bol. R. Soc. Esp. Hist. Nat. Ser. Biol.* **57:** 139-150

Fernández-Galiano T., Serrano S., Fernández-Galiano D. (1985) General morphology and stomatogenesis of two species of the genus *Entodinium* (Ciliophora, Entodiniomorphida). *Acta Protozool.* **24:** 181-186

Furness D. N., Butler R. D. (1983) The cytology of sheep rumen ciliates I. Ultrastructure of *Epidinium caudatum* Crawley. *J. Protozool.* **30:** 676-687

Furness D. N., Bulter R. D. (1985a) The cytology of sheep rumen ciliates II. Ultrastructure of the *Eudiplodinium maggii*. *J. Protozool.* **32:** 205-214

Furness D. N., Butler R. D. (1985b) The cytology of sheep rumen ciliates III. Ultrastructure of the Genus *Entodinium* (Stein). *J. Protozool.* **32:** 699-707

Grain J. (1966) Etude cytologique de quelques ciliés holotriches endocommensaux des ruminants et des équidés. *Protistologica* **2(1):** 59-141; **2(2):** 5-51

Grain J. (1994) Class Vestibuliferea de Puytorac *et al*., 1974. In: Traité de Zoologie: Anatomie, Systématique, Biologie. Tome II. Fascicule II. Infusories Ciliés. (Eds. P. Grassé, P. de Puytorac), Masson, Paris, 311-379

Hammerschmidt B., Schlegel M., Lynn D., Leipe D., Sogin M., Raikov I. (1996) Insights into the evolution of nuclear dualism in the ciliates revealed by phylogenetic analysis of rRNA sequences. *J. Eukaryot. Microbiol.* **43:** 225-230

Hirt R. P., Dyal P. L., Wilkinson M., Finlay B. J., Roberts D. M., Embley T. M. (1995) Phylogenetic relationships among karyorelictids and heterotrichs inferred from small subunit rRNA sequences: resolution at the base of the ciliate tree. *Mol. Phylogenet. Evol.* **4:** 77-87

Ito A., Imai S. (1998) Infraciliary bands in the rumen ophryoscolecid ciliate *Ostracodinium gracile* (Dogiel, 1925) observed by light microscopy. *J. Eukaryot. Microbiol.* **45:** 628-636

Ito A., Imai S. (2000) Ciliates from the caecum of capybara (*Hydrochoerus hydrochaeris*) in Bolivia II. The family Cycloposthiidae. *Europ. J. Protistol.* **36:** 169-200

Leipe D. D., Bernhard D., Schlegel M., Sogin M. L. (1994) Evolution of 16S-like ribosomal RNA genes in the ciliophoran taxa Litostomatea and Phyllopharyngea. *Europ. J. Protistol.* **30:** 354-361

Lubinsky G. (1957a) Studies on the evolution of the Ophryoscolecidae (Ciliata: Oiligotricha). II. On the origins of the higher Ophryoscoledidae. *Can. J. Zool.* **35:** 135-140

Lubinsky G. (1957b) Studies on the evolution of the Ophryoscolecidae (Ciliata: Oligotricha). III. Phylogeny of the Ophryoscolecidae based on their comparative morphology. *Can. J. Zool.* **35:** 141-159

Lynn D. H., Small E. (1997) A revised classification of the Phylum Ciliophora Dolfein, 1901. *Rev. Soc. Mex. Hist. Nat.* **47:** 65-78

Rambaut A. (1996) Se-Al (Sequence Alignment Editor). Ver. 1.0a1. Private release software, Oxford

Sorenson M. D. (1999) TreeRot. Ver. 2. Boston University, Boston, MA

Strüder-Kypke M. C., Wright A-D. G., Fokin S. I., Lynn D. H. (2000) Phylogenetic relationships of the genus *Paramecium* inferred from small subunit rRNA gene sequences. *Mol. Phylogenet. Evol.* **14:** 122-130

Swofford D. L. (1998) PAUP* Phylogenetic Analysis using Parsimony (*and Other Methods). Ver. 4.0b3. Sinauer Associates, Sunderland, MA

Van Hoven W., Gilchrist F., Hamilton-Attwell V. (1987) Intestinal ciliated protozoa of African rhinoceros: Two new genera and five new species from the white rhino (*Ceratotherium simum* Burchell, 1817). *J. Protozool.* **34:** 338-342

Williams A., Coleman G. (1991) The Rumen Protozoa. Springer-Verlag, New York

Wolska M. (1964) Infraciliature of *Didesmis ovalis* Fior. and *Blepharozoum trizonum* (Hsiung) - Fam. *Buetschliidae* (Ciliata, Rhabdophorina). *Acta Protozool.* **6:** 153-158

Wolska M. (1965) Remarks on the adoral ciliature in the Order Entodiniomorpha. *Acta Protozool.* **3:** 321-324

Wolska M. (1971) Studies on the family Blepharocorythidae Hsiung. VI. Phylogenesis of the family and the description of the new genus *Circodinium* gen. n. with the species *C. minium* (Gassovsky, 1918). *Acta Protozool.* **15:** 171-194

Wright A-D. G. (1998) Molecular phylogeny of the endosymbiotic ciliates (Litostomatea: Trichostomatia) of vertebrate animals inferred from 18S rRNA gene sequences. PhD thesis. The University of Guelph

Wright A-D. G., Lynn D. H. (1997a) Phylogenetic analysis of the rumen ciliate family Ophryoscolecidae based on 18S ribosomal RNA sequences with new sequences from *Diplodinium*, *Eudiplodinium* and *Ophryoscolex*. *Can. J. Zool.* **75:** 963-970

Wright A-D. G., Lynn D. H. (1997b) Monophyly of the trichostome ciliates (phylum Ciliophora: class Litostomatea) tested using new 18S rRNA sequences from the vestibuliferids, *Isotricha intestinalis* and *Dasytricha ruminantium*, and the haptorian, *Didinium nasutum*. *Europ. J. Protistol.* **33:** 305-315

Wright A-D. G., Dehority B., Lynn D. H. (1997) Phylogeny of the rumen ciliates *Entodinium*, *Epidinium* and *Polyplastron* (Liotstomatea: Entodiniomorphida) inferred from small subunit ribosomal RNA sequences. *J. Eukaryot. Microbiol.* **44:** 61-67

Received on 29th April, 2002; accepted on 13th September, 2002

Acta Protozool. (2003) 42: 7 - 10

ACTA
PROTOZOOLOGICA

Organelle Movement in *Actinophrys sol* and Its Inhibition by Cytochalasin B

Toshinobu SUZAKI[1], Mikihiko ARIKAWA[1], Akira SAITO[1], Gen OMURA[1], S. M. Mostafa Kamal KHAN[1], Miako SAKAGUCHI[2,3] and Klaus HAUSMANN[3]

[1]Department of Biology, Faculty of Science; [2]Research Institute for Higher Education, Kobe University, Kobe, Japan; [3]Institute of Biology/Zoology, Free University of Berlin, Berlin, Germany

Summary. Movement of extrusomes in the heliozoon *Actinophrys sol* was characterized at surfaces of the cell body and giant food vacuoles where microtubules are absent. Extrusomes moved in a saltatory manner at an average velocity of 0.5 μms^{-1}. The highest velocity observed was 2.1 μms^{-1}. Cytochalasin B (50 µg/ml) strongly inhibited extrusome movement at the surfaces of newly-formed food vacuoles, suggesting that the actomyosin system is involved in the organelle transport in *Actinophrys*.

Key words: actinophryid, actomyosin, extrusome, heliozoa, organelle transport.

INTRODUCTION

Transport of intracellular organelles is a ubiquitous feature of eukaryotic cells (e.g. Rebhun 1972, Hyams and Stebbings 1979, Schliwa 1984). In many instances, microtubules have been postulated as important elements along which bidirectional particle transport takes place (Koonce and Schliwa 1985, Hayden and Allen 1984, and references therein). In addition to the microtubule-associated movement, there are other examples in which organelles are transported in the absence of microtubules (reviewed in Hyams and Stebbings 1979), which include movement of organelles (extrusomes and mitochondria) in the heliozoon cell surface.

Address for correspondence: Toshinobu Suzaki, Department of Biology, Faculty of Science, Kobe University, 1-1 Rokkodai-cho, Nada-ku, Kobe 657-8501, Japan; Fax: +81-78-803-5722; E-mail: Suzaki@kobe-u.ac.jp

Edds (1975a) showed that organelle movement of the heliozoon *Echinosphaerium* still occurred in artificial axopodia where a glass microneedle substituted for the microtubular axoneme, and colchicine did not inhibit the motion in either the normal or the artificial axopodia (Tilney 1968, Edds 1975a). Organelle movement is also known to take place in the cortex of the heliozoon cell body where no microtubules are present (Fitzharris *et al.* 1972, Suzaki and Shigenaka 1982). The actomyosin system has therefore been suggested as a possible force-generating mechanism for this movement, although there is no direct evidence available so far.

Actinophrys cells form giant food vacuoles when they are fed with large ciliates such as *Colpidium* and *Paramecium* (Patterson and Hausmann 1981, Hausmann and Patterson 1982). Extrusomes move in the cytoplasm at the surfaces of such food vacuoles. Motions of individual extrusome particles can be observed easily on

food vacuoles, because this region of the cell is most distant from the cell body cytoplasm that usually hinders precise observation of extrusomes due to optical disturbances. In the present study, we characterized particle movement at the food vacuole surface and demonstrated that cytochalasin B inhibited particle movement there, which further strengthens the evidence for the involvement of the actomyosin system in organelle transport in heliozoa.

MATERIALS AND METHODS

The source of *Actinophrys sol* and the culture method have been described by Patterson (1979). Prior to every experiment, cells were kept in a conditioning medium (0.01% Knop solution containing 5 mM Hepes-KOH buffer at pH 7.0) for more than 1 h to make them adapted to the solution. Formation of food vacuoles was induced by adding *Colpidium* spp. (ciliate) as prey. For light microscopy, a Zeiss inverted microscope (IM 35) was used with a 63x plan apochromatic oil immersion objective and Nomarski differential interference contrast optics. Movement of extrusomes was recorded at real time speed with a video recorder (JVC BR6400 TR), and analyzed afterwards frame by frame. Cytochalasin B (Sigma) was dissolved at 5 mg/ml in dimethylsulfoxide (DMSO) before it was diluted with the above medium.

RESULTS AND DISCUSSION

Actinophrys sol formed giant food vacuoles when it was fed with large ciliates. The size of such food vacuoles sometimes exceeded the initial size of the cell body (Fig. 1). The food vacuole was surrounded by a thin layer of cytoplasm, in which numerous particles moved in a saltatory manner (Fig. 2). These particles are extrusomes (Patterson 1979), which can be seen as refractile spheres of about 0.5 µm in diameter under the light microscope. Since these organelles are known to discharge their contents when the cells capture food organisms, they are implicated in the process of prey adhesion and membrane supply for making food vacuoles (Suzaki *et al*. 1980; Patterson and Hausmann 1981; Hausmann and Patterson 1982; Sakaguchi *et al*. 1998, 2001).

Movement of these cytoplasmic particles was examined in detail at the food vacuole surface. Particles moved at variable velocities, with a range from ~ 0 to 2.1 μms^{-1} (Fig. 3). The average velocity was 0.55 μms^{-1}, which was almost the same as the one recorded at the surface of the cell body (0.52 μms^{-1}, Table 1). Particles moved independently from each other

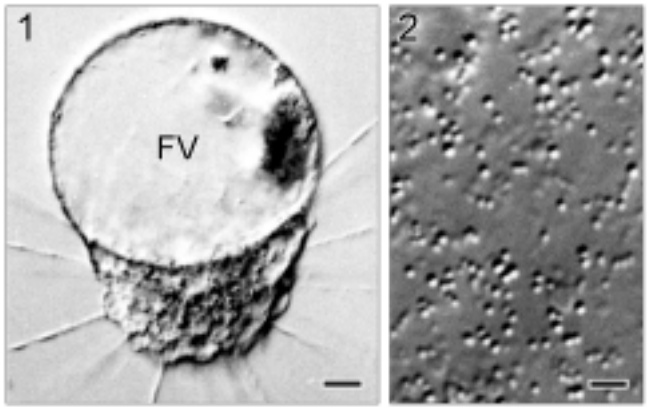

Figs 1, 2. Light micrographs of *Actinophrys sol*; **1** - low magnification picture showing a giant food vacuole (FV); **2** - highly magnified picture showing many extrusomes at the surface of a food vacuole. Scale bars: 10 µm (1); 2 µm (2).

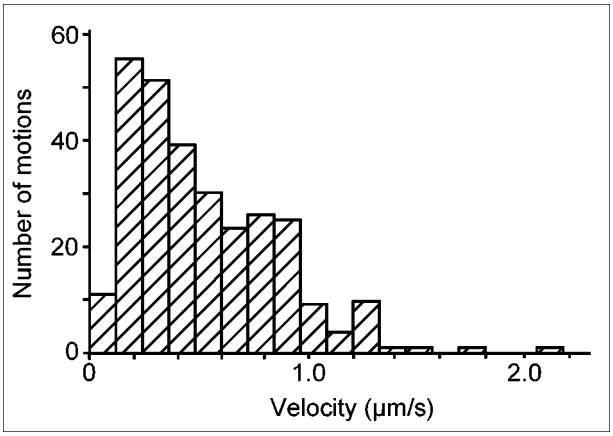

Fig. 3. Histogram of velocities (distance moved in 1 s) of particles at the surface of a newly-formed food vacuole. 10 motions were examined for each of 30 particles (total 300 motions examined).

with no evident track of movement, and frequently showed changes in direction and velocity (Figs 4, 5). The degree of regularity of the particle movement was examined by calculating Jarosch's regularity quotient (Qr, the ratio of mean square displacement of double intervals to the mean square displacement of single intervals) according to Kamiya (1959). Qr for particle movement of the food vacuole surface was 2.13 (30 particles were traced in both 5 and 10 s intervals), which suggests that the motion can be regarded as an irregular one with some energy-dependent driving process for it.

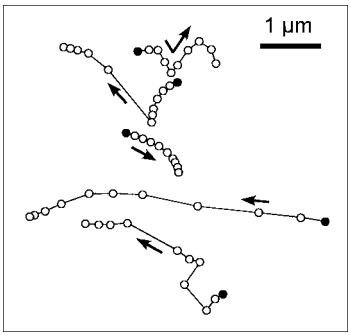

Fig. 4. Tracing of particles moving at the surface of a food vacuole. Each open circle represents the position of the particle at 1 s intervals (started from the position shown by the closed circles). Arrows indicate directions of movement.

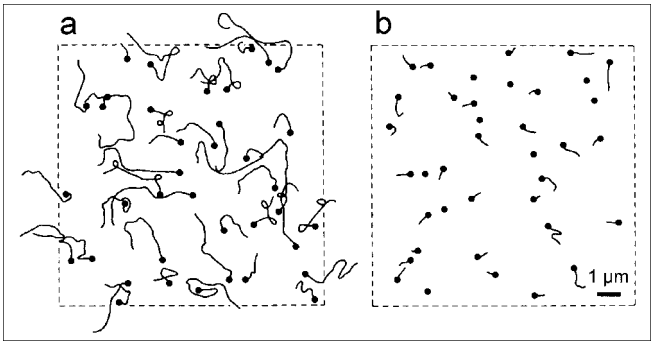

Figs 5a, b. Effect of cytochalasin B on particle movement at the surface of newly-formed food vacuoles (about 30 min after formation); **a** - control movement in 1% DMSO; **b** - 30 min after treatment with 50 µg/ml cytochalasin B in 1% DMSO. Particles were traced for 10 s from the position shown by the closed circles.

Table 1. Effect of cytochalasin B on particle movement at the surfaces of cell body and newly-formed food vacuole*.

		Average velocity ($\mu ms^{-1} \pm SD$)	Sample number**
Control***	Cell body	0.52 ± 0.34	30
	Food vacuole	0.55 ± 0.34	30
Cytochalasin B treated (50 µg/ml, 30 min)	Cell body	0.37 ± 0.15	38
	Food vacuole	0.05 ± 0.04****	38

* Examined about 30 min after formation; ** 9-10 particles were traced for each of 4 experiments; *** containing 1% DMSO; **** significantly different from control food vacuole ($p<0.001$).

Movement of particles at the surface of newly-formed food vacuoles (within 3 hours after formation) was inhibited by cytochalasin B at 50 µg/ml (Fig. 5 and Table 1). Particle movement resumed when the cells were washed in a control medium that did not contain cytochalasin B (the control medium contained 1% DMSO, which did not show any effect either on cell shape or on particle motility). Average velocity of the particles slightly decreased at the surface of the cell body, but it was not significant as compared with the inhibition observed at the food vacuole surface (Table 1).

The plasma membrane of the food vacuole is considered to be derived from the investing membrane of the extrusomes, which becomes available after the discharge of their contents to the prey organisms (Hausmann and Patterson 1982). This newly-formed membrane has different characteristics from other cell body surfaces, i.e., it is very adhesive to the prey organisms (Suzaki *et al*. 1980, Hausmann and Patterson 1982), and is easily fused with food vacuole membranes of neighboring heliozoon cells to form a large common food vacuole (Bovee and Cordell 1971, Patterson and Hausmann 1981). These properties of the food vacuole membrane may suggest that this new membrane surface possesses a reduced or a different type of surface coat. A large increase in the frequency of cell fusion after experimental removal of the surface coat has been shown in *Echinosphaerium* (Vollet and Roth 1974). Cytochalasin B inhibited particle movement most effectively at the food vacuole surface but had little or no effect in other parts of the cell (Table 1). This difference might be due to different permeability characteristics of the food vacuole membrane.

The inhibitory effect of cytochalasin B suggests that the actomyosin system might be involved in force generation for particle movement, although its exact mecha-

nism is still an open question. Microfilaments have been observed in the cytoplasm of *Echinosphaerium* (Tilney *et al.* 1966, Edds 1975b, Suzaki *et al.* 1980) and *Actinophrys* (Hausmann and Patterson 1982). They are, however, located either deep in the cytoplasm (Tilney *et al.* 1966) or in the food vacuole-forming pseudopodia (Suzaki *et al.* 1980, Hausmann and Patterson 1982), without any direct interaction with moving extrusomes. Movement of extrusomes is known to take place always along the inner surface of the plasma membrane and was inhibited when the extrusomes were removed from contact with the plasma membrane by treatment with chloral hydrate (Suzaki and Shigenaka 1982). Therefore, it seems to be plausible that the driving force for the movement of extrusomes may be generated through interaction with meshwork of single actin filaments located in the close vicinity of the inner surface of the plasma membrane, not with large bundles of microfilaments located deeper in the cytoplasm. The next and crucial step to understand the molecular mechanism of movement of the extrusomes is to demonstrate the presence of F-actin between the cell membrane and the food vacuole.

Acknowledgments. We thank Dr. R. W. Ridge for his critical reading of the manuscript. This work was supported by an Alexander von Humboldt Research Fellowship awarded to T. S.

REFERENCES

Bovee E. C., Cordell D. L. (1971) Feeding on gastrotrichs by the heliozoan *Actinophrys sol*. Trams. *Amer. Micros. Soc.* **90:** 365-369

Edds K. T. (1975a) Motility in *Echinosphaerium nucleofilum*. I. An analysis of particle motions in the axopodia and a direct test of the involvement of the axoneme. *J. Cell Biol.* **66:** 145-155

Edds K. T. (1975b) Motility in *Echinosphaerium nucleofilum*. II. Cytoplasmic contractility and its molecular basis. *J. Cell Biol.* **66:** 156-164

Fitzharris T. P., Bloodgood R. A., Mcintosh J. R. (1972) Particle movement in the axopodia of *Echinosphaerium*: Evidence concerning the role of the axoneme. *J. Mechanochem. Cell Motil.* **1:** 117-124

Hausmann K., Patterson D. J. (1982) Pseudopod formation and membrane production during prey capture by a heliozoon (Feeding by *Actinophrys sol*, II). *Cell Motil.* **2:** 9-24

Hayden J. H., Allen R. D. (1984) Detection of single microtubules in living cells: Particle transport can occur in both directions along the same microtubule. *J. Cell Biol.* **99:** 1785-1793

Hyams J. S., Stebbings H. (1979) Microtubule associated cytoplasmic transport. In: Microtubules, (Eds. K. Roberts, J. S. Hyams), Academic Press, New York and London, 487-530

Kamiya N. (1959) Protoplasmic streaming. In: Protoplasmatologia, Handbuch der Protoplasmaforschung, (Eds. L. V. Heilbrunn, I. W. Weber), Springer-Verlag, Berlin, **8:** 3c

Koonce M. P., Schliwa M. (1985) Bidirectional organelle transport can occur in cell processes that contain single microtubules. *J. Cell Biol.* **100:** 322-326

Patterson D. J. (1979) On the organization and classification of the protozoon, *Actinophrys sol* Ehrenberg, 1830. *Microbios* **26:** 165-208

Patterson D. J., Hausmann K. (1981) Feeding by *Actinophrys sol* (Protista, Heliozoa). 1. Light microscopy. *Microbios* **31:** 39-55

Rebhun L. (1972) Polarized intracellular particle transport: saltatory movements and cytoplasmic streaming. *Int. Rev. Cytol.* **32:** 93-137

Sakaguchi M., Hausmann K., Suzaki T. (1998) Food capture and adhesion by the heliozoon *Actinophrys sol*. *Protoplasma* **203:** 130-137

Sakaguchi M., Murakami H., Suzaki T. (2001) Involvement of a 40-kDa glycoprotein in food recognition, prey capture, and induction of phagocytosis in the protozoon *Actinophrys sol*. *Protist* **152:** 33-41

Schliwa M. (1984) Mechanisms of intracellular transport. In: Cell and Muscle Motility, (Ed. J. Shay), Plenum Publishing Co., New York, **5:** 1-82

Suzaki T., Shigenaka Y. (1982) Intra-axopodial particle movement and axopodial surface motility in *Echinosphaerium akamae*. In: Biological Functions of Microtubules and Related Structures, (Eds. H. Sakai, H. Mohri, G. G. Borisy), Academic Press, Tokyo and New York, 91-103

Suzaki T., Shigenaka Y., Watanabe S., Toyohara A. (1980) Food capture and ingestion in the large heliozoan, *Echinosphaerium nucleofilum*. *J. Cell Sci.* **42:** 61-79

Tilney L. G. (1968) Studies on the microtubules in heliozoa. IV. The effect of colchicine on the formation and maintenance of the axopodia and the redevelopment of pattern in *Actinosphaerium nucleofilum* (Barrett). *J. Cell Sci.* **3:** 549-562

Tilney L. G., Hiramoto Y., Marsland D. (1966) Studies on the microtubules in heliozoa. III. A pressure analysis of the role of these structures in the formation and maintenance of the axopodia of *Actinosphaerium nucleofilum* (Barrett). *J. Cell Biol.* **29:** 770-795

Vollet J. J., Roth L. E. (1974) Cell fusion by nascent membrane induction and divalent-cation treatment. *Cytobiologie* **9:** 249-262

Received on 15th May, 2002; accepted on 29th August, 2002

Acta Protozool. (2003) 42: 11 - 17

ACTA
PROTOZOOLOGICA

Pharmacological Evidence Suggests that the Lysozyme/PACAP Receptor of *Tetrahymena thermophila* is a Polycation Receptor

Michael KEEDY, Nathan YORGEY, Jeremy HILTY, Angela PRICE, David HASSENZAHL, and Heather KURUVILLA

Cedarville University, Department of Science and Mathematics, Cedarville, U.S.A.

Summary. Pituitary adenylate cyclase activating polypeptide (PACAP) is a peptide hormone that exists in two biologically active forms: PACAP-38 and PACAP-27. Several types of PACAP receptors have been characterized, and these have been classified into three families: the $VPAC_1$, the $VPAC_2$, and the PAC_1 receptors. In this study, we used *in vivo* behavioral assays along with pharmacological inhibitors to investigate the behavior of the lysozyme/PACAP receptor in *Tetrahymena.* This receptor behaves like a PAC_1 receptor in some respects; however, PACAP 6-38 serves as an agonist, rather than an antagonist, for this receptor. These results are consistent with the existence of a generalized polycation receptor rather than a PACAP-specific receptor.

Key words: chemorepellent, G-protein, PACAP-38, PKA, PKC, polycation receptor, *Tetrahymena*.

Abbreviations: BIS IV - bisindolylmaleimide IV; cAMP - adenosine 3'5'monophosphate; cGMP - guanosine 3'5' monophosphate; EC_{50} - concentration of repellent which causes 50% avoidance; EIA - enzyme-linked immunoassay; GDP-β-S - guanosine 5'-O-(2-thiodiphosphate); IP_3 - inositol 1,4,5 trisphosphate; PACAP - pituitary adenylate cyclase activating polypeptide; PKA - cAMP-dependent protein kinase; PKC - protein kinase C; Rp-cAMPs - Rp-adenosine-3', 5' cyclic monophosphorothioate.

INTRODUCTION

Pituitary adenylate cyclase activating polypeptide (PACAP) is a peptide hormone derived from a larger polypeptide precursor. This peptide exists in two biologically active forms: a 38-amino acid peptide, PACAP-38 (Miyata *et al*. 1989), and an N-terminal amidated 27-amino acid peptide, PACAP-27 (Miyata *et al*. 1990). Both forms of this peptide are polycations at physiological pH. Receptors for this peptide have been found in nearly every organ in the body (Vaudry *et al*. 2000). The nearly ubiquitous nature of this peptide in mammalian systems makes it an interesting ligand to study in other cell systems. PACAP-38 has previously been shown to act as a chemorepellent in *Tetrahymena thermophila* (Mace *et al.* 2000, Hassenzahl *et al.* 2001).

Since the initial discovery of PACAP, several types of receptors have been identified and classified based on their affinities for the following ligands: PACAP-38,

Address for correspondence: Heather Kuruvilla, Cedarville University, Department of Science and Mathematics, 251 North Main St., Cedarville, OH 45314, U.S.A.; Fax: (937) 766-7631; E-mail: kuruvilh@cedarville.edu

PACAP-27, vasoactive intestinal peptide (VIP), and other members of the same peptide hormone superfamily. Three receptor classes have been identified so far: the $VPAC_1$ receptor, the $VPAC_2$ receptor, and the PAC_1 receptor (Harmar *et al*. 1998). Of these three receptor types, previously obtained pharmacological data (Hassenzahl *et al*. 2001) suggest that the *Tetrahymena* receptor may share some characteristics with the PAC_1 class of receptors in terms of the second messenger pathways utilized. The pathways through which previously identified PAC_1 receptors signal include cyclic AMP (cAMP) as well as inositol trisphosphate (IP_3) and diacylglycerol (DAG)-mediated activation of protein kinase C (PKC) (Delporte *et al*. 1995, Hahm *et al*. 1998).

Two forms of the PAC_1 receptor have been identified. Type IA receptors have an equal affinity for PACAP-38 and PACAP-27, while type IB receptors have a higher affinity for PACAP-38 than for PACAP-27 (Harmar *et al*. 1998, Robberecht *et al*. 1991). Both types receptors have an affinity for VIP that is about 1000 times less than the affinity for PACAP-38. In addition, PAC_1 receptors are selectively inhibited by the antagonist PACAP 6-38, a fragment of PACAP-38 that binds to the receptor but does not activate the second messenger pathway (Harmar *et al*. 1998). These pharmacological profiles have not previously been evaluated in *Tetrahymena*.

Previous work in *Tetrahymena* has demonstrated that the lysozyme response is mediated through a receptor that shows specific, saturable binding (Kuruvilla *et al*. 1997). The receptor has also been isolated and characterized electrophoretically as a 42 kD protein (Kuruvilla and Hennessey 1998). Adaptation studies with PACAP-38 have shown that cells exposed to lysozyme for at least 10 min no longer show avoidance to PACAP- 38 and *vice versa* (Mace *et al*. 2000). The fact that both lysozyme and PACAP are polycations, combined with the previously mentioned adaptation data, suggests that these two ligands may utilize a common receptor and second messenger pathways.

Recent work in our laboratory indicates that signaling through the lysozyme/PACAP receptor of *Tetrahymena thermophila* involves both cAMP production and the activation of PKC (Hassenzahl *et al*. 2001). While this suggests the possibility of PAC_1 receptor involvement, the potencies of PACAP-27, VIP, and the PAC_1 receptor antagonist PACAP 6-38 have not been previously tested in *Tetrahymena*. In our current study, we have used *in vivo* behavioral assays as well as pharmacological inhibitors to suggest the presence of a receptor that shares some characteristics with the PAC_1 receptor family, specifically, ligand potency and the use of common signaling pathways. However, there is one notable difference: namely, the action of PACAP 6-38, an antagonist to PAC_1 receptors (Vaudry *et al*. 2000), which acts as an agonist (chemorepellent) in our system. These data suggest that the lysozyme/PACAP receptor is probably a generalized, G-protein linked, polycation receptor which signals through several second messenger pathways.

MATERIALS AND METHODS

Cell cultures

Tetrahymena thermophila B, strain SB715, a generous gift from T. M. Hennessey (SUNY at Buffalo) was used throughout the study. Cells were incubated in the axenic medium Dentler (1988) at 25°C for 48 h after inoculation without shaking and without addition of antibiotics.

Chemicals and solutions

As in earlier studies with lysozyme and PACAP (Kuruvilla *et al*. 1997, Mace *et al*. 2000, Hassenzahl *et al*. 2001), behavioral bioassays were carried out in a buffer containing 10 mM Trizma base, 0.5 mM MOPS, 50 μM $CaCl_2$, pH 7.0. PACAP-38 was obtained from Calbiochem, La Jolla, CA. PACAP-27 was obtained from Peninsula Laboratories, San Carlos, CA. PACAP 6-38 and VIP were obtained from the American Peptide Co, Sunnyvale, CA. The G-protein inhibitor guanosine 5'-O-(2-thiodiphosphate) (GDP-β-S) was obtained from Alexis Biochemicals, San Diego, CA. The PKC inhibitor Calphostin C and the PKA inhibitor Rp-cAMPs were obtained from BIOMOL Research Laboratories, Plymouth Meeting, PA. Another PKC inhibitor, BIS IV, was obtained from LC Laboratories, Woburn, MA. The cAMP EIA kit was obtained from Cayman Chemical, Grand Rapids, MI. All other chemicals were obtained from Sigma Chemical Company, St. Louis, MO.

Behavioral bioassays

In vivo behavioral assays were carried out as previously described (Mace *et al*. 2000, Hassenzahl *et al*. 2001). Briefly, cells were first washed twice in the assay buffer and then transferred to the first well of a 3-well spot microtiter plate. Individual cells were then transferred, using a micropipette, to a well containing either buffer or the inhibitor being tested. If an inhibitor was being tested, cells were adapted to the inhibitor for a minimum of 10 to 15 min before individual cells were transferred to a third well containing a combination of the chemorepellent and the test concentration of inhibitor and scored for avoidance (+ or -) for each trial. Cells were scored as (+) for avoidance if they showed backward swimming, characterized by jerky, backward motions, backward motions in a straight line, or backward "tumbling", with the cell rotating anterior-over-posterior or spinning rapidly, like a fan blade. If no inhibitor was being tested, cells were simply transferred from the buffer to a well containing the

chemorepellent of interest and scored for avoidance (+ or -) for each trial. The mean ± SD was calculated for a minimum of three trials and was expressed as " Cells Showing Avoidance, [%]".

EIA assays

Enzyme-linked immunoassays (EIAs) for cAMP were performed using an EIA kit from Cayman Chemical, Grand Rapids, MI, Catalog Number 581001. Briefly, two-day old cell cultures were washed twice in behavioral buffer and then placed into the same behavioral buffer containing 1 mM theophylline. Cells were then exposed to 0.1 µM PACAP-38, PACAP-27, or PACAP 6-38, or simply left in buffer. Aliquots of 1 ml, containing approximately 7.66E06 cells, were immediately frozen in liquid nitrogen. Upon thawing, the cell lysate was centrifuged at 12,500 g for 10 min to remove particulate matter. The supernatant was acetylated according to the EIA kit manufacturer's instructions (diluted 1:100 for maximum performance on the standard curve) and used for the EIA assay.

RESULTS

In vivo behavioral assays indicate that PACAP-38, PACAP-27, and PACAP 6-38 all act with similar potencies as chemorepellents in *Tetrahymena* (Fig. 1). The EC_{50} (concentration of repellent which causes 50% of cells to show avoidance) of all three compounds was approximately 10 nM. VIP, which was also a chemorepellent, was much less potent, with an EC_{50} of approximately 10 µM, 1000 times higher than that of the other three ligands (Fig. 1). The concentrations of repellent necessary to elicit 100% avoidance was 0.1 µM for PACAP-38, PACAP-27, and PACAP 6-38, and 100 µM for VIP (Fig. 1). These concentrations of repellent were used in the adaptation studies (Fig. 2), cross-adaptation studies (Table 1), inhibitor studies (Table 2), and cAMP assays which follow.

Chemorepellent responses to 0.1 µM PACAP-38, 0.1 µM PACAP-27, 0.1 µM PACAP 6-38, and 100 µM VIP all declined with time (Fig. 2). By four min, approximately 50% of the cells had adapted to the repellent, while a baseline (≤ 20%) avoidance response was seen at 10 min. Based on the behavior of *Tetrahymena* when placed in buffer under our assay conditions (10-20%; Kuruvilla *et al*. 1997, Mace *et al*. 2000, Hassenzahl *et al*. 2001), it appears that cells are fully adapted after 10 min of exposure to the repellents. All of the ligands showed a similar time course of adaptation (Fig. 2). As seen in previous studies with other repellents in *Tetrahymena*, adaptation to all of the repellents could be reversed by placing cells in buffer for about 10 min before reintroducing them to the repellent (unpublished observations; Kuruvilla *et al.* 1997).

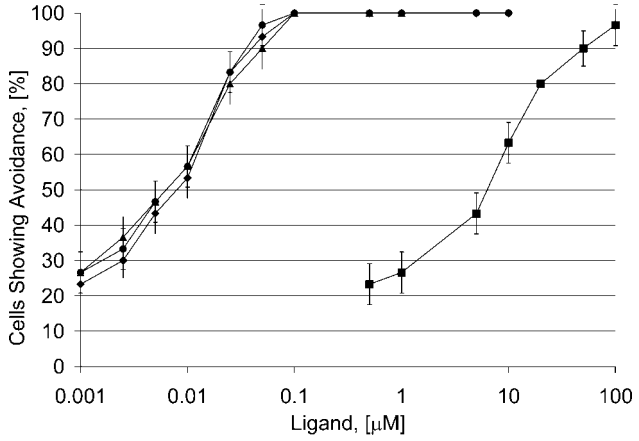

Fig. 1. PACAP-38, PACAP-27, PACAP 6-38, and VIP are effective chemorepellents in *Tetrahymena.* Behavioral bioassays (see Materials and Methods) were used to show the concentration dependencies for avoidance reactions to PACAP-38 (closed diamonds), PACAP-27 (closed triangles), PACAP 6-38 (closed circles), and VIP (closed squares). The percentage of cells showing avoidance was determined by observation of a single cell after transfer to the test solution. Each trial consisted of ten cells, which were individually scored as to whether or not avoidance occurred. Each point represents the mean ± SD of ≥ 3 trials. Error bars, representing the standard deviation, are shown for each point. The EC_{50} values for these repellents were approximately 10 nM for PACAP-38, PACAP-27, and PACAP 6-38 and 10 µM for VIP.

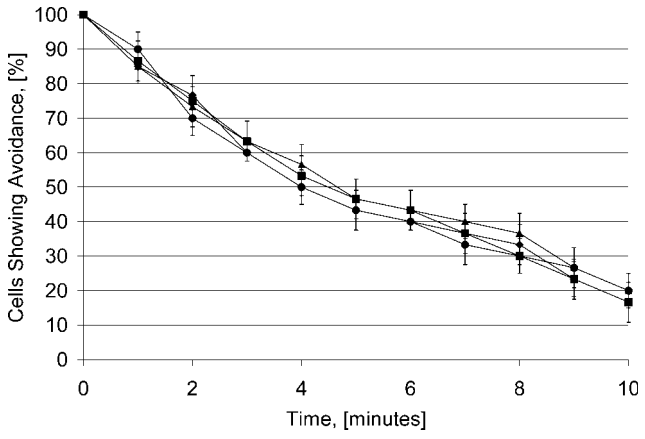

Fig. 2. Adaptation to PACAP-38 (closed diamonds), PACAP-27 (closed triangles), PACAP 6-38 (closed circles), and VIP (closed squares) all occurred over a similar time period (approximately 10 min), consistent with a common signaling mechanism. Each point represents the mean ± SD of ≥ 3 trials. Error bars, representing the standard deviation, are shown for each point.

Table 1. Cross-adaptation between members of the VIP/PACAP family.

	PACAP-38	PACAP-27	PACAP-6-38	VIP
PACAP-38	16.6 ± 5.8	20.0 ± 5.0	13.3 ± 5.8	20.0 ± 5.0
PACAP-27	16.6 ± 5.8	16.6 ± 5.8	20.0 ± 5.0	20.0 ± 5.0
PACAP 6-38	20.0 ± 5.0	20.0 ± 5.0	13.3 ± 5.8	16.6 ± 5.8
VIP	20.0 ± 5.0	20.0 ± 5.0	16.6 ± 5.8	20.0 ± 5.0

Means ± SD for ≥ 3 trials of 10 cells are listed. Each cell was adapted to the chemorepellent for 10 min before testing for cross-adaptation in a different repellent. In all experiments, adaptation to one chemorepellent in the VIP/PACAP family effectively eliminated avoidance to the other repellents in the family (avoidance in buffer alone under our assay conditions ranges from 10-20% (Kuruvilla *et al*. 1997, Mace *et al*. 2000).

Table 2 Effect of various pharmacological inhibitors upon avoidance behavior in various members of the VIP/PACAP family.

	No inhibitor	GDP-β-S 1mM	Rp-cAMPs 50 μM	Calphostin C 10 μM	BIS IV 50 μM	Neomycin 5 μM
PACAP-38, 0.1 μM	100 ± 0.0	16.6 ± 5.8	10 ± 5.0	16.6 ± 5.8	20.0 ± 5.0	16.6 ± 5.8
PACAP-27, 0.1 μM	100 ± 0.0	13.3 ± 5.8	10 ± 0.0	16.6 ± 5.8	16.6 ± 5.8	16.6 ± 5.8
PACAP 6-38, 0.1 μM	100 ± 0.0	6.6 ± 5.8	16.6 ± 5.8	20.0 ± 5.0	16.6 ± 5.8	20.0 ± 5.0
VIP, 100 μM	96.6 ± 5.8	20.0 ± 5.0	20.0 ± 5.0	20.0 ± 5.0	20.0 ± 5.0	20.0 ± 5.0

Means ± SD for ≥ 3 trials of 10 cells are listed. Each cell was incubated with the inhibitor for 10 min before testing for avoidance in the chemorepellent. In all experiments, exposure to the pharmacological inhibitor nearly eliminated avoidance to the chemorepellent (avoidance in buffer alone ranges from 10-20% under these assay conditions; Kuruvilla *et al*. 1997, Mace *et al*. 2000).

Cross-adaptation studies (Table 1) were also conducted to determine whether a cell adapted to one chemorepellent in the VIP/PACAP family would also be adapted to the other peptides in the family. Cells were first adapted to either 0.1 μM PACAP-38, 0.1 μM PACAP-27, 0.1 μM PACAP 6-38, or 100 μM VIP for 10 min and then exposed to one of the other three repellents. In all cases, adaptation to one repellent reduced avoidance to the other three repellents to baseline levels of 10-20% (Table 1).

Several potent and specific pharmacological inhibitors of second messenger pathways have been effective in eliminating avoidance to PACAP-38 in *Tetrahymena* (Mace *et al*. 2000, Hassenzahl *et al*. 2001). These compounds were tested using *in vivo* behavioral assays in order to determine whether the same second messenger pathways are involved in the signaling of the other ligands in the VIP/PACAP family (Fig. 2). The concentrations of inhibitors used in the current assay were based on previously published data (Mace *et al*. 2000, Hassenzahl *et al*. 2001).

The G-protein inhibitor, 1 mM GDP-β-S (Hassenzahl *et al*. 2001), effectively eliminated avoidance to 0.1μM PACAP-38, 0.1μM PACAP-27, 0.1μM PACAP 6-38, and 100 μM VIP (Table 2), lowering avoidance in all cases to the baseline avoidance of 10-20%. A cAMP analogue and competitive inhibitor of PKA, 50 μM Rp-cAMPs (Hassenzahl *et al*. 2001), also eliminated avoidance to all four chemorepellents, as did two PKC inhibitors, 10 μM Calphostin C (Hassenzahl *et al*. 2001), and 50 μM BIS IV (Hassenzahl *et al*. 2001), (Table 2). A competitive inhibitor of the lysozyme receptor (Kuruvilla *et al*. 1997) and an inhibitor of the PACAP-38 response (Mace *et al*. 2000), 5 μM neomycin sulfate, effectively eliminated the avoidance response to 0.1μM PACAP-38, 0.1μM PACAP-27, 0.1μM PACAP 6-38, and 100 μM VIP (Table 2).

Indirect determination of cytosolic cAMP levels was performed by EIA. These preliminary data (N=2) suggest that detectable levels of cAMP are present even in control cells (7.73 ± 0.02E-06 picomoles/cell). Exposure to PACAP-38 raised the cAMP level to 255% of the

control level (1.96 ± 0.11E-05 picomoles/cell), and PACAP-27 caused an increase in cAMP levels to 239% of the control level (1.85 ± 0.12E-05 picomoles/cell). Exposure to PACAP 6-38 caused a lesser increase, raising the level of cAMP to 131% of control levels (1.01 ± 0.08E-05 picomoles/cell). Although these data are preliminary, they are consistent with the Rp-cAMPs data mentioned above.

DISCUSSION

PAC_1 receptors are characterized by a number of common features, including a low affinity for VIP, signaling through cAMP and PKC, and inhibition by the PACAP fragment PACAP 6-38. Data from *in vivo* behavioral assays in *Tetrahymena* (Fig. 1) indicates that the potency of PACAP-38 and PACAP-27 is nearly identical, and the potency of VIP is nearly 1000 times lower than that of PACAP. These results are consistent with signaling through a PAC IA receptor. However, PACAP 6-38 acted as a repellent in our assay (Fig. 1) rather than an antagonist of receptor activity. This is in clear contrast to other systems where PACAP 6-38 serves as an antagonist to the PAC_1 receptor, binding to the receptor but not activating the second messenger pathway (Harmar *et al*. 1998). However, PACAP 6-27, also considered a competitive inhibitor of the PACAP receptor, has been shown to stimulate serotonin release from rat peritoneal mast cells (Seebeck *et al*. 1998). In this case, a receptor-independent mechanism of G-protein activation has been proposed. We have found that PACAP 6-27 is also an effective chemorepellent in our system (unpublished data), with potency nearly indistinguishable from PACAP 6-38. While a receptor-independent mechanism of signaling such as the one proposed for rat peritoneal mast cells is also possible in our system, the high potency of PACAP 6-38, which is nearly equivalent to that of PACAP-38 and PACAP-27, along with the shape of the activation curve, is more consistent with the existence of a receptor, linked to a G-protein. Use of common signaling pathways for all the ligands being studied (PACAP-38, PACAP-27, PACAP 6-38, and VIP) also supports the hypothesis that a common receptor is being used.

Time course studies of *in vivo* behavioral adaptation show a similar kinetic for all four repellents being tested. This result is consistent with the hypothesis that PACAP-38, PACAP-27, PACAP-6-38, and VIP are all signaling through a common receptor. Adaptation occurs over a fairly short time period (about 10 min) and is reversible. These data are consistent with an adaptation mechanism such as modification of the receptor or second-messenger pathway rather than a mechanism such as receptor-mediated endocytosis, which would require a longer period of time for adaptation and recovery or de-adaptation. In the case of lysozyme, which appears to work through the same receptor as PACAP-38 (Mace *et al*. 2000), receptor-mediated endocytosis is not the mechanism of adaptation (Cantor *et al*. 1999). Our current data support these earlier findings.

Cross-adaptation studies (Table 1) are also consistent with the hypothesis that all four ligands being tested (0.1 µM PACAP-38, 0.1 µM PACAP-27, 0.1 µM PACAP 6-38, and 100 µM VIP) share a common receptor and/or second messenger pathway. Adaptation to any one of the ligands in the VIP/PACAP family results in a lack of responsiveness to any of the other ligands, resulting in a baseline avoidance of 10-20%, similar to that seen in buffer alone (Kuruvilla *et al*. 1997, Mace *et al*. 2000).

The polycation, lysozyme, is a chemorepellent in *Tetrahymena* (Kuruvilla *et al*. 1997, Kuruvilla and Hennessey 1998). The lysozyme receptor has been purified by affinity chromatography, and a polyclonal antibody has been raised against the purified protein (Kuruvilla and Hennessey 1998). This antibody, along with a competitive inhibitor of the lysozyme receptor neomycin sulfate (Kuruvilla *et al*. 1997, Kuruvilla and Hennessey 1998) has been used to show that PACAP-38 and lysozyme share a common receptor in *Tetrahymena* (Mace *et al*. 2000). Avoidance to PACAP-38 may also be inhibited by the G-protein inhibitor GDP-β-S, the cAMP analogue Rp-cAMPs, and the PKC inhibitors Calphostin C and BIS IV (Hassenzahl *et al*. 2001). These potent, specific inhibitors can be effectively used to determine involvement of specific enzymes/receptors in the *in vivo* behavioral response of *Tetrahymena*.

In vivo behavioral assays done with 0.1 µM PACAP-38, 0.1 µM PACAP-27, 0.1 µM PACAP 6-38, or 100 µM VIP gave approximately 100% avoidance in all cases (Table 2). The G-protein inhibitor 1 mM GDP-β-S reduced avoidance to near the baseline response of ~10-20% in all cases (Table 2), implicating G-protein involvement in the signaling pathway. This is consistent with previous results for PACAP-38 and

lysozyme, which appear to share a receptor and signaling pathways (Mace *et al*. 2000, Hassenzahl *et al*. 2001).

The cAMP analogue, 50 µM Rp-cAMPs, also inhibited avoidance to 0.1 µM PACAP-38, 0.1 µM PACAP-27, 0.1 µM PACAP 6-38, and 100 µM VIP (Table 2). These data are also consistent with what has been seen for PACAP-38 and lysozyme (Hassenzahl *et al*. 2001). This indicates that cAMP is involved in signaling, possibly as an activator of PKA, or perhaps in another capacity, such as opening a plasma membrane calcium channel. A calcium influx has previously been implicated in the response of *Tetrahymena* to lysozyme (Kuruvilla and Hennessey 1998). These data also support the hypothesis of a common receptor/signaling pathway used by all four ligands.

Preliminary data from EIA experiments measuring the concentration of cAMP in the cytosol after PACAP stimulation showed that all PACAP isoforms tested stimulate cAMP production above control levels. This is consistent with our current Rp-cAMPs data, which suggests cAMP involvement in avoidance, as well as data from previous studies (Hassenzahl *et al*. 2001). Interestingly, PACAP 6-38, a PACAP receptor antagonist in many systems, caused less of an increase in cAMP production than the native PACAP forms (PACAP-38 and PACAP-27). Since the data are sparse, repeated studies will be necessary to determine whether this pattern is consistent. PACAP 6-38 was as potent an agonist in our system as were the native forms of PACAP, and future experiments continue to show lower cAMP levels elicited by PACAP 6-38, this would suggest that the high cAMP levels caused by the native forms of PACAP may not be necessary or sufficient to cause avoidance. The data discussed below implicate the PKC pathway as an integral part of avoidance, and recent data from our laboratory suggest that PKG may be important as well (unpublished observations). Clearly, cAMP is not the only essential component of this repellent pathway.

As seen in Table 2, the PKC inhibitors 10 µM Calphostin C and 50 µM BIS IV effectively reduced avoidance to 0.1 µM PACAP-38, 0.1 µM PACAP-27, 0.1 µM PACAP 6-38, and 100 µM VIP to near the baseline avoidance of 10-20%. This is consistent with previous results seen for PACAP-38 and lysozyme (Hassenzahl *et al*. 2001) and implicates PKC in the avoidance of chemorepellents in the PACAP family. These data also support the hypothesis of a shared second messenger pathway used by all four ligands.

Neomycin sulfate has been shown to be a competitive inhibitor of lysozyme binding to its receptor in *Tetrahymena* (Kuruvilla *et al*. 1997, Kuruvilla and Hennessey 1998) as well as an inhibitor of PACAP-38 binding (Mace *et al*. 2000). In this assay, 5 µM neomycin sulfate reduced avoidance to 0.1 µM PACAP-38, 0.1 µM PACAP-27, 0.1 µM PACAP 6-38, and 100 µM VIP to near the baseline of 10-20%. This, too, is consistent with previous results and supports the hypothesis that all four of these ligands are working through the previously identified lysozyme receptor. This low (5 µM) concentration of neomycin is 60 times lower than the concentration required to block calcium channels on the plasma membrane of *Paramecium* (~300 µM; Gustin and Hennessey 1988) and is consistent with previous inhibition data (Kuruvilla *et al*. 1997, Kuruvilla and Hennessey 1998, Mace *et al*. 2000).

In the current study, we have explored adaptation kinetics, cross-adaptation of cells adapted to one ligand and exposed to another, and the involvement of G-proteins, cAMP, and PKC in signaling. While some of the inhibitors used in our study may have pleiotropic effects on the cell, when taken collectively, our data suggest that PACAP avoidance in *Tetrahymena* occurs through activation of a G-protein linked receptor. The *Tetrahymena* receptor shows some similarities to previously described PAC_1 receptors (Miyata *et al*. 1989, Delporte *et al*. 1995, Hahm *et al*. 1998) in that it signals through cAMP and PKC. However, the N-terminal amino acids of PACAP do not appear to be required for receptor activation, since PACAP 6-38 is as potent a chemorepellent as PACAP-38 or PACAP-27. All of the PACAP isoforms used in the assay, as well as VIP, lysozyme (tested previously), and the lysozyme fragment CB_2 (Kuruvilla and Hennessey 1999) are positively charged polypeptides. Interestingly, the more highly charged molecules, such as PACAP (+ 12 at physiological pH), whose EC_{50} is 10 nM, are more potent than the less highly charged molecules, such as CB_2 (+ 4 at physiological pH) whose EC_{50} is 100 nm (Kuruvilla and Hennessey 1999, Mace *et al*. 2000). All of these data are consistent with signaling of these repellents through a polycation receptor, rather than through a specialized PACAP receptor. This polycation receptor is likely the previously isolated lysozyme receptor, based on the cross-adaptation studies, similar inhibition profiles, and the fact that the antibody raised against the lysozyme receptor blocks PACAP avoidance (Kuruvilla and Hennessey 1998, Mace *et al*. 2000, Hassenzahl *et al*. 2001). Molecular cloning of the receptor, perhaps using

the amino acid sequence previously isolated from the purified receptor preparation (Kuruvilla and Hennessey, 1998), will provide an important step toward identifying sequences responsible for ligand binding and allow for molecular characterization of this polycation receptor.

REFERENCES

Cantor J. M., Mace S. R., Kooy C. M., Caldwell B. D., Kuruvilla H. G. (1999) Adaptation to lysozyme does not occur via receptor-mediated endocytosis in *Tetrahymena thermophila. WWW J Biol*. 4. Available online at http://www.epress.com/w3jbio/vol4/cantor/paper.htm

Delporte C., Poloczek P., de Neef P., Vertongen P., Ciccarelli E., Svoboda M., Herchuelz A., Winand J., Robberecht P. (1995) Pituitary adenylate cyclase activating polypeptide (PACAP) and vasoactive intestinal peptide stimulate two signaling pathways in CHO cells stably transfected with the selective type PACAP receptor. *Mol. Cell Endocrinol.* **107:** 71-76

Dentler W. L. (1988) Fractionation of *Tetrahymena* ciliary membranes with Triton X-114 and the identification of a ciliary membrane ATPase. *J. Cell Biol.* **107:** 2679-2688

Gustin M., Hennessey T. M. (1988) Neomycin inhibits the calcium current of *Paramecium*. *Biochim. Biophys. Acta* **940:** 99-104

Hahm S. H., Hsu C., Eiden L. E. (1998) PACAP activates calcium influx-dependent and -independent pathways to couple met-enkephalin secretion and biosynthesis in chromaffin cells. *J. Mol. Neurosci.* **11:** 43-56

Harmar A. J., Arimura A., Gozes I., Journot L., Laburthe M., Pisegna J. R., Rawlings S. R., Robberecht P., Said S. I., Sreedharan S. P., Wank S. A., Waschek J. A. (1998). International union of pharmacology. XVIII. Nomenclature of receptors for vasoactive intestinal peptide and pituitary adenylate cyclase-activating polypeptide. *Pharmacol. Rev.* **50:** 265-270

Hassenzahl D. L., Yorgey N. K., Keedy M. D., Price A. R., Hall J. A., Myzcka C. C., Kuruvilla H. G. (2001) Chemorepellent signaling through the PACAP/lysozyme receptor occurs through both cAMP and PKC in *Tetrahymena thermophila*. *J. Comp. Physiol. A* **187:** 171-176

Kuruvilla H. G., Hennessey T. M. (1998) Purification and characterization of a novel chemorepellent receptor from *Tetrahymena thermophila. J. Memb. Biol.* **162:** 51-57

Kuruvilla H. G., Hennessey T. M. (1999) Chemosensory responses of *Tetrahymena thermophila* to CB_2, a 24-amino acid fragment of lysozyme. *J. Comp. Physiol. A.* **184:** 529-534

Kuruvilla H. G., Kim M. Y., Hennessey T. M. (1997) Chemosensory adaptation to lysozyme and GTP involves independently regulated receptors in *Tetrahymena thermophila*. *J. Euk. Microbiol.* **44:** 263-268

Mace S. R., Dean J. G., Murphy J. R., Rhodes J. L., Kuruvilla H. G. (2000) PACAP-38 is a chemorepellent and and agonist for the lysozyme receptor in *Tetrahymena thermophila*. *J. Comp. Physiol. A* **186:** 39-43

Miyata A., Arimura A., Dahl R. R., Minamino N., Uehara A., Jiang L., Culler, M. D., Coy, D.H. (1989) Isolation of a novel 38 residue-hypothalamic polypeptide which stimulates adenylate cyclase in pituitary cells. *Biochem. Biophys. Res. Commun.* **164:** 567-574

Miyata A., Jiang L., Dahl R. D., Kitada C., Kubo K., Fujino M., Minamino N., Arimura A. (1990) Isolation of a neuropeptide corresponding to the N-terminal 27 residues of the pituitary adenylate cyclase activating polypeptide with 38 residues (PACAP38). *Biochem. Biophys. Res. Commun.* **170:** 643-648

Robberecht P., Woussen-Colle M. C., De Neef P., Gourlet P., Buscail L., Vandermeers A., Vandermeers-Piret M. C., Christophe J. (1991) The two forms of the pituitary adenylate cyclase activating polypeptide [PACAP (1-27) and PACAP (1-38)] interact with distinct receptors on rat pancreatic AR 4-2J cell membranes. *FEBS Lett.* **286:** 133-136

Seebeck J., Kruse M. L., Schmidt-Choudbury A., Schmidt W. E. (1998) Pituitary adenylate cyclase activating polypeptide induces degranulation of rat peritoneal mast cells via high-affinity PACAP-receptor-independent activation of G-proteins. *Ann. NY Acad. Sci.* **865:** 141-146

Vaudry D., Gonzales B. J., Basille M., Yon L., Fournier A., Vaudry H. (2000). Pituitary adenylate cyclase-activating polypeptide and its receptors: From structure to function. *Pharm. Rev.* **52:** 269-324

Received on 19th August, 2002; accepted on 10th October, 2002

Acta Protozool. (2003) 42: 19 - 29

ACTA
PROTOZOOLOGICA

How Cytotoxic is Zinc? A Study on Effects of Zinc on Cell Proliferation, Endocytosis, and Fine Structure of the Ciliate *Tetrahymena*

Jytte R. NILSSON

Department of Cell Biology, Institute of Zoology, University of Copenhagen, Copenhagen, Denmark

Summary. Addition of 0.5-2.0 mM zinc (Zn^{2+}) to proliferating *Tetrahymena* cultures in 2% proteose peptone (PP) medium induced varying lag periods (~½-4 h) before proliferation resumed at almost normal (0.5, 0.75 mM) or decreased rates (1, 1.5, 2 mM). Initially cells in 1 mM Zn^{2+} moved slowly whereas in higher concentrations a dose-dependent number of cells ceased to move exhibiting rocking movements; the cells recovered, however, and regained motility during the lag period. All Zn-treated cells had small refractive granules which increased in number during the lag period, decreased when cell proliferation resumed, and increased again in non-proliferating cells in high density cultures. The endocytic capacity of the cells was elevated in the low concentrations but suppressed dose-dependently in 1-2 mM Zn^{2+}, concommitantly with an increase in cells not forming vacuoles (up to 80%), corresponding to the immobile cells mentioned above. *Tetrahymena* exposed to Zn^{2+} in dilute, 1% and 0.5% PP, medium showed the same trend of growth pattern and endocytosis as in 2% PP but at lower Zn concentrations. The maximum sublethal concentrations in 0.5%, 1%, and 2% PP growth medium permitting cell proliferation, were 0.2, 1.0, and 2.0 mM Zn^{2+}, respectively, a linear relationship between the amount of organic matter and toxicity. Fine structurally, Zn^{2+}-treated cells had dilated endoplasmic reticulum (induced protein synthesis), electron-dense granules (fused with food vacuoles), and a variety of vesicles, some containing electron-dense dots (Zn?). Apart from the early strong reaction, *Tetrahymena* adapted quickly to excess amounts of Zn^{2+}, perhaps because an ion regulation pathway for Zn^{2+} is already operating in the cells.

Key words: cell motility, cytoplasmic granules, homeostasis, *Tetrahymena pyriformis*, zinc.

INTRODUCTION

Zinc (Zn^{2+}) is an interesting metal nutritionally essential to living organisms in trace amount (μM). The element has multiple intracellular functions as a catalytic or structural constituent of more than 300 enzymes (Vallee and Falchuk 1993, Vallee and Maret 1993) and a cofactor of gene regulatory proteins and transcription factors (Zeng and Kägi 1994). The wide involvement of Zn in biological functions has resulted in an expanding interest in understanding the Zn metabolism.

A deficiency in Zn affects proper functioning of various organs, e.g., the nervous system, skin, intestine (Goyer 1991), and disturbs cell development, differentiation, and cell division (Vallee and Falchuk 1993). The latter disorders affect the immune system, mainly the T-cell population, causing disease advances of, e.g., AIDS, cancer G1 disorder, renal disorder, and aging heightening apoptosis (Fraker and King 2001). All these

Address for correspondance: Jytte R. Nilsson, Department of Cell Biology, Institute of Zoology, University of Copenhagen, Universitetsparken 15, DK-2100 Copenhagen Ø, Denmark; Fax: (+45) 35.32.12.00; E-mail: jrnilsson@zi.ku.dk

disorders, apart from inherited ones, are reversed by Zn supplementation (Vallee and Falchuk 1993). Excess amounts of Zn does not seem to have any adverse long time effects in humans (Vallee and Falchuk 1993) but whereas some reports indicate that Zn may inhibit apoptosis (Zalewski *et al*. 1991), others suggest that Zn actually induces apoptotic cell deaths (Haase *et al*. 2001, Iitaka *et al*. 2001) and propose Zn as a potential cytotoxic agent in treatment of thyroid cancer (Iitaka *et al*. 2001).

As an essential trace element in living organisms, regulation of the intracellular concentration of Zn^{2+} is of utmost importance. Homeostasis of the metal is mediated by metal-binding proteins and metallothioneins (MTs), small proteins binding heavy metals (Kojima and Kägi 1978, Brady 1982, Cherian and Chan 1993, Vallee and Maret 1993) and found in all organisms (Kojima and Kägi 1978, Piccinni 1989, Cherian and Chan 1993, Vallee and Falchuk 1993). Administration of Zn to rats caused a 3-fold increase in mRNA encoding for MT hence supporting a regulatory involvement of the protein in Zn homeostasis (Shapiro and Cousins 1980). MTs have been studied widely, not least in organisms exposured to cadmium (Cd) which induces synthesis of Cd-Zn metallothioneins (Kägi and Vallee 1960, Vallee and Maret 1993) which also happens in *Tetrahymena* (e.g. Yamagushi *et al*. 1978; Nakamura *et al*. 1981a, b; Piccinni *et al*. 1990), a ciliate used much as a model cell system in cytotoxicology (e.g. Nilsson 1989, Sauvant *et al*. 1999). On exposure to Cd, *Tetrahymena* homogenates contain a 3-fold increased amount of Zn in the supernatant but an unchanged amount in the sediment (Piccinni *et al*. 1990).

The role of MTs is not solely that of detoxication of heavy metals, as they are general regulators of the normal Zn-Cu metabolism in living organisms (Brady 1982, Bremner 1993, Cherian and Chan 1993). MTs are also present in untreated *Tetrahymena* and increase in amount when cell proliferation ceases at high cell density (Santovito *et al*. 2000).

In view of the general importance of understanding how cells regulate the intracellular concentration of Zn^{2+}, the present study was undertaken by exposing *Tetrahymena* to excess amounts of the metal. Early studies on effects of Zn on *Tetrahymena* were reviewed some years ago (Nilsson 1989). It was revealed that a high concentration of Zn^{2+} was tolerated by cells in media with a high content of organic matter, in fact, 100-fold higher in 2% proteose peptone (PP) than in distilled water (cf. Nilsson 1989). Moreover, Zn accumulated in small cytoplasmic granules (Dunlop and Chapman 1981, Jones *et al*. 1984). Such small refractive granules appear commonly in *Tetrahymena* under stress conditions and when growth ceases due to high cell density; they have been proposed to play a role as intracellular ion regulators in detoxication of heavy metals (cf. Nilsson 1976, 1989). Yet, how cytotoxic is Zn^{2+} really?

The present study describes effects of Zn^{2+} on cell proliferation, rate of endocytosis, and fine structure of *Tetrahymena* in proliferating cultures. The findings are discussed in relation to published literature on effects of Zn on the organism. The data show good agreement with previous findings but additional new information is reported, especially on the early reaction of cells to excess Zn.

MATERIALS AND METHODS

Tetrahymena pyriformis GL was grown axenically at 28°C in 2% proteose peptone (PP) enriched with 01% yeast extract and inorganic salts, including 0.4 µM Zn (Plesner *et al*. 1964). The experimental 100-ml cultures in 500-ml Fernbach flasks were agitated and aerated. Two cultures in exponentiel growth (20-40,000 cells/ml) were mixed and divided into 50-ml cultures of which 3 cultures received zinc chloride (stock: 100 mM) in an equal volume of distilled water to establish different Zn^{2+} concentrations, and the last culture, the control, received the same amount of water without Zn^{2+}. When addition of the metal decreased the pH of the growth medium (pH 7.0), pH was readjusted with NaOH. To test the effect of Zn^{2+} in reduced amounts of organic matter, cultures (50-80,000 cells/ml) were diluted with 10 mM Hepes buffer (pH 7.0) to obtain media of 1% and 0.5% PP, respectively; the dilution was made 1 h before testing. All cultures were followed for a 24-h period.

In vivo observations were made at low power microscopy of freely swimming cells (for cell shape and motility) and at high power of compressed cells (for cellular details) using a Reichert microscope with anoptral optics.

The cell density of the cultures was determined electronically (Coulter Multisizer II, Counter Electronics Ltd., England). Triplicate 0.5-ml cell samples were withdrawn from the cultures at hourly intervals and fixed with an equal volume of 1% glutaraldehyde in phosphate buffer (pH 7.2). The cell samples were diluted with 0.45% NaCl prior to counting.

The endocytic capacity was determined by a 10-min exposure of 2-ml cell samples to 2 ml carmine particles (0.4 mg/ml) suspended in the same medium as that of the cells. At the end of exposure, the cell suspension was fixed in 4 ml 1% buffered glutaraldehyde. After washing the cells, the number of labelled food vacuoles was counted in 100 cells (Nilsson 1976). The endocytic capacity of treated populations was expressed as the percent of that of control cells (100%).

For electron microscopy, 4-ml cell samples were fixed for 10 min in 2% glutaraldehyde in 0.1 M sodium cacodylate buffer (pH 7.2). The cells were washed in buffer and postfixed for 1 h in buffered

1% osmium tetroxide, washed, dehydrated in a graded series of ethanol, and embedded in epon. The sectioned material was contrasted with uranyl acetate and lead citrate before examination in a Zeiss EM 109 electron microscope.

RESULTS

Normal 2% proteose peptone medium

Addition of 0.5-2.0 mM Zn^{2+} to the medium affected growth of *Tetrahymena* by inducing a dose-dependent lag period before cell proliferation resumed (Fig. 1). After the lag period, cells in 0.5 and 0.75 mM Zn^{2+} resumed proliferation at almost normal rate, whereas cells in 1.0, 1.5, and 2.0 mM Zn^{2+} exhibited decreased rates of proliferation. After 24 h the cells in 0.5-1.0 mM Zn^{2+} had reached the maximum high cell density of control cultures (~ 1,000,000 cells/ml) and cells in 1.5 mM Zn^{2+} a little less (~ 700,000 cells/ml), whereas cells in 2 mM Zn^{2+} doubled 3 times only (~ 300,000 cells/ml).

In vivo observations revealed an initial dose-dependent effect of Zn^{2+} on cell motility. Visually swimming of cells in 0.5 and 0.75 mM was unaffected but in 1 mM their rate became more leisurely (~½ h) and some cells became immobile (~1 h); however, in 1.5 and 2 mM a high fraction of the cells (up to 80% in 2 mM Zn^{2+}) became motionless (with rocking movements) and a few cells had enlarged contractile vacuoles and were spherical of shape, yet a few cells behaved normally. Within the lag period, however, the cells had restored shape, regained motility, and were swimming normally before cell proliferation resumed. A fluffy precipitate formed within 1 h after addition of 2 mM (Fig. 3) and it was ingested by the cells; moreover, sometimes a few dead cells (< 0.1 %) were observed which indicates that 2 mM Zn^{2+} is a critical concentration, i.e. the highest Zn^{2+} concentration permitting cell proliferation in this medium.

The endocytic capacity of *Tetrahymena*, i.e. to form food vacuoles, was affected dose-dependently by Zn^{2+} (Fig. 2). The rate of endocytosis (closed symbols) was elevated in 0.5 and 0.75 mM Zn^{2+} but decreased in 1-2 mM Zn^{2+}, independently of a 1- or 3-h exposure. Whereas about 10% of the control cells (division stages) in proliferating populations do not form food vacuoles (e.g. Nilsson 1989), the number of cells not forming food

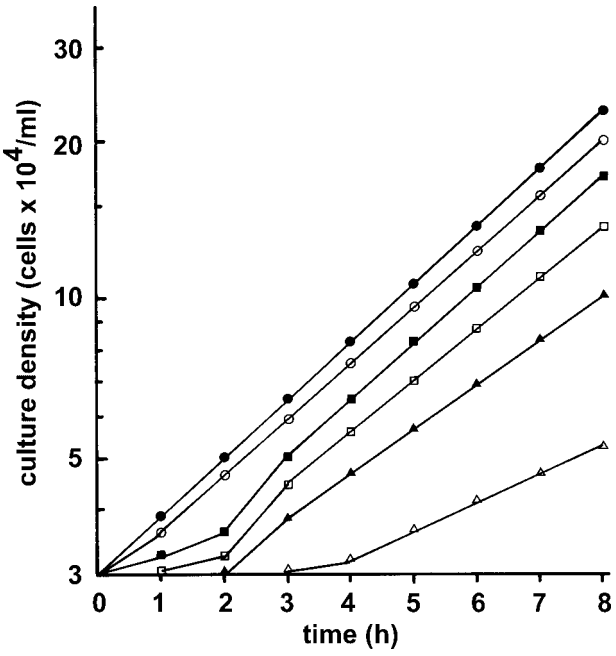

Fig. 1. Effect of Zn^{2+} on the growth rate of *Tetrahymena* in the normal 2% PP medium: control (closed circle), 0.5 mM (open circle), 0.7 mM (closed square), 1.0 mM (open square), 1.5 mM (closed triangle), 2.0 mM (open square). Means of 5-10 experiments per concentration.

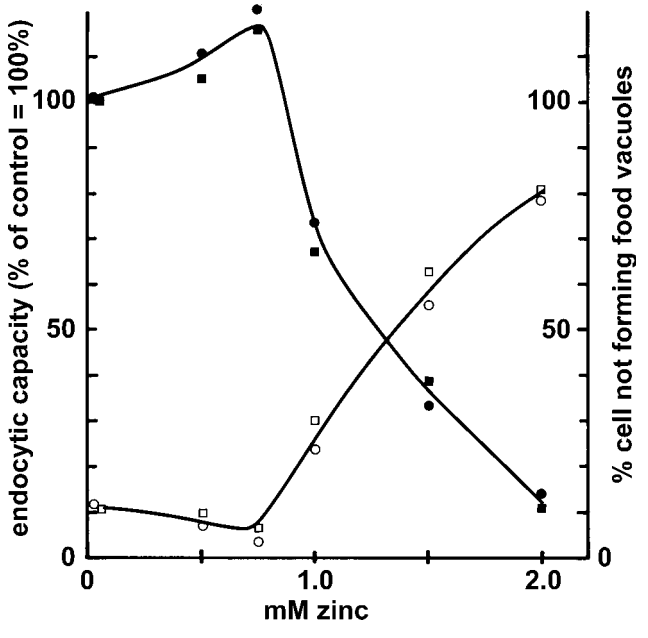

Fig. 2. Effect of a 1- (closed circle) and 3 h - (closed square) exposure to Zn^{2+} (abscissa) on the endocytic capacity of the *Tetrahymena* population (left ordinate, closed symbols) and on the fraction of cells not forming food vacuoles (right ordinate, open symbols). Normal 2% PP medium. Means of 5-10 experiments per concentration.

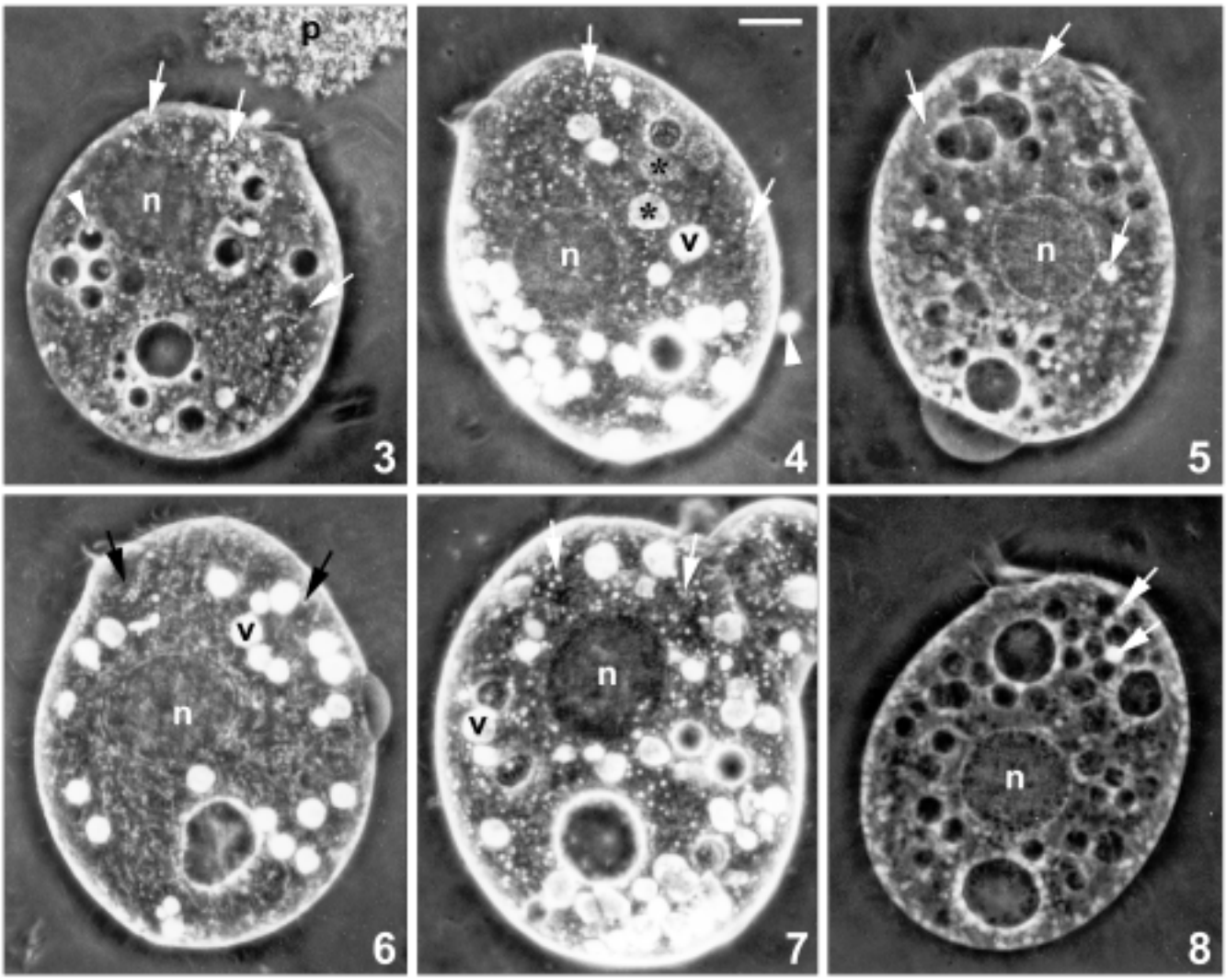

Figs 3-8. Appearance, and turnover, of small refractive granules in *Tetrahymena* (compressed *in vivo*) exposed to Zn in the normal 2% PP; (Figs 3-6) and dilute 1% PP (Fig. 7) growth medium as compared to untreated control (Fig. 8). **3 -** after 1 h in 2 mM Zn the cell contains many small granules (arrows), some have fused with food vacuoles (arrowheads); outside cell, a patch of Zn-PP precipitate (p); **4 -** after 5 h in 2 mM Zn cell contains many small granules (arrows) but also refractive food vacuoles (v) some of composite nature (star) as formed after fusion with granules, a defecation ball (arrowhead) outside cell; **5 -** after 5 h in 0.5 mM Zn, the population proliferates and the cell has few small refractive granules (arrows) but also some larger ones; **6 -** after 5 h in 1 mM Zn the proliferating cell has few small granules (arrows) but still refractive food vacuoles (v); **7 -** after 5 h in 1 mM Zn in 1% PP medium the cell contains numerous small granules (arrows), as well as refractive food vacuoles (v), resembling cell in 2 mM Zn in the normal 2% PP medium (Fig. 4); **8 -** the 5-h control cell has initiated granule formation due to high population density: small refractive granules and a single larger one (arrows). Nucleus (n). Scale bar 10 µm.

vacuoles during the 10-min test increased markedly in high Zn^{2+} concentrations (open symbols); these cells were not in division but in number they correspond to that of the immobile cells mentioned above. Interestingly, cells forming food vacuoles did so at the normal rate, i.e. up to 6 vacuoles/10 min (cell cycle stage dependent); the finding indicates a close relationship between cell motility and capacity for endocytosis. By 24 h all Zn-treated cells had recovered and formed food vacuoles at the same rate as that of control cells.

Conspicuously, all Zn-treated cells contained small refractive granules which accumulated during the lag period (Figs 3, 4). The granules remained present at a low value in proliferating cells but increased again in number at high cell density (Figs 5, 6). Such small refractive granules also appear in control cells when

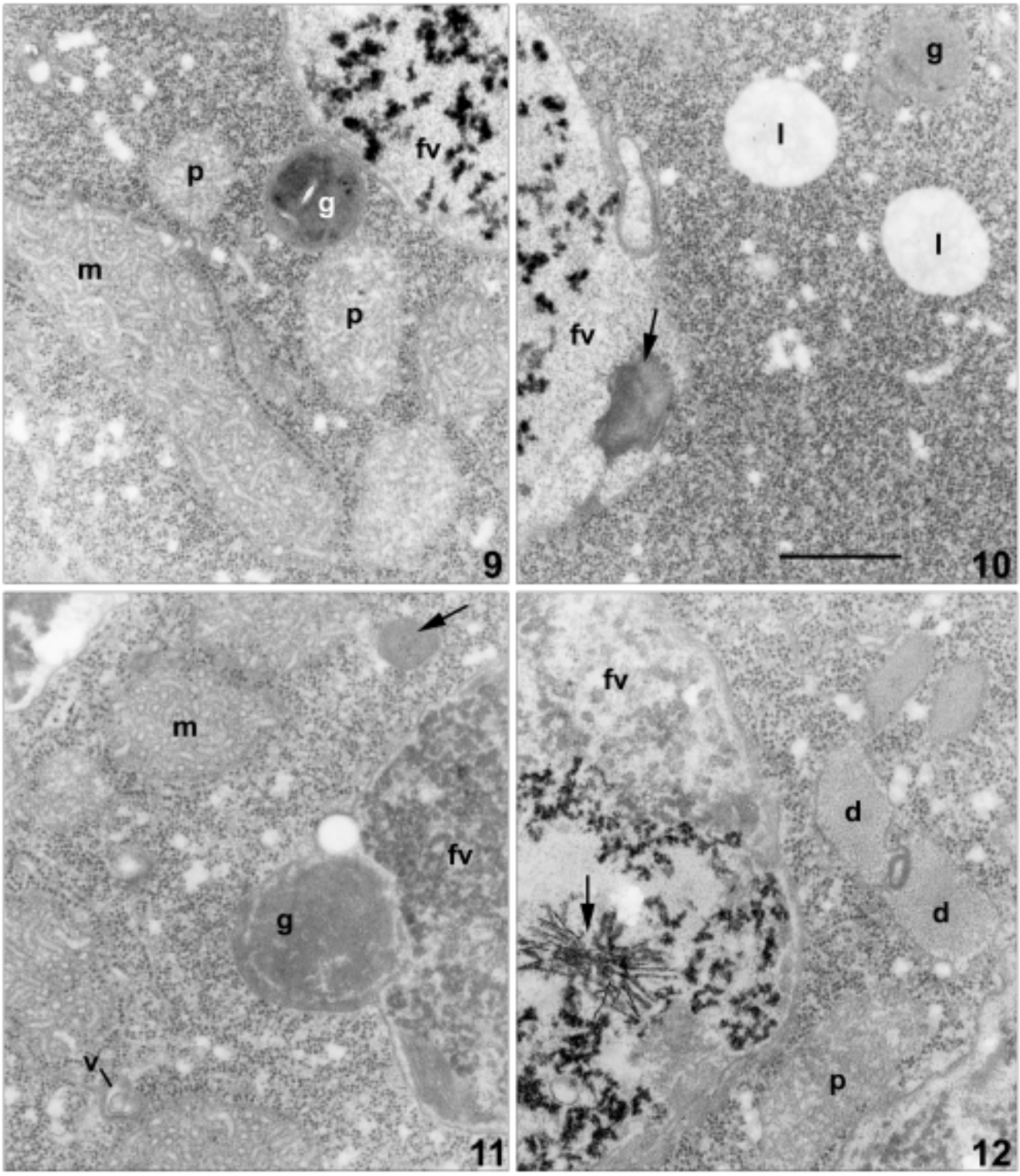

Figs 9-12. Turnover of dense (refractive) granules in *Tetrahymena* exposed to 1.5 mM Zn^{2+} for 1 h (Figs 9, 10) and 5 h (Fig. 11) and to 1.0 mM Zn^{2+} for 3 h (Fig. 12) in 2% PP medium. **9** - dense granule (g) close to a food vacuole (fv) indicative of near fusion; **10** - opposite side af the same food vacuole (fv) as shown in Fig. 9 containing a laminated structure (arrow) indicative of completed fusion with a dense granule, in the cytoplasm a less dense granule (g) and lipid droplets (l), growth inhibited related structures; **11** - after 5 h in 1.5 mM Zn^{2+} cell proliferation has initiated (see Fig. 1) and a granule (g) is fusing with a food vacuole (fv), electron-dense material (arrow) within the grazing section of another granule and a vesicle (v) with laminated substructure; **12** - part of food vacuole (fv) in cell after 3 h in 1 mM Zn^{2+} containing electron-dense material after uptake of Zn-PP precipitate, note the crystal-like structure (arrow), in the cytoplasm delated endoplasmic structures (d). Mitochondria (m), peroxisomes (p). Scale bar 0.5 µm.

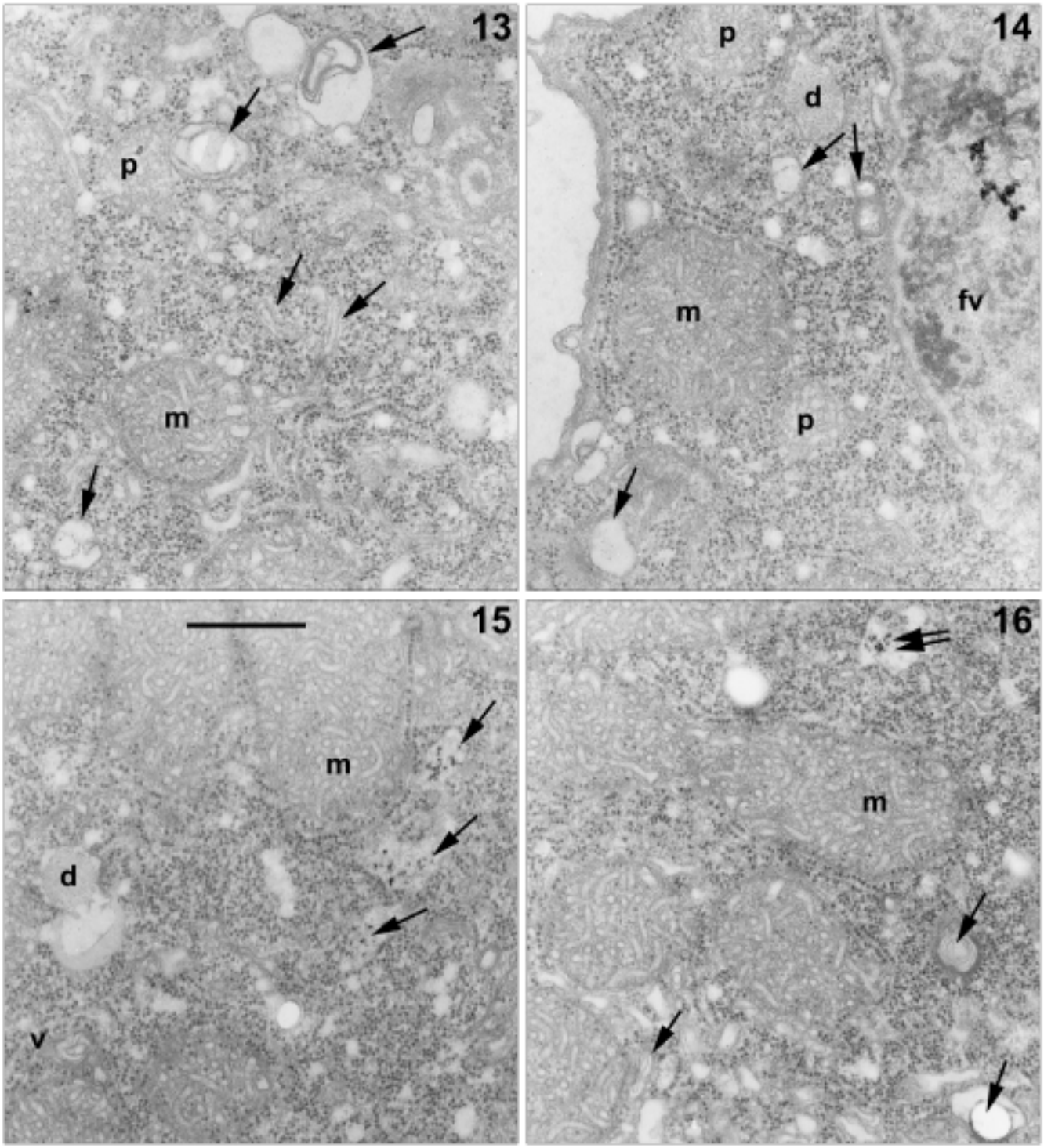

Figs 13-16. Cytoplasmic structures possibly involved in lowering and controlling the intracellular Zn^{2+} concentration in *Tetrahymena* exposed for 3 h to 1 mM (Figs 13, 14) and for 5 h to 1.5 mM Zn^{2+} (Figs 15, 16) in 2% PP medium. **13** - various vesicles (arrows) and tubular structures believed to be accumulating the metal; **14** - dilated endoplasmic structure with amorphous material (d), laminated structure, and vesicles (arrows) with fine dense dots (Zn?); **15** - dilated structures (d) with distinct dense (Zn?) material (arrows), vesicle with laminated structure (v); **16** - dilated structure with dense (Zn?) material (double arrow), vesicles with laminated contents or "empty" ones and tubular structures (arrows). Mitochondria (m), peroxisomes (p). Scale bar 0.5 µm.

proliferation ceased due to high cell density (Fig. 8). The early appearance of the granules on exposure to excess Zn indicates a rapid entry of the metal, increasing the intracellular concentration, followed by an efficient mechanism of removal or capture of the ions. The later decrease in number of granules before proliferation is resumed, seems to relate to an apparent fusion of granules with food vacuoles (e.g. Figs 3, 4), giving rise to a refractive content of these, unrelated to ingestion of the fluffy precipitate, and in turn to extrusion via refractive defecation balls (Fig. 4) which accummulated with time at the bottom of the cultures.

Dilute (1.0, 0.5%) proteose peptone media

In order to establish a relationship between the tolerated concentration of Zn^{2+} and the amount of organic matter, the normal growth medium (2% PP) was diluted to 1.0 and 0.5% PP, respectively. In these media Zn^{2+} was tolerated only at lower concentrations by *Tetrahymena* than in the 2% PP medium but otherwise the effects on the cells followed the same trends (data not shown) as shown for cells in 2% PP (Figs 1, 2).

In 1% PP, 0.1 mM Zn^{2+} affected cell proliferation only slightly (like 0.75 mM Zn^{2+} in 2% PP). A concentration of 0.5 mM Zn^{2+} induced a 3-h lag period before proliferation resumed (almost like 1.5 mM in 2% PP). In 1.0 mM Zn, a 5-h lag period was induced but even though the cells were affected more (Fig. 7) than cells in 2 mM Zn^{2+} in 2% PP (Fig. 4), the cell population had doubled twice by 24 h. Hence in 1% PP medium, 1.0 mM Zn is considered the highest tolerated concentration.

In 0.5% PP, 0.1 mM Zn^{2+} induced a 2-h lag period before the cells started to proliferate (like in 1 mM Zn^{2+} in 2% PP). In 0.2 mM, the cells exhibited a 4-h lag period before proliferation resumed (almost like 2 mM Zn^{2+} in 2% PP) but the percentage of immobile cells was high during the lag period. Cells in 0.5 mM Zn^{2+} were affected severely and many had grossly enlarged contractile vacuoles and were spherical of shape and some cells died; the population had not increased in density after 24 h but the cells had regained motility and normal shape. The highest Zn^{2+} concentration permitting cell proliferation in the 0.5% PP medium was then 0.2 mM.

In both dilute media *Tetrahymena* was affected by Zn^{2+} in the same manner as that described above for cells in the normal 2% PP medium but at respective lower concentrations. With respect to the effect of Zn^{2+} on cell motility, appearance of the small refractive granules (see Figs 4, 7), and on the capacity of cells to form food vacuoles, all findings showed the same trends as those described above for cells in 2% PP medium but at the respective, low concentrations of Zn^{2+}.

Fine structure

Fine structurally, Zn-treated cells showed signs of suppressed growth initially in the high concentrations as reflected in some change in nucleolar structure (not shown), appearance of lipid droplets, glycogen islands, and not least of small, electron-dense granules (Figs 9-11). The dense granules were especially numerous early on exposure to Zn^{2+} during the lag period; however, already at this stage, and throughout exposure to Zn^{2+}, the granules appeared to fuse with food vacuoles and remnants of their contents appeared within the food vacuoles (Figs 9-11) which contained varying amounts of electron-dense (Zn?) matter (Figs 9-10, 12) after ingestion of soluble Zn or Zn-containing precipitate. The finding indicates an intracellular turnover of the granules and thereby elimination of accumulated Zn through defecation as suggested light microscopically (Fig. 4). Moreover, the cells had dilated endoplasmic reticulum, indicative of induced protein synthesis (Figs 12, 14) and an abundance of various small vesicles and tubular structures (Figs 13-16), some with electron-dense dots (Zn?), not seen in the control cells. With time in Zn, some of these structures (Figs 15, 16) contained distinct electron-dense material (Zn?), resembling the contents of food vacuoles (Figs 9-10, 12) in which electron-dense material, even crystal-like structures (Fig. 12), could derive from ingestion of the fluffy Zn-containing precipitate formed with the PP medium at high Zn^{2+} concentrations.

DISCUSSION

The present findings on how excess amount of Zn^{2+} affects growth of *Tetrahymena* are in good agreement with earlier reports (summerized in Table 1) using growth media of 2% proteose peptone (PP) (Jones *et al*. 1984, Larsen and Svensmark 1991) and 1% PP (Dunlop and Chapman 1981). The unusual short lag periods noted in the present study in up to 1 mM Zn^{2+}, indicate a moderate effect only on, or high adaptation of, the cells as they resume growth at almost normal rate. The phenomenon is likely to relate to Zn^{2+} being an essential metal for which the cells already have a regulatory mechanism. The present findings confirm also that toxicity of Zn^{2+} increases when the amount of organic

Table 1. Effects of zinc chloride on *Tetrahymena.*

Medium	Zn^{2+} amount	Lag/growth rate	Specific remarks	Reference
2% PP	0.5 mM	no inhibition	granules (Zn)	Jones *et al*.1984
	1.0 mM	reduced rate	granules (Zn)	
	5.0 mM	kills cells/5 days	granules (Zn)	
2% PP	0.5 mM	unaffected	granules	Larsen and Svensmark 1991
	1.0 mM	2-h/decreased	granules	
	2.0 mM	5-h/decreased	granules	
2% PP	0.5 mM	~½-h/unaffected	granules	Present study
	0.75 mM	~1-h/affected	granules	
	1.0 mM	2-h/decreased	granules	
	1.5 mM	~2-h/decreased	granules/immobility	
	2.0 mM	4-h/decreased	granules/immobility	
1% PP	94 µM	undisturbed	granules (Zn)	Dunlop and Chapman 1981
	0.9 mM	decreased	granules (Zn)	
	1.8 mM	kills all cells		
1% PP	0.1 mM	~1-h/decreased	granules	Present study
	0.5 mM	3-h/decreased	granules/immobility	
	1.0 mM	>5-h/recovery	granules/immobility	
0.5% PP	0.1 mM	2-h/decreased	granules/immobility	Present study
	0.2 mM	5-h/decreased	granules/immobility	
	0.5 mM	24-h/ceased	granules/immobility	
0.2% PP	130 µM	50% inhibition		Yamagushi *et al*. 1973
	1.0 mM	growth ceases		
Tap water	~4 µM	4-h survival		Ruthven and Cairns 1973
	19 µM	kills in10 min		
Distill. w.	20 µM	96-h survival		Carter and Cameron 1973
	40 µM	24-h/30% mortality		
Hard w.*	0.4 mM	8-h LD_{50}		Chapman and Dunlop 1981
IM**	8 µM	1-h LD_{50}		Svensmark and Larsen 1988

*Hard water - 500 ppm of Ca^{2+} (12.5 mM), Mg^{2+} (20.6 mM), or Ca^{2+} + Mg^{2+} (16.5 mM); **IM - inorganic salts (Plesner *et al*. 1964).

matter in the medium (2-0.5% PP) decreases (Table 1). Tolerance is low in the absence of organic matter (~20 µM Zn^{2+}) (Carter and Cameron 1973, Ruthven and Cairns 1973, Svensmark and Larsen 1988) but increases (Table 1) in presence of high amounts of inorganic calcium (Ca) and magnesium (Mg) salts (Chapman and Dunlop 1981). The protective power of organic matter may relate to the high affinity of Zn for forming more or less labile complexes with ligands, such as, amino acids, peptides, and various proteins (Albert 1981, Vallee and Falchuk 1993). In 2% PP medium, the amounts of 0.5, 1, and 2 mM Zn^{2+} found as free ions or very labile complexes, were 17, 15, and 11%, respectively, (Larsen and Svensmark 1991); the decreasing percentage may relate to formation of the fluffy precipitate seen at high Zn^{2+} concentrations. The Zn-PP precipitate was preferentially ingested by the cells which then became exposed to a higher (unknown) amount of the metal than that added to the medium.

Metallothionein (MT) is an important protein which binds Zn as already mentioned. The amount of MT is low in proliferating *Tetrahymena* but increases when growth ceases in old cultures (Santovito *et al*. 2000). Although it remains to be established, MT is expected to increase markedly in *Tetrahymena* exposured to excess Zn, as happens in other organisms (Shapiro and Cousins 1980, Cherian and Chan 1993), and when the ciliate is exposed to Cd (Piccinni *et al*. 1990). With a high binding affinity for Zn, 7 Zn atoms per MT-molecule (e.g. Vallee and Falchuk 1993), MT may act as a modulator as it captures and releases Zn readily (Brady 1982, Cherian and Chan 1993, Vallee and Maret 1993). In the cytoplasm MT may function by releasing Zn when needed (Brady 1982, Bremner 1993, Cherian and Chan 1993), whereas storage of Zn would be expected to be within membrane-bound compartments.

Tetrahymena exposed to Zn^{2+} had small refractive granules as also reported by other investigators (see

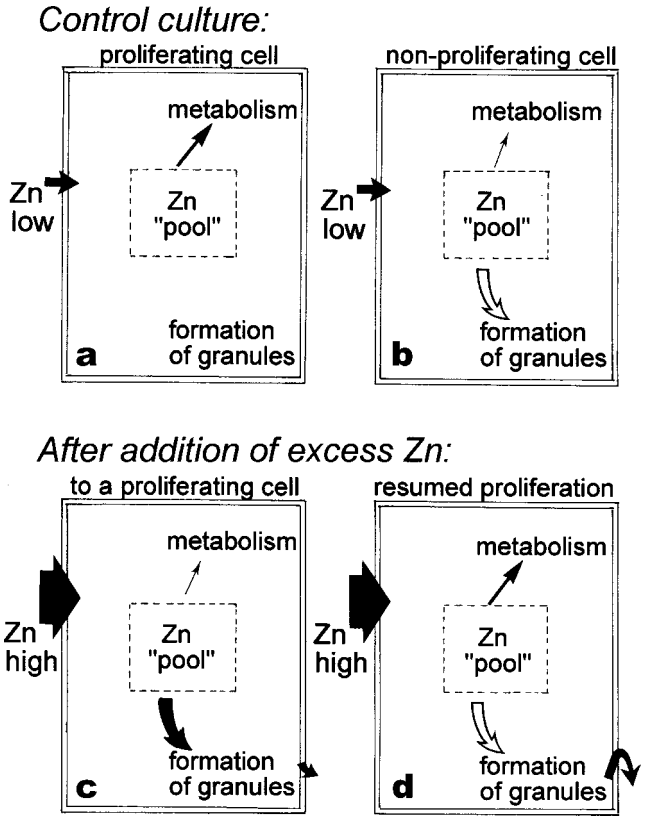

Fig. 17. Proposed intracellular state of Zn homeostasis in *Tetrahymena* assuming a constant intracellular "Zn pool". Control cells at low external Zn^{2+} concentration (a, b) and proliferating cells exposured to excess amounts of Zn^{2+} (c, d). **a** - proliferating control cell, Zn^{2+} enters plasma membrane in balance with an intracellular "pool" of available Zn^{2+} and drainage of remaining Zn^{2+} through metabolism; **b** - non-proliferating control cell: entry of Zn^{2+} through plasma membrane is unchanged but intracellular drainage through metabolism is decreased, excess Zn will be exported through pathway of granule formation for storage as a minor component with Ca, Mg, K, and P; **c** - on exposure of proliferating cells to excess Zn^{2+}, massive entry of Zn^{2+} through plasma membrane rising the intracellular concentration (causing immobility), less Zn is drawn through metabolism (proliferation ceased), the inbalance activates the pathway to granule formation where Zn may become a major cation in the refractive granules, some Zn is passed out of the cell *via* defecation balls, the chaotic state is stabilized during lag period; **d** - end of lag period with restored homeostasis, massive entry of Zn^{2+} through plasma membrane unchanged, intracellular "Zn pool" restored, drainage through metabolism increased to normal as cells proliferate, but not enough to eliminate the pathway of granule formation completely, turnover of accumulated Zn *via* defecation. - When high cell density has been reached the situation resembles that of (b) but with large increase in number of granules.

Table 1). The granules increased in number during the lag period and remained present throughout the exposure to Zn^{2+}. However, when cell proliferation resumed, the number of granules decreased, indicating a turnover, but it increased again at high cell density when cell proliferation ceased. The small refractive granules are not seen in proliferating control cells but they appear normally in *Tetrahymena* in high density cultures when cell proliferation is decreasing (Rosenberg 1966; Munk and Rosenberg 1969; Nilsson 1976, 1989), a cyclic event. The granules contain Ca, Mg, potassium (K) and phosphorus (P) (Rosenberg 1966) with a constant cations/P ratio in an organic matrix (Coleman *et al.* 1972) and they have been proposed to be involved in the intracellular ion regulation as storage sites for excess metals. The cyclic appearance/disappearance of the granules relates to the activity of an associated pyrophosphatase with an optimum at pH 6.0 which is different from the optimum of pH 7.5 of a soluble pyrophosphatase in *Tetrahymena* (Munk and Rosenberg 1969). In the presence of excess Zn, the refractive granules also contained Zn in addition to Ca and P (Dunlop and Chapman 1981) and Mg and K (Jones *et al.* 1984) and after 24 h, Zn became the major cation with Ca and Mg as minor components (Jones *et al.* 1984). As would be expected, Zn was also detected in minor amount in granules in old control cells (Dunlop and Chapman 1981). In the present study, the dense granules fused with food vacuoles, hence any Zn accumulated within them, would together with ingested Zn, become defecated from the cells; this finding indicates a constant turnover of accumulated Zn in *Tetrahymena* exposed to excess amount of Zn. In humans several Zn-transporter proteins (ZnTs) have been identified to be involved in Zn efflux (ZnT1), in vesicular sequestration of the cation (ZnT2, ZnT3), and in export of Zn (ZnT4) out of cells (Milon *et al.* 2001). Moreover, in human HeLa cells excess Zn accumulates in intracellular vesicles (Chimienti *et al.* 2001) like the granules in *Tetrahymena*. Whether specific Zn transporter proteins are involved in Zn metabolism in ciliates remains to be shown.

The initial, dramatic effect of high Zn^{2+} concentrations on motility of *Tetrahymena* has not been reported previously. Immobility, associated with rocking movements of the cells, was a gradual effect developing within ~0.5 h and strongly indicates an interference of Zn with Ca metabolism. Availability and change in the intracellular ionic Ca concentration play an important role in proper functioning of ciliary movement (Machemer 1988). In a related ciliate *Paramecium* fixed while actively swimming, excess Zn deposited at high Ca sites (Fischer *et al.* 1976), a finding suggesting entry of Zn^{2+} through Ca^{2+} gates. In *Tetrahymena* a cation channel for K^+ and Ca^{2+} has been isolated from ciliary membranes and the channel was found to be permeated also by other cations (Oosawa *et al.* 1988); Zn was not

tested but it is likely to enter the cells *via* these Ca^{2+} channels. That Zn interferes with Ca metabolism is also indicated by suppressed uptake of ^{45}Ca in *Tetrahymena* exposured to 0.5 and 1 mM Zn^{2+} (Jones *et al*. 1984). Moreover, in rat liver cells 0.5 mM Zn^{2+} stimulates the activity of Ca, Mg ATPases in plasma and lysosomal membranes (Adachi *et al*. 1996), and Zn enters rat neurons through Ca channels (Büsselberg 1995). Inactivation of cilia, i. e. cell immobility, is Ca-dependent and induced by membrane depolarization which causes a slight rise in the intraciliary Ca concentration (Machemer 1988). It seems likely that the immobility induced in *Tetrahymena* by exposure to excess Zn, is caused by massive entry of the metal through Ca channels in the ciliary membrane whereby Ca homeostasis is disturbed, causing a slight rise in the intraciliary Ca^{2+} concentration whereby ciliary beating is inactivated. The cells recovered, however, and regained motility during the lag period, i.e. they adapted to the high external Zn concentration, indicating restoration of Zn homeostasis.

In proliferating cultures *Tetrahymena* is assumed to have an established Zn homeostasis. In homeostasis, a balance exists between the amount of Zn entering the cell and a constant cytoplasmic "pool" of available Zn, ionic and temporary in binding proteins, and drainage of the metal through metabolism as proposed in Fig. 17a. When proliferation ceases, the same amount of Zn will enter the cell but as less Zn is drawn through metabolism, excess Zn is directed through the pathway of granule formation (Fig. 17b) where it is stored together with Ca, Mg, K and P in small refractive granules. In excess amount of Zn, the element enters the cell massively which disturbs homeostasis causing an increase in the intracellular Zn^{2+} concentration, cell proliferation ceases so less Zn is drawn through metabolism, and the increased Zn^{2+} concentration is lowered by activating (induced protein synthesis?) the pathway to granule formation (Fig. 17c). Once a new balance is established between entry of Zn and the intracellular handling of the metal, the cells will proliferate and drainage of Zn through metabolism will return to previous value (Fig. 17a) but not enough to eliminate the pathway of granule formation (Fig. 17d), i.e. cells proliferating in excess Zn will still have granules, but in a lower number than during the lag period (Fig. 17c) because accumulated Zn is turned over and defecated (Fig. 17d). Likewise, when the culture reaches high cell density, proliferation ceases and less Zn is drawn through metabolism so the number of granules increases in the non-proliferating cells. In fact, if non-proliferating cells, i.e. active in granule formation (Fig. 17b), were exposed to excess Zn, they would probably adapt more quickly with less effect on cell motility than that observed in the present study.

In conclusion, proliferating *Tetrahymena* exposed to high sublethal amounts of Zn^{2+} experiences a major hazard initially. Due to a massive entry of Zn, cell motility is affected but once the cells have circumvented the hurdle and restored homeostasis (during the lag period), they can resume proliferation. Hence, apart from the initial hazard, excess amount of Zn has no adverse long time effects on *Tetrahymena*, only a somewhat prolonged generation time, i.e. the metabolic cost of the intracellular handling of excess Zn.

REFERENCES

Adachi T., Arai K., Ohkuma S. (1996) A comparative study of (Ca^{2+}-Mg^{2+})-ATPase on the lysosomal membrane and ecto-ATPase on the plasma membrane from rat liver. *Biol. Pharm. Bull.* **19:** 1291-1297

Albert A. (1981) Selective Toxicity. Chapman and Hall, London, New York

Brady F. O. (1982) The physiological function of metallothionein. *Trends Biochem. Sci.* **7:** 143-145

Bremner I. (1993) Involvement of metallothionein in the regulation of mineral metabolism. In: Metallothionein III. (Eds. K. T. Suzuki, N. Imura, M. Kimura). Birkhäuser Verlag, Basel, 111-124

Büsselberg D. (1995) Calcium channels as target sites of heavy metals. *Toxicol. Lett.* **82/83:** 255-261

Carter J. W., Cameron I. L. (1973) Toxicity bioassay of heavy metals in water using *Tetrahymena pyriformis*. *Wat. Res.* **7:** 951-961

Chapman G., Dunlop S. (1981) Detoxication of zinc and cadmium by the freshwater protozoan *Tetrahymena pyriformis*. I.The effect of water hardness. *Environ. Res.* **26:** 81-86

Cherian M. G., Chan H. M. (1993) Biological functions of metallothionein - a Review. In: Metallothionein III. (Eds. K. T. Suzuki, N. Imura, M. Kimura). Birkhäuser Verlag, Basel, 87-109

Chimienti F., Jourdan E., Favier A., Seve M. (2001) Zinc resistance impairs sensitivity to oxidative stress in HeLa cells: protection through metallothioneins expression. *Free Radic. Biol. Med.* **31:** 1179-1190

Coleman J. R., Nilsson J. R., Warner R. R., Batt P. (1972) Qualitative and quantitative electron probe analysis of cytoplasmic granules in *Tetrahymena pyriformis*. *Exp. Cell Res.* **74:** 207-219

Dunlop S., Chapman G. (1981) Detoxication of zinc and cadmium by the freshwater protozoan *Tetrahymena pyriformis*. II. Growth experiments and ultrastructural studies on sequestration of heavy metals. *Environ. Res.* **24:** 264-274

Fischer G., Kaneshiro E. S., Peters P. D. (1976) Divalent cation affinity sites in *Paramecium aurelia*. *J. Cell Biol.* **69:** 429-442

Fraker P. J., King L. E. (2001) A distinct role for apoptosis in the changes in lymphopoiesis and myelopoiesis created by deficiencies in zinc. *FASEB J.* **15:** 2572-2578

Goyer R. A. (1991) Toxic effects of metals. In: Casarett and Doull's Toxicology. (Eds. M. O. Amdur, J. Doull, C. D. Klaassen). 4 ed. Pergamon Press, New York, 623-680

Haase H., Wätjen W., Beyersmann D. (2001) Zinc induces apoptosis that can be suppressed by lanthanum in C6 rat glioma cells. *Biol. Chem.* **382:** 1227-1234

Iitaka M., Kakinuma S., Fujimaki S., Oosuga I., Fujita T., Yamanaka K., Wada S., Katayama S. (2001) Induction of apotosis and necrosis by zinc in human thyroid cancer cell lines. *J. Endocr.* **169:** 417-424

Jones A. R., Taylor M., Simkiss K. (1984) Regulation of calcium, cobalt and zinc by *Tetrahymena elliotti*. *Comp. Biochem. Physiol.* **78A:** 493-500

Kojima Y., Kägi J. H. R. (1978) Metallothionein. *Trends Biochem. Sci.* **3:** 90-92

Kägi J. H. R., Vallee B. L. (1960) Metallothionein: a cadmium- and zinc-containing protein from equine renal cortex. *J. Biol. Chem.* **235:** 3460-3465

Larsen J., Svensmark B. (1991) Labile species of Pb, Zn and Cd determined by anodic stripping staircase voltammetry and their toxicity to *Tetrahymena*. *Talanta* **38:** 981-988

Machemer H. (1988) Motor control of cilia. In: *Paramecium* (Ed. H.-D. Görtz) Springer Verlag, Berlin, 216-235

Milon B., Dhermy D., Pountney D., Bourgeois M., Beaumont C. (2001) Differential subcellular localization of hZip1 in adherent and non-adherent cells. *FEBS Lett.* **507:** 241-246

Munk N., Rosenberg H. (1969) On the deposition and utilization of inorganic pyrophosphate in *Tetrahymena pyriformis*. *Biochim. Biophys. Acta* **177:** 629-640

Nakamura Y., Katayama S., Okada Y., Suzuki F., Nagata Y. (1981a) The isolation and characterization of a cadmium and zinc-binding protein from *Tetrahymena pyriformis*. *Agr. Biol. Chem.* **45:** 1167-1172

Nakamura Y., Maekawa Y., Katayama S., Okada Y., Suzuki F., Nagata Y. (1981b) Induction of a metallothionein-like protein in *Tetrahymena pyriformis* by metal ions. *Agr. Biol. Chem.* **45:** 2375-2377

Nilsson J. R. (1976) Physiological and structural studies on *Tetrahymena pyriformis* GL. With special reference to endocytosis and to structural changes during the cell cycle and in response to alterations in the cellular environment. *C. R. Trav. Lab. Carlsberg* **40:** 215-355

Nilsson J. R. (1989) *Tetrahymena* in cytotoxicology: with special reference to effects of heavy metals and selected drugs. *Europ. J. Protistol.* **25:** 2-25

Oosawa Y., Sokabe M., Kasai M. (1988) A cation channel for K^+ and Ca^{2+} from *Tetrahymena* cilia in planar lipid bilayers. *Cell Struct. Func.* **13:** 51-60

Piccinni E. (1989) Response to heavy metals of uni- and multicellular organisms: homologies and analogies. *Boll. Zool.* **56:** 265-271

Piccinni E., Irato P., Guidolin L. (1990) Cadmium-thionein in *Tetrahymena thermophila* and *Tetrahymena pyriformis*. *Europ. J. Protistol.* **26:** 176-181

Plesner P., Rasmussen, L., Zeuthen E. (1964) Techniques used in the study of synchronous *Tetrahymena*. In: Synchrony in Cell Division and Growth. (Ed. E. Zeuthen). Interscience Publ., New York, 543-563

Rosenberg H. (1966) The isolation and identification of "volutin" granules from *Tetrahymena*. *Exp. Cell Res.* **41:** 397-410

Ruthven J. A., Cairns J., Jr. (1973) Response of fresh-water protozoan artificial communities to metals. *J. Protozool.* **20:** 127-135

Santovito G., Irato P., Piccinni E. (2000) Regulation of metallothionein (MT) in *Tetrahymena*: induction of MT-mRNA and protein by cadmium exposure. *Europ. J. Protistol.* **36:** 437-442

Sauvant M. P., Pepin D., Piccinni E. (1999) *Tetrahymena pyriformis*: a tool for toxicological studies. A review. *Chemosphere* **38:** 1631-1669

Shapiro S. G., Cousins R. J. (1980) Induction of rat liver metallothionein mRNA and its distribution between free and membrane-bound polyribosomes. *Biochem. J.* **190:** 755-764

Svensmark B., Larsen J. (1988) Determination of the labile species of zinc by anodic stripping staircase voltammetry, with special reference to correlation with the toxicity to *Tetrahymena*. *Talanta* **35:** 953-957

Vallee B. L., Falchuk H. (1993) The biochemical basis of zinc physiology. *Physiol. Rev.* **73:** 79-118

Vallee B. L., Maret W. (1993) The functional potential and potential functions of metallothioneins: A personal perspective. In: Methallothionein III (Eds. K. T. Suzuki, N. Imura, M. Kimura), Birkhäuser Verlag, Basel, 1-27

Yamagushi N., Wada O., Ono T., Yazaki K., Toyokawa K. (1973) Detection of heavy metal toxicity by *Tetrahymena pyriformis* culture method. *Ind. Health* **11:** 27-31

Yamagushi N., Wada O., Ono T., Nagahashi M. (1978) Responses of *Tetrahymena pyriformis* to cadmium exposure - With special reference to a metallothionein-like protein. *Ind. Health* **16:** 15-21

Zalewski P. D., Forbes I. J., Giannakis C. (1991) Physiological role for zinc in prevention of apoptosis (gene-directed death). *Biochem. Biophys. Res. Commun.* **24:** 1093-1101

Zeng J., Kägi J. H. R. (1994) Zinc fingers and metallothionein in gene expression. In: Handbook of Experimental Pharmacology (Eds. R. A. Goyer, M. G. Cherian) **115:** 333-347

Received on 17th July, 2002; accepted on 2nd October, 2002

Acta Protozool. (2003) 42: 31 - 39

ACTA
PROTOZOOLOGICA

Bacterial Endocytobionts within Endosymbiotic Ciliates in *Dreissena polymorpha* (Lamellibranchia: Mollusca)

Sergei I. FOKIN[1], Laure GIAMBERINI[2], Daniel P. MOLLOY[3] and Abraham bij de VAATE[4]

[1]Biological Institute, St. Petersburg State University, Russia; [2]UPRES Ecotoxicité, Biodiversité et Santé Environnementale, Université de Metz, France; [3]Division of Research & Collections, New York State Museum, Albany, NY USA; [4]Institute for Inland Water Management & Waste Water Treatment, Lelystad, Netherlands

Summary. This paper documents a multi-level microcosm system: *Dreissena*-ciliates-bacteria-viruses. In the first comprehensive investigation of endocytobionts present in the cytoplasm of endosymbiotic ciliates from mussels, bacteria are described from *Conchophthirus acuminatus* and an undescribed *Ophryoglena* sp. species which are, respectively, commensal and parasitic in the freshwater bivalve *Dreissena polymorpha*. Light microscopy, electron microscopy, Feulgen staining, and *in situ* observation indicated that in some populations of *C. acuminatus* practically all individuals were infected with cytoplasmic bacteria. Some of these bacteria were in the α-subgroup of proteobacteria. *In situ* hybridization indicated that some other eubacteria with a very similar morphology were also present in the cytoplasm of *C. acuminatus*. Using *in situ* hybridization with appropriate oligonucleotide probes, a large amount of bacteria, most of which were also in the α-subgroup, were observed in the cytoplasm of each specimen of *Ophryoglena* sp. examined. Some bacteria with virus particles were also observed in a population of the *Ophryoglena* sp. The bacteria in *C. acuminatus* were not likely the same as in the *Ophryoglena* sp. The presence of α-subgroup proteobacteria in the cytoplasm of both endosymbiotic ciliates, in conjunction with previous reports of these bacteria in free-living species, indicates that they are widely established endocytobionts in these protists.

Key words: bacteria, *Conchophthirus acuminatus*, *Dreissena polymorpha*, *in situ* hybridization, *Ophryoglena* sp.

INTRODUCTION

The freshwater macrofouling bivalve *Dreissena polymorpha*, commonly known as the zebra or wandering mussel, has been continually spreading throughout Eastern and Western Europe since the beginning of the 19th century. Although considerable research has been carried out to understand the ecological interrelationships of this bivalve with other aquatic organisms, relatively little effort has been made to investigate the diversity, distribution, and significance of endosymbiotic organisms present within these mussels. This gap of information is currently being addressed as a project of the International Research Consortium on Molluscan Symbionts (IRCOMS) (Molloy *et al.* 2001, Molloy 2002). IRCOMS investigations have documented that ciliates are the most common endosymbionts of *D. polymorpha*. Five host-specific ciliates (*Conchophthirus acuminatus*, *C. klimentinus*, *Hypocomagalma dreissenae*, *Sphenophrya dreissenae*, and *S. naumiana*) are known from the mantle cavity of this mussel and at least one undescribed *Ophryoglena* sp. from its digestive gland. The nature of the symbiotic relationships of these

Address for correspondence: Sergei I. Fokin, Tuchkov 3, apt. 6, 199053, St. Petersburg, Russia; E-mail: fokin@peterlink.ru

species with their dreissenid hosts is typically not well defined, but appears to range from commensalism, e.g., *C. acuminatus*, to parasitism, e.g., *Ophryoglena* sp. (Molloy *et al.* 1997, Laruelle *et al.* 1999).

Intracellular bacteria have been observed in the cytoplasm, nuclei, and perinuclear space of a number of free living ciliate species, but their phylogenetic positions have rarely been determined (Görtz 1983, 1998; Fokin 1993; Fokin and Karpov 1995; Fokin *et al.* 1996, 2000). In this IRCOMS investigation, we report bacterial endocytobionts within endosymbiotic ciliates, in particular, within two species from *D. polymorpha*: the commensal *C. acuminatus* (Scuticociliatida, Conchophthiridae) (Fig. 1) and the undescribed parasitic *Ophryoglena* sp. (Hymenostomatida, Ophryoglenidae) (Fig. 2).

MATERIALS AND METHODS

Organisms: *Dreissena polymorpha* populations from the following five locations were dissected to collect endosymbiotic ciliates: lake Bodensee at Konstanz and a lake near Karlsruhe in Germany, from the Volkerak and Haringvliet waterbodies in the Netherlands, and from the Ivankovskoye reservoir in Russia. *C. acuminatus* was obtained from all locations, and the *Ophryoglena* sp. from all except the Karlsruhe lake. Although the majority ciliate populations examined contained bacteria in their cytoplasm, the research efforts outlined below focused primarily on specimens of *C. acuminatus* from Karlsruhe and Volkerak and on the *Ophryoglena* sp. from Bodensee, Volkerak, and Haringvliet.

Microscopy: live ciliates were temporarily immobilized following the methods of Skovorodkin (1990). Photomicrographs were taken with DIC and fluorescence optics (Axioskop, Zeiss, Germany and Zeiss confocal laser scanning microscope, LSM 410).

Staining: Feulgen procedure was done according to previous work (Fokin 1989). For *in situ*- hybridization, cells were fixed with 4% formaldehyde (w/v, freshly prepared from paraformaldehyde) in phosphate buffered saline solution (PBS) pH 7.2, for 2 h and washed with PBS. Cells were incubated with oligonucleotide probes in hybridization buffer (Fokin *et al.* 1996). A eubacterial specific probe (5'-GCTGCCTCCCGTAGGAGT-3'), labeled with fluorescein (FITC) and an α-subgroup of proteobacteria specific probe (5'-GCGTTCGCTCTGAGCCAG-5'), labeled with tetramethylrhodamine (TRITC) (Amann *et al.* 1990, 1991) were used.

Specimens were examined using a Zeiss LSM 410 with a plan neofluar 100x oil immersion objective. For detection of FITC and TRITC, an argon-ion laser (488 nm) and a helium-neon laser (543 nm) with appropriate emission filters, BP 510-525 nm, and 575-640 nm, respectively, were used. Color pictures were taken by a Polaroid recorder on a Zeiss LSM 410.

Electron microscopy: immediately after collection, during zebra mussel dissection, the ciliates were immersed in 2% glutaraldehyde (Grade I, Sigma Chemical Co.) in 0.025 M sodium cacodylate buffer (pH 7.4) for 90 min at 4°C. After centrifugation at 200 G, the cell pellets were rinsed in buffer solution (0.05 M) and post-fixed with 1% osmium tetroxide (Sigma) buffered with sodium cacodylate. To facilitate manipulations, the cells after fixation were first embedded in agar. Following their dehydration through graded alcohol, the ciliates were embedded in Epon-Araldite (Sigma). Ultra-thin sections (60-80 nm), cut with a diamond knife on a LKB Ultratom V ultramicrotome, were placed on copper grids and stained with uranyl acetate and lead citrate. Ultrastructural observations were made using a Jeol CX100 (80KV) transmission electron microscope.

RESULTS

Bacteria in the cytoplasm of *Conchophthirus acuminatus* (Figs 1, 11)

Prevalence of infection was high, and in some *C. acuminatus* populations practically all individuals were infected. Using DIC and phase-contrast microscopy, relatively large bacteria (2.0-6.0 x 0.5-0.7 μm) were detected in four of the five *C. acuminatus* populations investigated, with infection intensities ranging from about 5 to 70 of these large bacteria per ciliate. Whereas bacteria were occasionally visible in live intact cells, they were more easily seen in squashed preparations. The best methods of detection, however, were Feulgen-staining and the *in situ* hybridization.

According to the DIC pictures of squashed living cells, the bacteria appeared to be well distributed throughout the cytoplasm. From light microscopic observations, it seemed that at least some bacteria were located in individual vacuoles. Electron microscopic images, however, did occasionally reveal membranes surrounding some bacteria, but whether these were truly endocytobiotic vacuoles was unclear. A clear zone frequently separated the bacteria from host cytoplasmic structures (Figs 3-5). Bacteria were sometimes observed close to the cisternae of endoplasmic reticulum without ribosomes (Fig. 5). No clear nucleoid structures were found inside of the bacteria. In rare cases, a portion of the bacterial "cytoplasm" appeared to have a different density (Fig. 5). The cell wall structure suggests that all bacteria could be Gram-negative (Figs 3, 4).

Using an *in situ* hybridization procedure with two oligonucleotide probes, at least two types of bacteria were detected in the cytoplasm: an α-subgroup of proteobacteria and one more type of eubacteria (Figs 12, 15). Since all bacteria had similar dimensions and shapes, we were not able to discriminate among them morphologically, but the two types always were located in

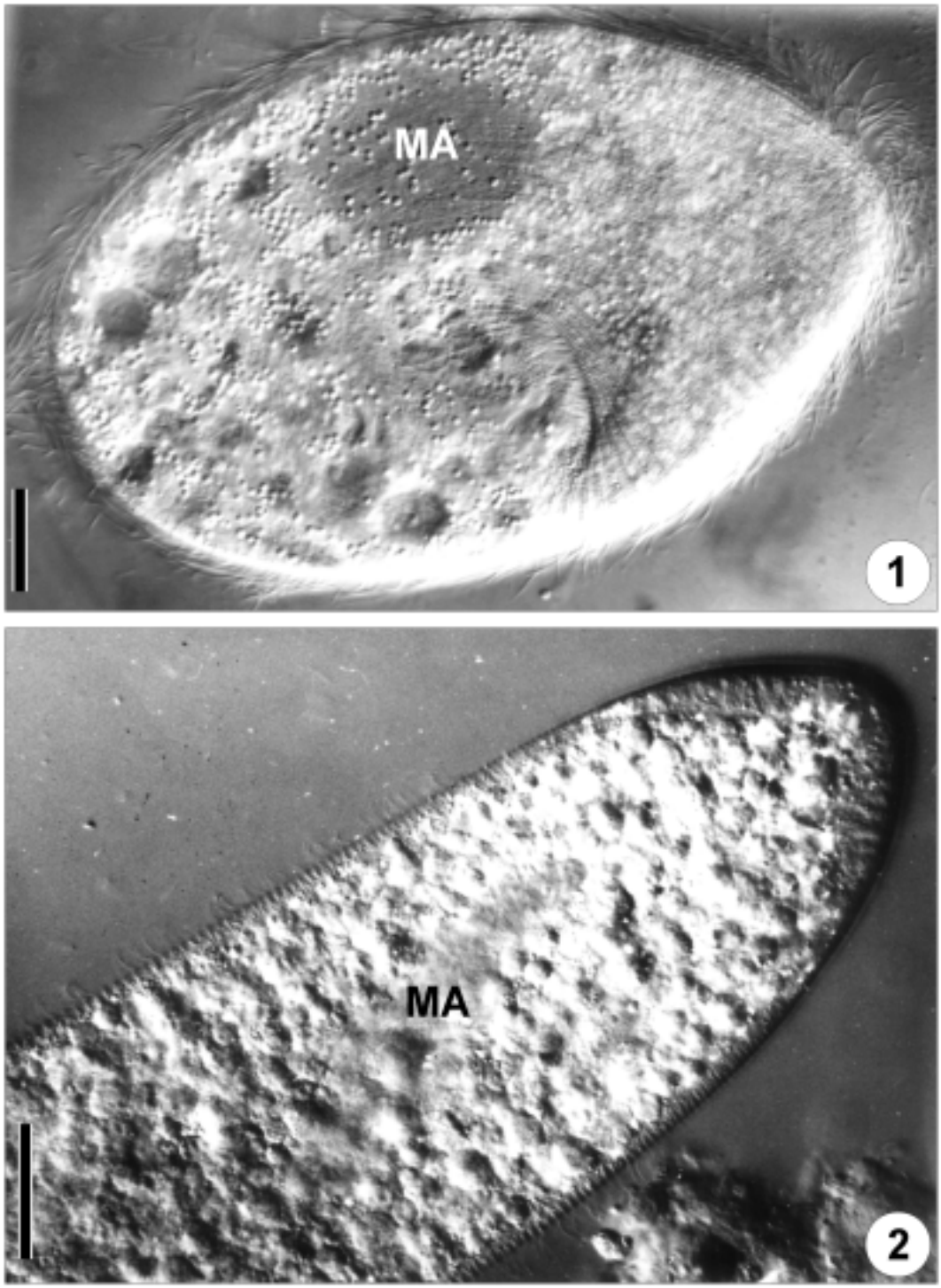

Figs 1-2. Ciliates investigated. **1** - *Conchophthirus acuminatus*, an endocommensal from the mantle cavity of *Dreissena polymorpha*; and **2** - *Ophryoglena* sp., a parasite of the digestive gland of *D. polymorpha*. Living cells, DIC contrast, MA - macronucleus. Scale bars 10 µm (1); 20 µm (2).

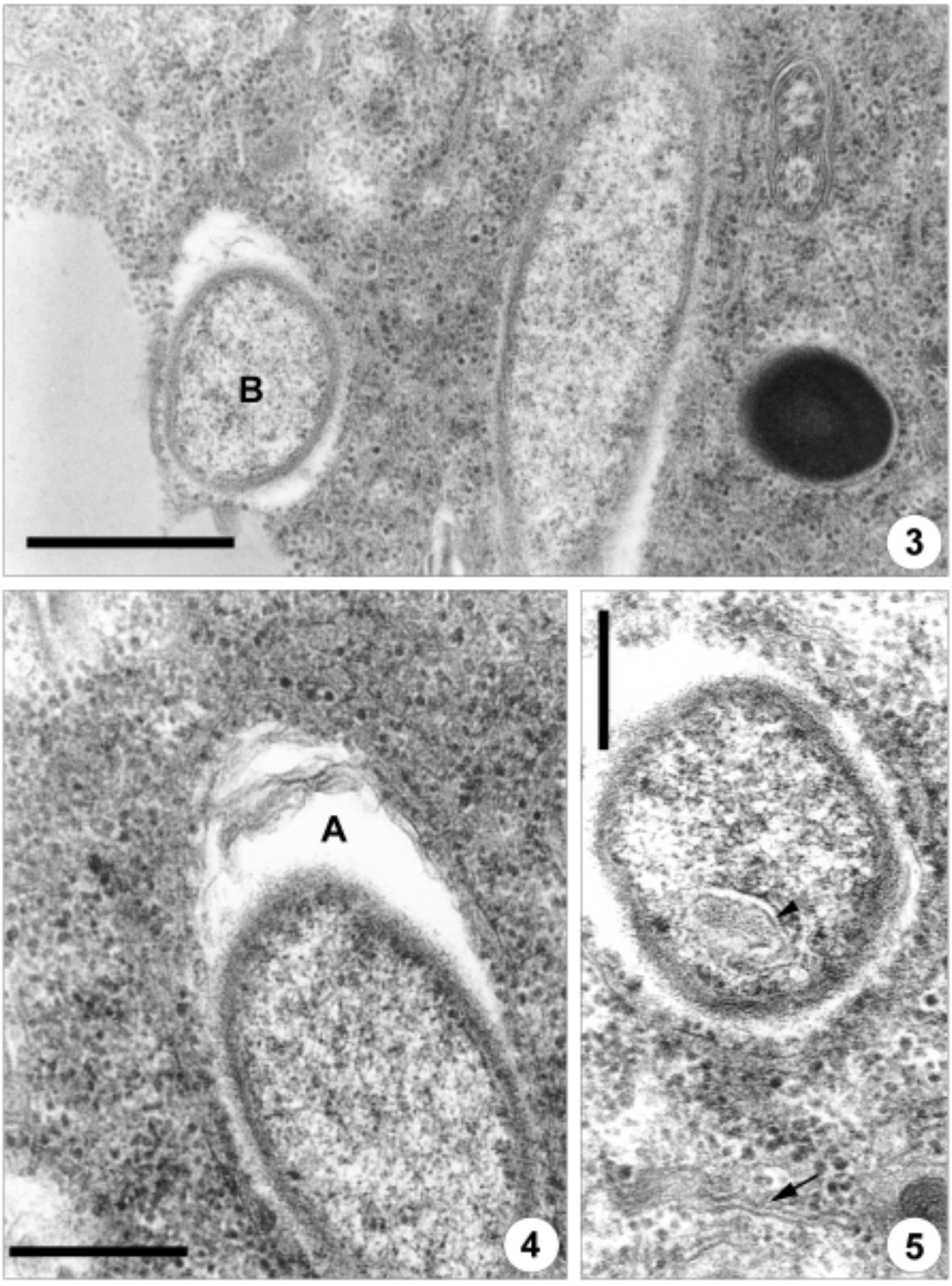

Figs 3-5. Electron micrographs of bacteria in the cytoplasm of *Conchophthirus acuminatus.* A - clear space separates the bacteria from host cytoplasmic structures; membranes surrounding some bacteria may be associated with individual endocytobiotic vacuoles. B - bacteria, arrowhead - region of bacterial cytoplasm with different density, large arrow - cisternae of endoplasmic reticulum. Scale bar 0.5 µm.

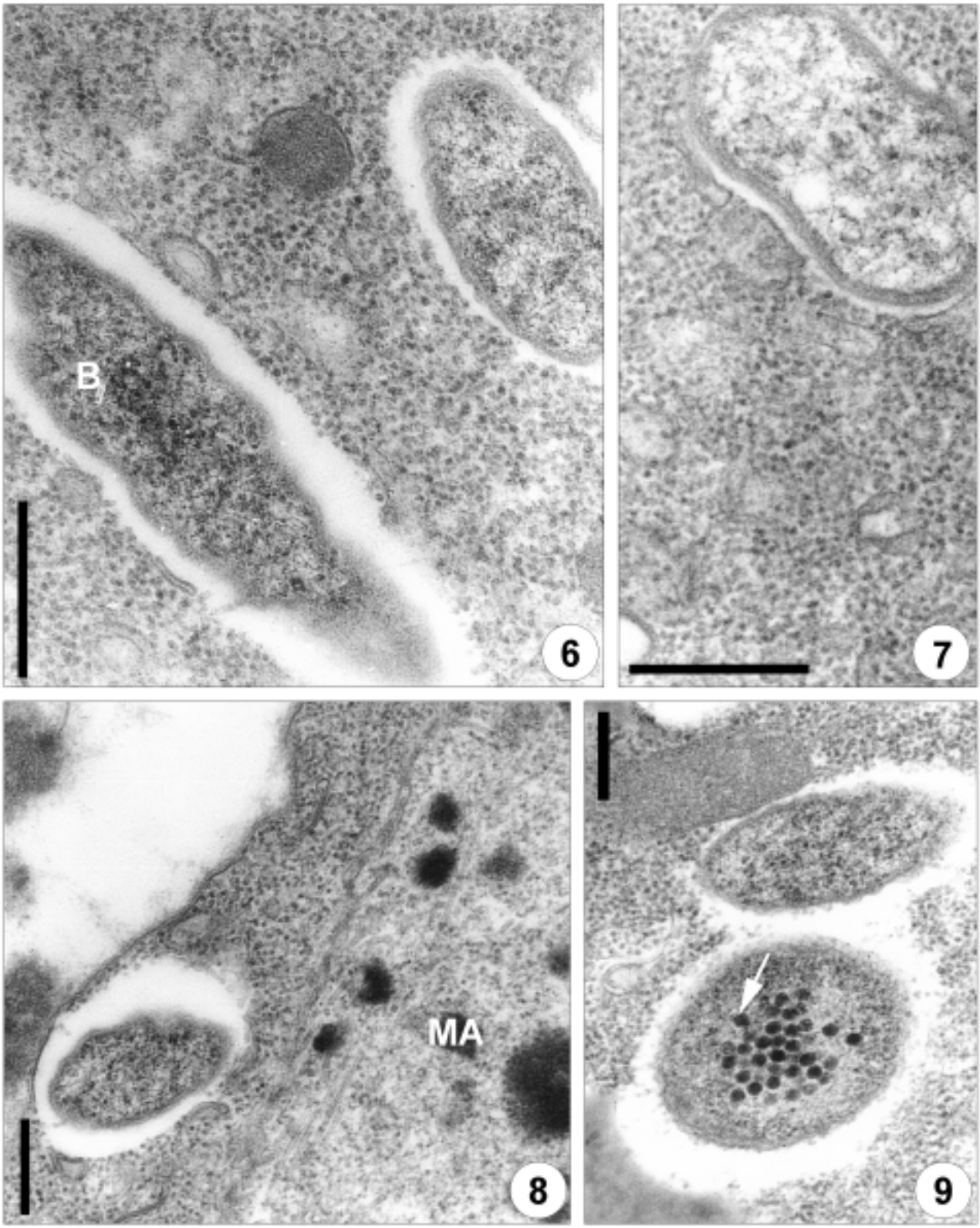

Figs 6-9. Electron micrographs of bacteria in the cytoplasm of *Ophryoglena* sp. **6, 8, 9** - no host membrane surrounding the bacteria was observed; instead, clear space separated the bacteria from host cytoplasmic structures. **7** - another type of bacterium was found, apparently, enclosed in an individual host vacuole; **9** - virus particles were observed in some of the bacteria in one of *Ophryoglena* population. B - bacteria, arrow - virus particles, MA - macronucleus. Scale bar 0. 5 µm.

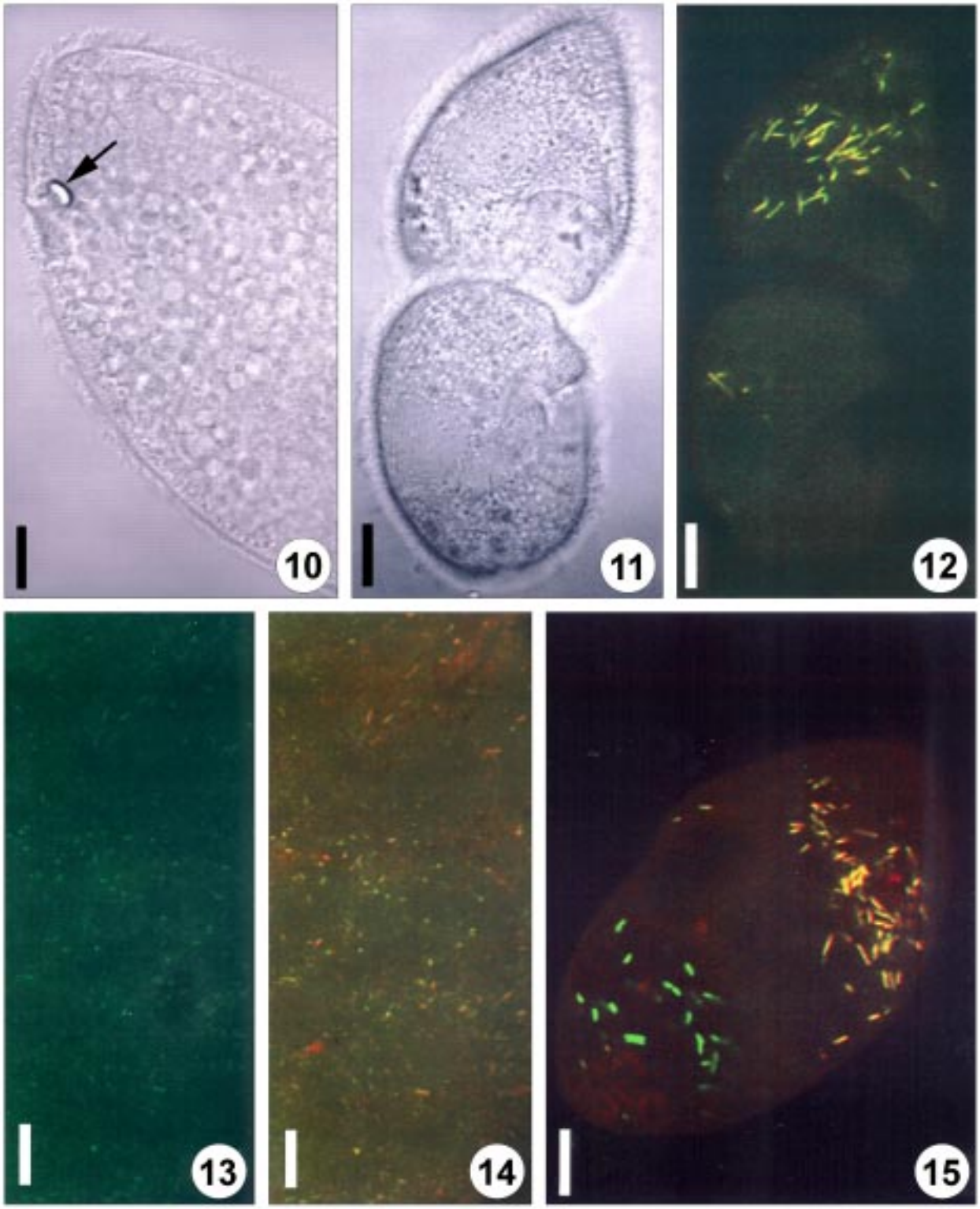

Figs 10-15. *In situ* hybridization. **10** - *Ophryoglena* sp. cell - the organelle of Lieberkühn (arrow). **11** - *Conchophthirus acuminatus* in division process; **12** - the same dividing cells labeled with eubacteria- and α-subgroup-specific probes. Bacteria in the cytoplasm (double labeling yellow). **13** - bacteria in the cytoplasm of *Ophryoglena* sp., the same cell as presented on fig.10. A labeling with eubacteria-specific probe (green); **14** - the same region with double labeling. Main bacteria are labeled as α-subgroup bacteria (orange) and some are labeled just as eubacteria (green). **15** - two different types of bacteria in the cytoplasm of *C. acuminatus*. Double labeling: populations of α-subgroup bacteria (orange) and some other eubacteria (green). The populations do not mix in the cytoplasm. Figs 10, 11 - DIC; Figs 12-15 - fluorescence microscopy. Scale bars 10 μm (10-12, 15); 6 μm (13, 14).

separate parts of the cell (Fig. 15). The α-subgroup was the most frequent type detected, and the *C. acuminatus* in some mussels appeared to have only this type (Fig. 12). Distribution of the bacteria during ciliate division appeared to be arbitrary (Figs 11, 12), with some progeny possibly receiving no bacteria. Experimental infection of aposymbiotic *C. acuminatus* with bacteria was not attempted.

Bacteria in the cytoplasm of *Ophryoglena* sp. (Figs 2, 10)

In living *Ophryoglena* it was impossible to detect any endocytobionts because of the opacity of the cytoplasm (Fig. 2), but bacteria were visible in squashed preparations of live specimens. *In situ* observations indicated that at least two types of bacteria (usually totaling more than 100 individuals) were present in each ciliate. Electron microscopy revealed that one type was rod-shaped, 1.5-2.0 x 0.3-0.5 μm. No host membrane was observed surrounding this type, but a clear space separated individual bacterial cells from host cytoplasmic structures (Figs 6, 8, 9). The second type of bacterium was short and rod-like, measured about 1.0 x 0.4 μm, and appeared enclosed in individual host vacuoles (Fig. 7). The two-membrane cell wall structure typical of Gram-negative bacteria was present in both types (Figs 6, 7). Both types of bacteria were generally located everywhere in the cytoplasm, sometimes even close to the nuclei (Fig. 8). The inner structure of the short bacteria was distinctive, differing from that of the larger rod-shaped type as well as the bacteria in *C. acuminatus* (Figs 3, 6, 7). In one population of *Ophryoglena* from the Netherlands, virus particles were observed in bacteria which morphologically resembled the larger rod-shaped type (Fig. 9).

Using the *in situ* hybridization procedure with two oligonucleotide probes, α-subgroup proteobacteria were identified in the cytoplasm of the *Ophryoglena* sp., along with a smaller number of other eubacteria (Figs 13, 14). From the size of the bacteria observed, it appeared that the large rod-shaped bacteria belonged to the α-subgroup and that the short ones were a mixture of both α-subgroup proteobacteria and other eubacteria (Figs 13, 14).

DISCUSSION

This is the first comprehensive investigation of bacteria present in the cytoplasm of endosymbiotic ciliates from mussels. Previous investigations of bacterial endocytobionts in ciliates have focused mostly on free-living host species. It is also the first detailed investigation of the cytoplasm of either *C. acuminatus* or the undescribed *Ophryoglena* sp.

Conchophthirus acuminatus

Conchophthirus acuminatus is an obligate commensal of the mantle cavity, and *Dreissena* spp. are its only known hosts (Molloy *et al.* 1997, Laruelle *et al.* 1999). Intensity of infection can be over several thousand ciliates per mussel (Burlakova *et al.* 1998, Karatayev *et al.* 2000), and the species is widely distributed in European *Dreissena* populations (Molloy *et al.* 1997).

Four from five *C. acuminatus* populations we sampled in this study were infected, but these bacteria are not present in a number European *C. acuminatus* populations (authors, unpublished data). However, we observed a high prevalence of bacterial infection in these four *C. acuminatus* populations, suggesting that where present, infection is usually of high intensity. The range in infection intensity recorded (i.e., 5 to 70 bacteria per host) was understandable since we observed that bacteria did not appear to be equally distributed between ciliate progeny during *C. acuminatus* division (Figs 11, 12).

Intracellular bacteria are known to be site specific, e.g., residing in the cytoplasm, in the micro- or macronuclei, or in the perinuclear space (Heckmann and Görtz 1991, Fokin 1993, Fokin and Karpov 1995). Some bacterial endocytobionts cannot live together in the same region of the host cell (Fokin 1993). Using *in situ* hybridization, we recorded two different types of bacteria in *C. acuminatus* and noted their presence in separate regions of the host cytoplasm (Fig. 15). In addition to a possible inhibitory (i.e., antibiotic) effect of one type of bacterium on another, we suggest that the lack of a uniform bacterial distribution might be due in part to a heterogeneous distribution of key host metabolites or nutrients. The ability of these bacteria to be cultivated outside of their host was not tested. Because of the relative ease of collection of infected *C. acuminatus*, this ciliate could be a very valuable organism for studying the dynamics of niche preferences among intracellular bacteria.

***Ophryoglena* sp.**

Although ophryoglenine ciliates have been extensively studied (Canella 1976, Puytorac *et al.* 1983, Lynn *et al.* 1991, Kuhlmann 1993), their endocytobionts have never been investigated. Moreover, the *Ophryoglena*

sp. from the zebra mussel digestive gland is only currently being described as a new species (authors, in preparation) and has received very limited research attention. Since this *Ophryoglena* sp. is parasitic, the role of its cytoplasmic bacteria may be more specialized than in free living ciliates. Evidence of this is that every *Ophryoglena* specimen examined in this study was infected by similar types of bacteria. A continual problem in investigating the majority of intracellular bacteria within ciliates has been the inability to cultivate them outside of their host. Preliminary tests indicate that this is true for the bacteria of *Ophryoglena* as well. This suggests that the majority of these bacteria found in ciliates likely are obligate symbionts.

Overview

Our observations of α-subgroup proteobacteria in two endosymbiotic ciliate species, in conjunction with reports of these bacteria from a number of free-living ciliate species (Görtz 1998, Brigge *et al.* 1999, Fokin *et al.* 2000, Fokin unpublished data), indicate that they are widely established endocytobionts in these protists.

This paper documents a multi-level microcosm system: *Dreissena*-ciliates-bacteria-viruses. The presence of different bacteria inside ciliate cells has been well documented (Heckmann and Görtz 1991, Fokin 1993, Brigge *et al.* 1999), but never as part of such a multilevel microcosm. Such a system could be a useful one for microbiological and ecological investigations. The cytoplasm is an initial environment for establishment of any endocytobiont, and thus, among the cytoplasmic bacteria both phylogenically old and young forms can be found. Thus, investigations of cytoplasmic bacteria or cytoplasmic stages of endonucleobionts could, therefore, potentially have significant impacts on theories of ecology and evolution of symbiotic microbes (Fokin *et al.* 2000).

The relationship between *Dreissena*'s endosymbiotic ciliates and their endocytobiotic bacteria had previously never been studied. It is likely that future investigations of ciliates from other *Dreissena* populations will reveal even a wider diversity of intracellular bacteria than reported herein.

Acknowledgements. We are grateful to our colleagues Prof. H.-D. Görtz, Dr. F. Brümmer and Dr. T. Brigge (Stuttgart University, Germany) for their help with sampling and confocal laser scanning microscopy. This research was funded in part by a grant from the National Science Foundation Division of International Programs (to Robert E. Baier and D. P. M.) and a travel grant from the Université de Metz (to D. P. M.) and a grant from the German Science Foundation DFG 436 RUS 17/75/95 (to H.-D. Görtz and S.I.F.).

REFERENCES

Amann R. I., Binder B. J., Oslon R. J., Chrisholm S. W., Devereux R., Stahl D. A. (1990) Combination of 16S rRNA-targeted oligonucleotide probes with flow cytometry for analyzing mixed microbial population. *Appl. Environ. Microbiol.* **56:** 1919-1925

Amann R. I., Springer N., Ludwig W., Görtz H.-D., Scheifer K.-H. (1991) Identification in situ and phylogeny of uncultured bacteria endosymbionts. *Nature* **351:** 161-164

Brigge T., Fokin S., Brümmer F., Görtz H.-D. (1999) Molecular probes for localization of endosymbiotic bacteria in ciliates and toxic dinoflagellates. *J. Euk. Microbiol.* **46:** 11a

Burlakova L. E., Karatayev A. Y., Molloy D. P. (1998) Field and laboratory studies of zebra mussel (*Dreissena polymorpha*) infection by the ciliate *Conchophthirus acuminatus* in the Republic of Belarus. *J. Invert. Pathol.* **71:** 251-257

Canella M. F. (1976) Biologie des Ophryoglenina (Ciliés hyménostomes histophages). *Ann. Univ. Ferrara,* Sect. III, **3 (Suppl. 2):** 1-510

Fokin S. I. (1989) Bacterial endobionts of the ciliate *Paramecium woodruffi*. III. Endobionts of the cytoplasm. *Cytologia* (St. Petersburg) **31:** 964-970 (in Russian with English summary)

Fokin S. I. (1993) Bacterial endobionts of ciliates and their employment in experimental protozoology. *Cytologia* (St. Petersburg) **35:** 59-91 (in Russian with English summary)

Fokin S. I., Karpov S. A. (1995) Bacterial endocytobionts inhabiting the perinuclear space of Protista. *Endocytobiosis Cell Res.* **11:** 81-94

Fokin S. I., Brigge T., Brenner J., Görtz H.-D. (1996) *Holospora* species infecting the nuclei of *Paramecium* appear to belong into two groups of bacteria. *Europ. J. Protistol.* **32 (Suppl. 1):** 19-24

Fokin S. I., Sabaneyeva E. V., Borkchsenius O. N., Scheikert M., Görtz H.-D. (2000) *Paramecium calkinsi* and *Paramecium putrinum* (Ciliophora, Protista) harboring alpha-subgroup bacteria in the cytoplasm. *Protoplasma* **213:** 176-183

Görtz H.-D. (1983) Endonuclear symbionts in ciliates. *Intern. Rev. Cytol.* **14 (Suppl.):** 145-176

Görtz H.-D. (1998) Aquatic symbionts and pathogens - ancient and new. In: Digging for Pathogens (Ed. C. L. Greenblatt) Balaban Publishers, Rehovot, Philadelphia, 97-122

Heckmann K., Görtz H.-D. (1991) Prokaryotic symbionts of ciliates. In: The Prokaryotes, (Eds. A. Balows, H. G. Truper, M. Dworkin, W. Harder, K.-H. Scheifer) 2 ed., Springer Verlag, Berlin & New York, 3865-3890

Karatayev A.Y., Molloy D. P., Burlakova L. E. (2000) Seasonal dynamics of *Conchophthirus acuminatus* (Ciliophora: Conchophthiridae) infection in *Dreissena polymorpha* and *D. bugensis* (Bivalvia: Dreissenidae). *Europ. J. Protistol.* **36:** 397-404

Kuhlmann H.-W. (1993) Life cycle dependent phototactic orientation in *Ophryoglena catenula. Europ. J. Protistol.* **29:** 344-352

Laruelle F., Molloy D. P., Fokin S. I., Ovcharenko M. A. (1999) Histological analysis of mantle-cavity ciliates in *Dreissena polymorpha*: Their location, symbiotic relationship, and distinguishing morphological characteristics. *J. Shellfish Res.* **18:** 251-257

Lynn D. H., Frombach S., Ewing M. S., Kocan K. M. (1991) The organelle of Lieberkühn as a synapomorphy for the Ophryoglenina (Ciliophora: Hymenostomatida). *Trans. Am. Microsc. Soc.* **110:** 1-11

Molloy D. P. (2002) International Research Consortium on Molluscan Symbionts: A Research Network Organized by the New York State Museum. Available from: http//www.nysm.nysed.gov/biology/ircoms/bio_ircoms.html

Molloy D. P., Karatayev A. Y., Burlakova L. E., Kurandina D. P., Laruelle F. (1997) Natural enemies of zebra mussels: predators, parasites, and ecological competitors. *Rev. Fish. Sci.* **5:** 27-97

Molloy D. P., Giamberini L., Morado J. F., Fokin S. I., Laruelle F. (2001) Characterization of intracytoplasmic prokaryote infections in *Dreissena* sp. (Bivalvia: Dreissenidae). *Dis. Aquat. Org.* **44:** 203-216

Puytorac de P., Perez-Paniagua F., Garcia-Rodriguez T., Detcheva R., Savoie A. (1983) Observations sur la stomatogenèse du cilié Oligohymenophora *Ophryoglena mucifera*, Mugard, 1948. *J. Protozool.* **30:** 234-247

Skovorodkin I. N. (1990) A device for immobilization of biological objects in the light microscope studies. *Cytologia* (St. Petersburg) **32:** 515-519 (in Russian with English summary)

Received on 22nd July, 2002; accepted on 23rd November, 2002

Acta Protozool. (2003) 42: 41 - 46

ACTA
PROTOZOOLOGICA

The Occurrence of *Trichodina domerguei* Wallengren, 1897 and *Trichodina tenuidens* Fauré-Fremiet, 1944 (Peritrichia) on Three-spined Stickleback, *Gasterosteus aculeatus* L., 1758 Found in a Brackish and Freshwater Environment

Ahmet ÖZER

Ondokuzmay s Üniversity, Sinop Fisheries Faculty, Sinop, Turkey

Summary. *Trichodina domerguei* Wallengren, 1897 and *Trichodina tenuidens* Fauré-Fremiet, 1944 infestations on three-spined stickleback (*Gasterosteus aculeatus* L., 1758) were studied in the period from January to May 2000 in the Black Sea coasts of Sinop, Turkey. The overall infestation prevalence and mean intensity level were 60.9% and 109.1 ± 21.5 trichodinids per fish, respectively. Statistically significant differences existed for the trichodinid species among sites on the fish, among length classes and between the sexes of fish hosts. While *T. tenuidens* itself represent a new parasite record, *Gasterosteus aculeatus* is a new host record for *T. domerguei* in Turkey. Many structures of the parasites were smaller in March, when the habitat was brackish, compared to May, when waters were fresh.

Key words: fish ectoparasite, *Gasterosteus aculeatus, Trichodina domerguei, T. tenuidens.*

INTRODUCTION

Trichodinids are a widely dispersed group of ectoparasites. Many species are morphologically variable and show low host specificity which make their determination difficult (Lom and Dykova 1992). Host specificity in trichodinids appears highly variable, some species (i.e. *Trichodina domerguei* Wallengren, 1897; *T. acuta* Lom, 1961 and *T. nigra* Lom, 1961) infesting a large number of host species, while others (i.e. *T. intermedia* Lom, 1961 and *T. tenuidens* Fauré-Fremiet, 1944) infest only one or two host species (Lom 1970 a, b). *Trichodina domerguei* and *T. tenuidens* are both commonly found parasitising three-spined (*Gasterosteus aculeatus* L., 1758) and nine-spined sticklebacks (*Pungitius pungitius* L., 1758). Along with the fact that many trichodinids have several hosts, the site of infestation of trichodinids on the host seems to be variable (Van As and Basson 1987). While *T. domerguei* primarily infects the skin and rarely the gills, for *T. tenuidens* it is the reverse with the gills being the principle site of infection (Lom and Stein 1966, Calenius 1980, Gaze 1995).

In this study, the existence of *T. domerguei* and *T. tenuidens* in relation to different length classes and

Address for correspondence: Ahmet Özer, Ondokuzmay s Üniversitesi, Sinop Su Ürünleri Fakültesi, 57000 Sinop, Turkey; Fax: (+90) 368 2715530; E-mail: ahmetozer100@hotmail.com

the sex of three-spined sticklebacks as well as environmental conditions are investigated. While *T. tenuidens* itself represents a new parasite record in Turkey, *Gasterosteus aculeatus* is a new host record for *T. domerguei* in Turkey. This study is also the first that both trichodinid species are observed in a brackish and freshwater environment.

MATERIALS AND METHODS

Specimens of *Gasterosteus aculeatus* were collected by gill net and cast net from S rak rka açlar stream which connects with the Black Sea on the coast of Sinop. S rak rka açlar stream is characteristically slightly brackish during the late autumn and early spring months (October to March) when the water level rises and connects with the Black Sea. In summer and early autumn, however, the water level drops, the connection is broken and the stream turns to freshwater.

Sampling was carried out on a monthly basis. Following the May collection however, as the water levels dropped fish became harder to collect as they moved upstream and into deeper waters. For parasitological examinations, fish were transported alive in local water directly to the Sinop Fisheries Faculty Laboratory. A total of 151 fish were investigated over the period January to May 2000. Sticklebacks were weighed, the total length measured and their sex determined at post-mortem. The total number of trichodinids were determined by screening all body surfaces including the fins and gills using a light microscope at x200 magnification. For species identification and determination of infestation site, following total counts, samples of *Trichodina* were taken from each fish specimen and dry smears were made in accordance with Klein's silver nitrate ($AgNO_3$) method (Lom and Dykova 1992).

The prevalence and mean intensity levels of the trichodinids were determined according to Bush *et al.* (1997). The prevalence and mean intensity values of *T. domerguei* and *T. tenuidens* were given for pooled data rather than by species.

Kruskal-Wallis test (Nonparametric ANOVA) was performed to find out the significant differences in the mean intensity values of trichodinids for infestation sites, length classes of fish as well as for the months in which this study was conducted. The difference between parasite loading on male and female sticklebacks as well as the differences in the morphometric dimensions measured in March and May were tested by the Mann-Whitney U-test. All the statistical tests performed at the significance level of 5% and were given in Table 1 along with the results of the possible comparisons.

RESULTS

Throughout the investigation period, *T. domerguei* and *T. tenuidens* were the only species identified (Figs 1A, B). Both trichodinid species were found to have slightly smaller dimensions in brackish water in March than those recorded in May when waters became fresh (Table 2). Some particular parts of the trichodinids also had statistically significant differences when compared between March and May (Table 2). The overall infestation prevalence (%) and mean intensity levels recorded from a total of 151 fish specimens were 60.9% and 109.1 ± 21.5 trichodinids per infested fish, respectively (Table 1). Both levels were also recorded for all body parts as well as for the sex and length classes of *Gasterosteus aculeatus* (Table 1). Statistically significant differences were determined in relation to the sex and length classes of fish and are shown in Table 1. However, it must be noted that no statistically significant differences were determined between the infestation values of each of the three length classes of fish in all months, thus the data were pooled and analysed for three length classes regardless of sampling months (Table 1).

Monthly occurrences of both species were recorded. No trichodinids were observed in January but, an increase in both the infestation prevalence and mean intensity levels were recorded throughout the investigation period as can be seen in Fig. 2. Statistically significant differences were determined in the mean intensity values of trichodinids in February and March versus May ($P<0.01$). In addition, proportions of 1/8 *T. domerguei /T. tenuidens* in February and 1/10 *T. domerguei/ T. tenuidens* in March and April and 1/1 *T. domerguei /T. tenuidens* in May were observed in stained slides of each month.

DISCUSSION

Trichodinids are geographically a widely dispersed group of ectoparasites in freshwater, marine and euryhaline environments. About 70 species were identified in marine fishes (Kinne 1984) and more than 112 from freshwater fishes worldwide (Lom and Dykova 1992). Some trichodinids including *T. domerguei* and *T. tenuidens* parasitising *Gasterosteus aculeatus* and *Pungitius pungitius* have been recorded in euryhaline waters (Lom and Stein 1966, Calenius 1980).

The morphological data of the species *T. domerguei* and *T. tenuidens* fall within the size ranges given by other authors (Lom and Stein 1966, Calenius 1980, Gaze 1995). The morphological variations of denticle form and appearance of central circle in *T. tenuidens* observed in this study are also in agreement with the statement of Lom and Stein (1966) that this species was found to be among the most variable of trichodinid species. During

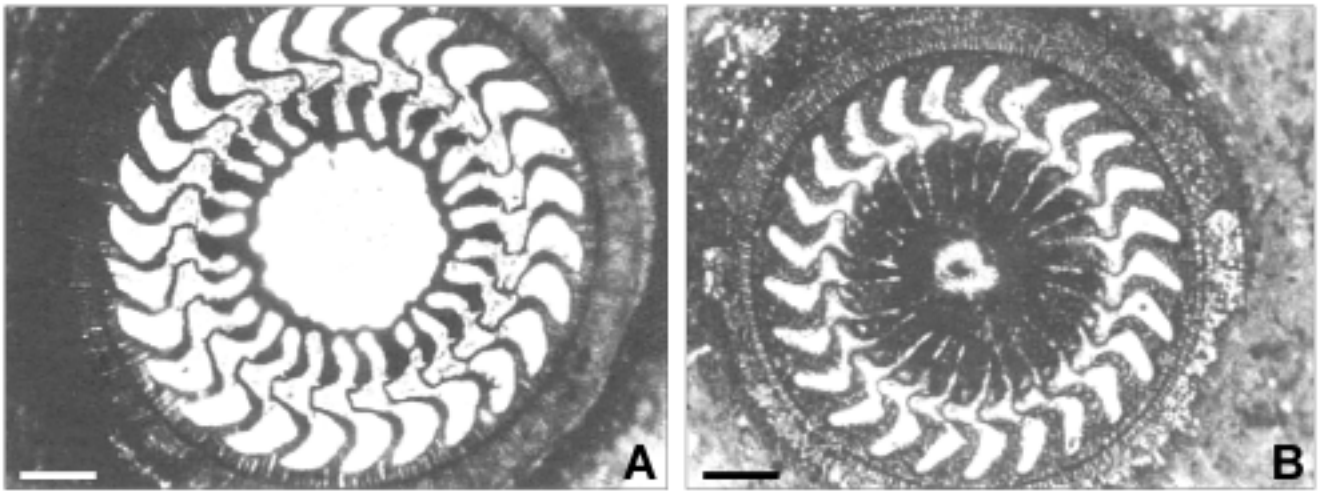

Figs 1A, B. A - *Trichodina domerguei* Wallengren, 1897; **B** - *Trichodina tenuidens* Fauré-Fremiet, 1944. Specimens stained by silver-nitrate. Scale bar 10 µm.

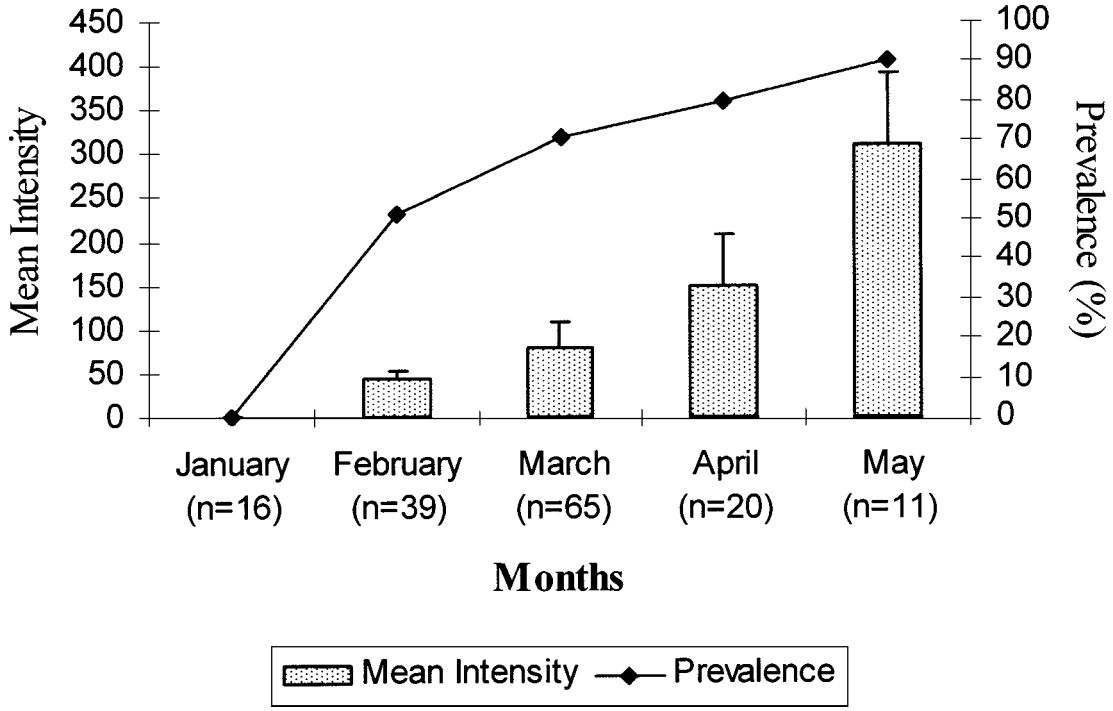

Fig. 2. Monthly infestation prevalence (%) and mean intensity levels of *Trichodina domerguei* and *T. tenuidens* on *Gasterosteus aculeatus*. n - represents the number of fish examined in each month.

Table 1. Infestation prevalence (%) and mean intensity levels of *Trichodina domerguei* and *T. tenuidens* on *Gasterosteus aculeatus* and the results of statistical tests performed.

	Infestation prevalence (%)	Mean intensity ± S.E	Possible comparisons	Statistial test used	Significance
Infestation site					
			(gills) *vs.* (skin) *vs.* (fins)	Kruskal-Wallis	P = 0.0001
Gills (n = 85)	60.9	87.9 ± 19.8			
			(gills) *vs.* (skin)	Dunn's	P < 0.001
Skin (n = 65)	56.3	32.9 ± 14.1			
			(gills) *vs.* (fins)	Dunn's	P < 0.001
Fins (n = 60)	43.1	7.4 ± 1.1			
			(skin) *vs.* (fins)	Dunn's	P > 0.05
Sex of fish					
Female (n = 116)	56.9	125.1 ± 28.9	(female) *vs.* (male)	Mann-Whitney U	P < 0.05
Male (n = 34)	70.6	65.9 ± 16.8			
Length classes of fish (mm)					
			(<60) *vs.* (61-69) *vs.* (70>)	Kruskal-Wallis	P = 0.0076
≤ 60 (n = 28)	35.7	11.1 ± 1.1			
			(<60) *vs.* (61-69)	Dunn's	P < 0.01
61 - 69 (n = 83)	72.4	122.3 ± 30.9			
			(<60) *vs.* (70>)	Dunn's	P < 0.05
70 ≥ (n = 40)	72.3	114.4 ± 27.8			
			(61 - 69) *vs.* (70>)	Dunn's	P > 0.05
Overall	60.9	109.1 ± 21.5			

Table 2. Biometric data of *Trichodina domerguei* and *T. tenuidens.*

	Trichodina domerguei (measured in March) (range; mean ± S.E)	*Trichodina domerguei* (measured in May) (range; mean ± S.E)	*Trichodina tenuidens* (measured in March) (range; mean ± S.E)	*Trichodina tenuidens* (measured in May) (range; mean ± S.E)
Host	*Gasterosteus aculeatus*	*Gasterosteus aculeatus*	*Gasterosteus aculeatus*	*Gasterosteus aculeatus*
Location	skin, fins, gills	skin, fins, gills	gills, skin	gills, skin
Adhesive disc diameter	48-56 (52 ± 0.53)	50-57.5 (53.5 ± 0.55)	40-57 (44.9 ± 1.3)	43-60 (47.5 ± 1.1)
Border membrane width	5-6.2 (5.4 ± 0.06)	5-6.3 (5.5 ± 0.07)	4.7-5.8 (5.4 ± 0.06)	4.9-5.9 (5.5 ± 0.06)
Denticle ring diameter	29-38.1 (33.8 ± 0.62)	30-38.6 (34.7 ± 0.53)	30.2-32 (31.0 ± 0.13)	30.9-32.4 (31.3 ± 0.16)
Denticle number	24-28 (26)	24-29 (26)	24-29 (25)	24-30 (25)
Number of radial pins per denticle	8-11 (9)	8-11 (9)	8-10 (9)	8-11 (9)
Denticle length	11-12.1 (12.5 ± 0.07)*	12-13.9 (13.3 ± 0.08)*	6.6-8.2 (7.1 ± 0.11)	6.6-8.5 (7.3 ± 0.15)
Blade length	5.0-6.1 (5.6 ± 0.06)	5.2-6.4 (5.8 ± 0.08)	4.8-6.6 (5.3 ± 0.11)	4.9 - 6.7 (5.5 ± 0.14)
Thorn length	4.4-5.4 (4.9 ± 0.07)*	4.9-5.8 (5.1 ± 0.05)*	5.6-7.4 (6.4 ± 0.17)	5.8-7.5 (6.5 ± 0.15)
Central part width	2-3 (2.2)	2-3 (2.3)	1.6-2.3 (1.7)	1.6-2.3 (1.8)
Central circle diameter	16.2-19.1 (18.1 ± 0.24)	16.8-19.5 (18.4 ± 0.19)	12-13 (12.5 ± 0.07)*	12-13.2 (12.8 ± 0.07)*

All measurements are in µm and based on 20 trichodinid specimens measured for each species. Mean values with superscript letter (*) represent statistically significant differences at P<0.05 when compared between March and May.

the months January, February and March when the stream mouth was in connection with the Black Sea, salinities of about 3, 4 and 3 ‰, respectively, were recorded and the dimensions of both trichodinid species were found to be slightly smaller in agreement with the findings of Lom (1970a) and Gaze (1995) who reported smaller specimen sizes in marine populations.

Host specificity in trichodinids seems to be highly variable, some species such as *T. domerguei*, *T. acuta* and *T. nigra* infest a large number of host species (Lom and Stein 1966, Lom 1970a, Calenius 1980) while *T. tenuidens* parasitises only one or two host species (Lom 1970b, Calenius 1980). It must be noted that several other fish species also inhabit the sampling site in this study, including *Aphanius chantrei* Gaillard, 1895, *Neogobius melanostomus* Pallas, 1811, *Mugil cephalus* L., 1758 and *Liza aurata* Risso, 1810, but *T. tenuidens* was not recorded on these fish species in contrast to *T. domerguei* which infected *N. melanostomus* as well. These findings on the host specificity of these trichodinid species also agree with the results of above mentioned authors.

The site of infection of trichodinids on host fish was categorised by Van As and Basson (1987) into four different groups based on site preference. Of the total number of trichodinid specimens, regardless of the actual species, counted throughout the study period, the infestation prevalence (%) and mean intensity levels were the highest on the gills as was shown in Table 1. *Trichodina tenuidens* was the dominant species and recorded mainly from the gills and rarely from the skin in accordance with Lom and Stein (1966), Calenius (1980) and Gaze (1995). On the other hand, most of the skin specimens were *T. domerguei* in this study. The above mentioned authors also reported this species to be skin specific and rarely found on the gills as well.

Seasonal and temperature dependant variations on the occurrence of trichodinids have been shown to occur (Özer and Erdem 1998, 1999). Spring was reported to be the mostly favoured season for trichodinid multiplication by the above mentioned authors and an increase was observed between the months February and May as in the present study. The obvious increase seen in both the infestation prevalence and mean intensity levels (Fig. 2) could be a result of the increase in temperature as the protozoan infestations in fish are strongly dependant on the ecological conditions such as temperature.

The number of studies on the existence of trichodinid parasites on both male and female fish is rare and almost no statistically significant difference in their existence is found (Özer 2000). However, the difference on the mean intensity levels of the trichodinids found on both sexes of fish in the present study is statistically significant. Pickering (1977), Pickering and Christie (1980) and Urawa (1992) attributed these differences to several factors such as rhythmical changes in epidermis thickness of male fish, a decrease in the number of AB-positive mucous cells and an increase in PAS-positive mucous cells.

The size of three-spined sticklebacks was a factor affecting the number of *T. domerguei* and *T. tenuidens* in this study and the differences in the parasite mean intensities among the different fish length classes were statistically significant. In general, the severity of most ecto- and endoparasitic infections increases with the age of the host fish, possibly as a result of the greater accumulation period and/or the larger space for feeding and breeding of the parasite. Özer and Erdem (1998) noted a tendency to increase in the mean intensity of *Trichodina* spp. in relation to the length of common carp. Our findings on the intensity levels of *T. domerguei* and *T. tenuidens* agree with those reported by the above mentioned authors.

Studies on the parasite fauna in farmed and wild fish in Turkey are quite rare. Özer and Erdem (1998, 1999) and Özer (2000) carried out extensive studies on the occurrence of trichodinids on common carp in the Sinop region of Turkey. This is the first study conducted on the trichodinids of three-spined sticklebacks found in a brackish environment in Turkey and *T. tenuidens* represents a new species record for Turkey.

Acknowledgements. The author is grateful to Dr. Jirí Lom, Czech Republic, and Dr. W.H. Gaze, U.K., for their kind help in the description of trichodinid species found in this study.

REFERENCES

Bush A. O., Lafferty K. D., Lotz J. M., Shostak A. W. (1997) Parasitology meets ecology on its own terms: Margolis *et al.* revisited. *J. Parasitol.* **83:** 575-583

Calenius G. (1980) Parasites of fish in Finland. III. Ciliates of the family *Urceolariidae* (Dujardin, 1851). *Acta Acad. Aboensis*, Ser. B **40:** 1-16

Gaze W. H. (1995) Studies on the biosystematics of trichodinid ciliates parasitic on British freshwater fish. Ph. D. Thesis.University of Stirling, Scotland

Kinne O. (1984) Diseases of Marine Animals. Biologische Anstalt Helgoland, Hamburg

Lom J. (1970a) Trichodinid ciliates (Peritrichia: Urceolariidae) from some marine fishes. *Folia Parasitol.* (Praha) **17:** 113-125

Lom J. (1970b) Observations on trichodinid ciliates from freshwater fishes, *Arch. Protistenkd.* **112:** 153-177

Lom J., Dykova I. (1992) Protozoan Parasites of Fish. Elsevier, Amsterdam

Lom J., Stein G. (1966) Trichodinids from sticklebacks and a remark on the taxonomic position of *Trichodina domerguei* (Wall). *Acta Societ. Zool. Bohem*. **30:** 30-40

Özer A. (2000) The occurrence of three species of *Trichodina* (Ciliophora: Peritrichia) on *Cyprinus carpio* in relation to culture conditions, seasonality and host characteristics. *Acta Protozool.* **39:** 61-66

Özer A., Erdem O. (1998) Ectoparasitic Protozoa fauna of the common carp (*Cyprinus carpio* L., 1758) caught in the Sinop region of Turkey. *J. Nat. Hist*. **32:** 441- 454

Özer A., Erdem O. (1999) The relationship between occurrence of ectoparasites, temperature and culture conditions; a comparison of farmed and wild common carp (*Cyprinus carpio* L., 1758) in the Sinop region of northern Turkey. *J. Nat. Hist*. **33:** 483-491

Pickering A. D. (1977) Seasonal changes in the epidermis of the brown trout, *Salmo trutta* (L.). *J. Fish Biol*. **10:** 561-565

Pickering A. D., Christie P. (1980) Sexual differences in the incidence and severity of ectoparasitic infestation of the brown trout, *Salmo trutta* L. *J. Fish Biol*. **16:** 669-683

Urawa S. (1992) *Trichodina truttae* Mueller, 1937 (Ciliophora:Peritrichida) on juvenile chum salmon (*Onchorhynchus keta*): Pathogenicity and host-parasite interactions. *Gyobyo Kenkyu* **27:** 29-37

Van As J. G., Basson L. (1987) Host specificity of trichodinid ectoparasites of freshwater fish. *Parasitol. Today* **3:** 88-90

Received on 28th August, 2002; accepted on 27th November, 2002

Acta Protozool. (2003) 42: 47 - 54

ACTA
PROTOZOOLOGICA

Cultellothrix velhoi gen. n., sp. n., a new Spathidiid Ciliate (Ciliophora: Haptorida) from a Brazilian Floodplain Soil

Wilhelm FOISSNER

Universität Salzburg, Institut für Zoologie, Salzburg, Austria

Summary. *Cultellothrix velhoi* sp. n. was discovered in floodplain soil from the Paraná River near the town of Maringá, Brazil, South America. Its morphology was investigated using live observation and protargol impregnation. *Cultellothrix* belongs to the gymnostomatous ciliate family Spathidiidae, where it represents a new genus characterized by the lateral location of the dorsal brush. *Cultellothrix velhoi* sp. n. differs from the European congener, *C. lionotiformis* (Kahl, 1930a) comb. n. (basionym: *Spathidium lionotiforme* Kahl, 1930a), by the smaller body size, the possession of a postoral extrusome row, and the lack of ordinary somatic ciliary rows between the circumoral and brush kineties. It is argued that the redescription of *S. lionotiforme* Kahl, 1930a by Foissner (1984) is based on an unfortunate misidentification. Foissner's species is *Spathidium scalpriforme* Kahl, 1930a, which is assigned to the genus *Arcuospathidium* and lowered to subspecies rank: *Arcuospathidium cultriforme scalpriforme* (Kahl, 1930a) comb. n., stat. n.

Key words: *Arcuospathidium cultriforme scalpriforme* comb. n., stat. n., *Cultellothrix lionotiformis* comb. n., *Cultellothrix velhoi* gen. n., sp. n., litostomateous ciliates, South America, *Spathidium lionotiforme*, terrestrial Protozoa.

INTRODUCTION

Spathidium is one of the largest ciliate genera known. Kahl (1930b) already compiled nearly 100 species, and about the same number has been described later (Foissner, unpubl.). Unfortunately, many descriptions lack sufficient details, leaving doubt about the validity of the species. However, recent studies confirm that there are many distinct *Spathidium* species and even indicate a high number of still undescribed taxa (Dragesco and Dragesco-Kernéis 1979; Foissner 1984, 1996, 1999, 2000; Leitner and Foissner 1997; Foissner *et al.* 2002).

Dragesco and Dragesco-Kernéis (1979) and Foissner (1984) split *Spathidium* into the genera *Spathidium* (continuous circumoral kinety with somatic kineties still attached to circumoral kinety fragments; oral bulge elongate elliptical), *Protospathidium* (with circumoral kinety fragments distinctly separated from each other and attached to somatic kineties), *Arcuospathidium* (somatic ciliary rows directed dorsally at both sides of oral bulge and separated from continuous circumoral kinety; oral bulge cuneate), *Epispathidium* (somatic

Address for correspondence: Wilhelm Foissner, Universität Salzburg, Institut für Zoologie, Hellbrunnerstrasse 34, A-5020 Salzburg, Austria; Fax. ++43 (0) 662 8044 5698

ciliary rows separated from continuous circumoral kinety and so strongly curved anteriorly that the circumoral kinety is seemingly doubled), and *Supraspathidium* (with many contractile vacuoles; poor generic feature). Recently, Foissner *et al*. (2002) added three further genera, all based on new species discovered in Namibian soils: *Apospathidium* (with nematodesmata-bearing somatic monokinetids), *Semispathidium* (with discoidal oral bulge and continuous circumoral kinety), and *Apertospathula* (circumoral kinety shortened at left end). Here, I add a further new genus, *Cultellothrix*, based on a new species discovered in floodplain soil from Brazil.

MATERIALS AND METHODS

The soil sample, which contained *Cultellothrix velhoi* sp. n., was collected in May 2001 by Dr. L. Felipe Machado Velho in the high Paraná River floodplain near the town of Maringá (53°15'W 22°40'S, altitude about 500 m), State of Mato Grosso do Sul, Brazil. It was taken from the Aurelio Lagoon, that is, a marginal lagoon associated with the Baia River, a tributary to the Paraná River. The dark, humic soil was mixed with much partially decomposed plant litter, had pH 5.1 (in water), was air-dried in the Salzburg laboratory for about one month, and then stored in a plastic bag. In November 2001, the about 300 g soil were put in a Petri dish (13 cm ø) and saturated, but not flooded with distilled water to obtain a "non-flooded Petri dish culture", as described in Foissner *et al*. (2002). About two weeks after rewetting, a small population of *C. velhoi* developed and was studied *in vivo* and with Foissner's protargol protocol (Foissner 1991).

Counts and measurements on prepared specimens were performed at a magnification of x 1000. *In vivo* measurements were conducted at magnifications of x 100-1000. Although these provide only rough estimates, it is worth giving such data as specimens may change in preparations. Illustrations of live specimens were based on *in vivo* measurements and free-hand sketches, while those of prepared cells were made with a camera lucida. Terminology is according to Kahl (1930a, b) and Corliss (1979).

RESULTS

Cultellothrix gen. n.

Diagnosis: Spathidiidae with dorsal brush on left side and ciliature in *Arcuospathidium* pattern.

Table 1. Morphometric data on *Cultellothrix velhoi* sp. n.

Characteristics[a]	x	M	SD	SE	CV	Min	Max	n
Body, length	105.7	103.0	18.1	4.4	17.1	77.0	140.0	17
Body, width	29.2	25.0	9.7	2.4	33.4	21.0	50.0	17
Anterior body end to end of circumoral kinety (mouth length), distance	53.8	55.0	10.4	2.5	19.3	38.0	75.0	17
Mouth, width in anterior third	3.8	4.0	0.6	0.2	16.6	3.0	5.0	10
Anterior body end to macronucleus, distance	56.3	58.0	12.1	2.9	21.5	41.0	80.0	17
Dorsal brush row 1, length[b]	32.2	32.0	7.6	1.9	23.7	20.0	43.0	17
Dorsal brush row 1, number of dikinetids	29.0	28.0	7.3	1.8	25.1	18.0	40.0	17
Dorsal brush row 2, length[b]	32.7	35.0	8.0	2.0	24.6	20.0	47.0	17
Dorsal brush row 2, number of dikinetids	23.2	24.0	4.4	1.1	18.8	16.0	29.0	17
Dorsal brush row 3, length[b]	9.2	10.0	1.5	0.4	16.0	7.0	12.0	17
Dorsal brush row 3, number of dikinetids	7.1	7.0	1.3	0.3	19.1	5.0	10.0	17
Macronuclear figure, length	26.9	22.0	10.7	2.6	39.7	17.0	56.0	17
Macronucleus, length (spread)[c]	40.7	40.0	-	-	-	25.0	56.0	17
Macronucleus, width	5.8	6.0	1.2	0.3	20.8	4.0	9.0	17
Macronucleus, number	1.0	1.0	0.0	0.0	0.0	1.0	1.0	17
Micronucleus, length	2.9	3.0	0.4	0.1	14.6	2.2	4.0	17
Micronucleus, width	2.6	2.5	0.5	0.1	20.8	2.0	4.0	17
Micronucleus, number	1.0	1.0	0.0	0.0	0.0	1.0	1.0	17
Somatic kineties, postoral number[d]	11.7	12.0	1.1	0.3	9.4	10.0	14.0	17
Kinetids in a right side kinety, number	27.2	28.0	5.0	1.2	18.5	18.0	35.0	17
Dorsal brush rows, number	3.0	3.0	0.0	0.0	0.0	3.0	3.0	17

[a] Data based on mounted, protargol-impregnated (Foissner's method), selected (cells with large rotifers ingested strongly inflated and thus excluded) specimens from a non-flooded Petri dish culture. [b] Distance from circumoral kinety to last brush dikinetid. [c] Approximate values. [d] Including dorsal brush rows. Measurements in µm. CV - coefficient of variation in %, M - median, Max - maximum, Min - minimum, n - number of individuals investigated, SD - standard deviation, SE - standard error of arithmetic mean, x - arithmetic mean.

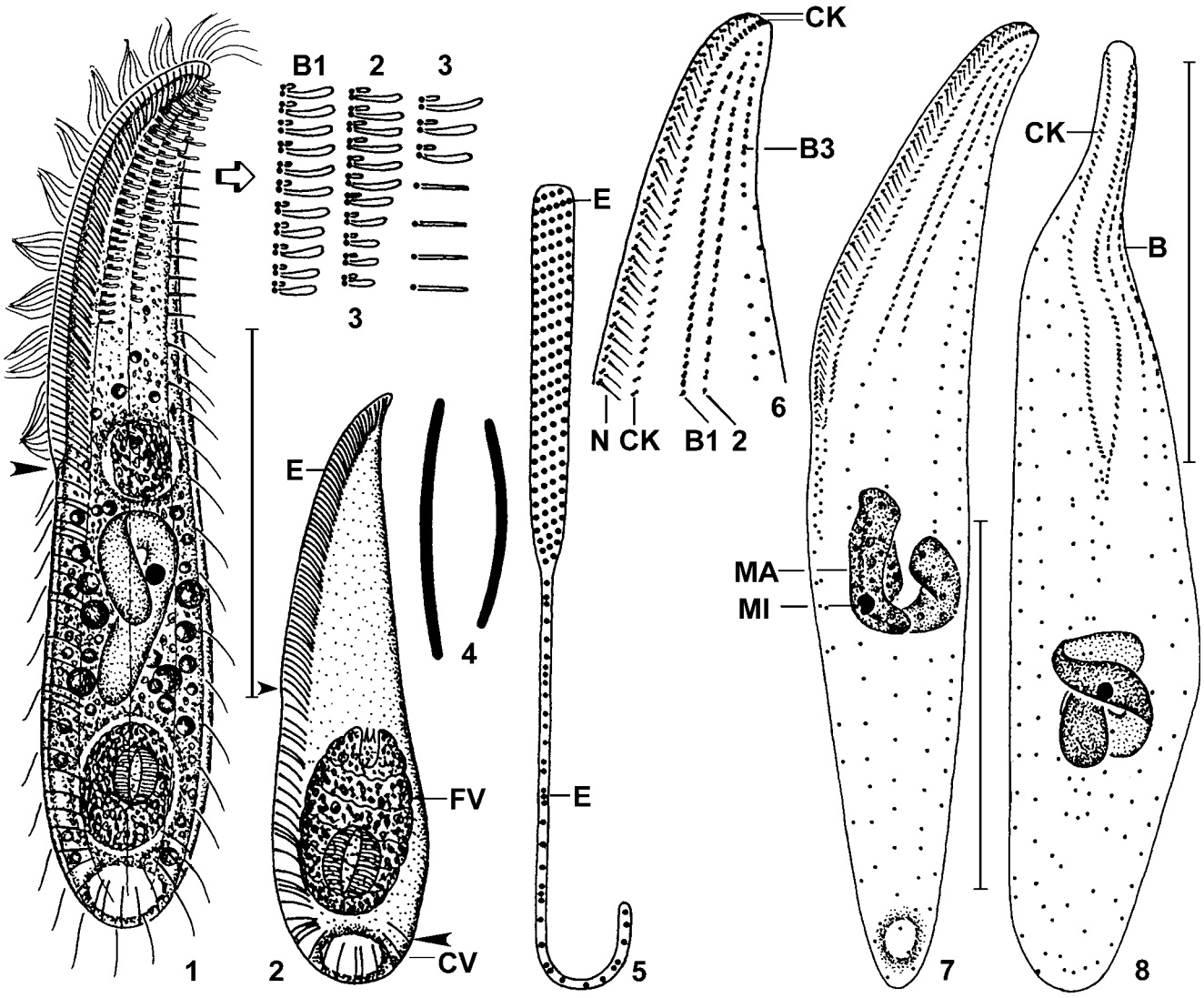

Figs 1-8. *Cultellothrix velhoi* sp. n. from life (1-5) and after protargol impregnation (6-8). **1 -** left side view of a representative, knife-shaped specimen with dorsal brush occupying anterior left side of cell. The oral apparatus extends to mid-body (arrowhead); **2 -** left side view of a broadly knife-shaped specimen having just ingested a rotifer (FV). Note the postoral extrusome row (arrowheads), which extends onto the dorsal side of the cell and is difficult to recognize *in vivo* because the individual extrusomes are fine and often hidden by cell inclusions (Fig. 1); **3 -** posterior portion of dorsal brush with bristles up to 5 µm long. Note monokinetidal bristle tail of row 3; **4 -** extrusomes are curved rods with a size of about 6-7 x 0.3 µm; **5 -** arrangement of extrusomes, which form short, oblique rows in the oral bulge and a single, postoral row extending to dorsal side of cell; **6, 7 -** ciliary pattern of left side. Note lack of an ordinary somatic ciliary row between circumoral kinety and dorsal brush, a main difference to *C. lionotiformis*, which has at least two such rows (Figs 12a, b). Dorsal brush rows 1 and 2 are distinctly more narrowly spaced than the other ciliary rows; **8 -** ventral view showing the parallel-sided circumoral kinety with cuneate proximal portion. B - dorsal brush; B1, 2, 3 - dorsal brush rows; CK - circumoral kinety; CV - contractile vacuole; E - extrusomes; FV - food vacuole with a rotifer; MA - macronucleus; MI - micronucleus; N - nematodesmata (oral basket rods). Scale bars 50 µm.

Type species: *Cultellothrix velhoi* sp. n.

Etymology: composite of the Latin noun *cultellus* (small knife) and the Greek noun *thrix* (hair ~ cilium ~ ciliate), referring to the conspicuous knife-shape of the two species known. Feminine gender.

***Cultellothrix velhoi* sp. n.**

Diagnosis: size about 120 x 25 µm *in vivo*. Knife-shaped with blade (oral portion) approximately half of body length. Macronucleus about 40 µm long, usually

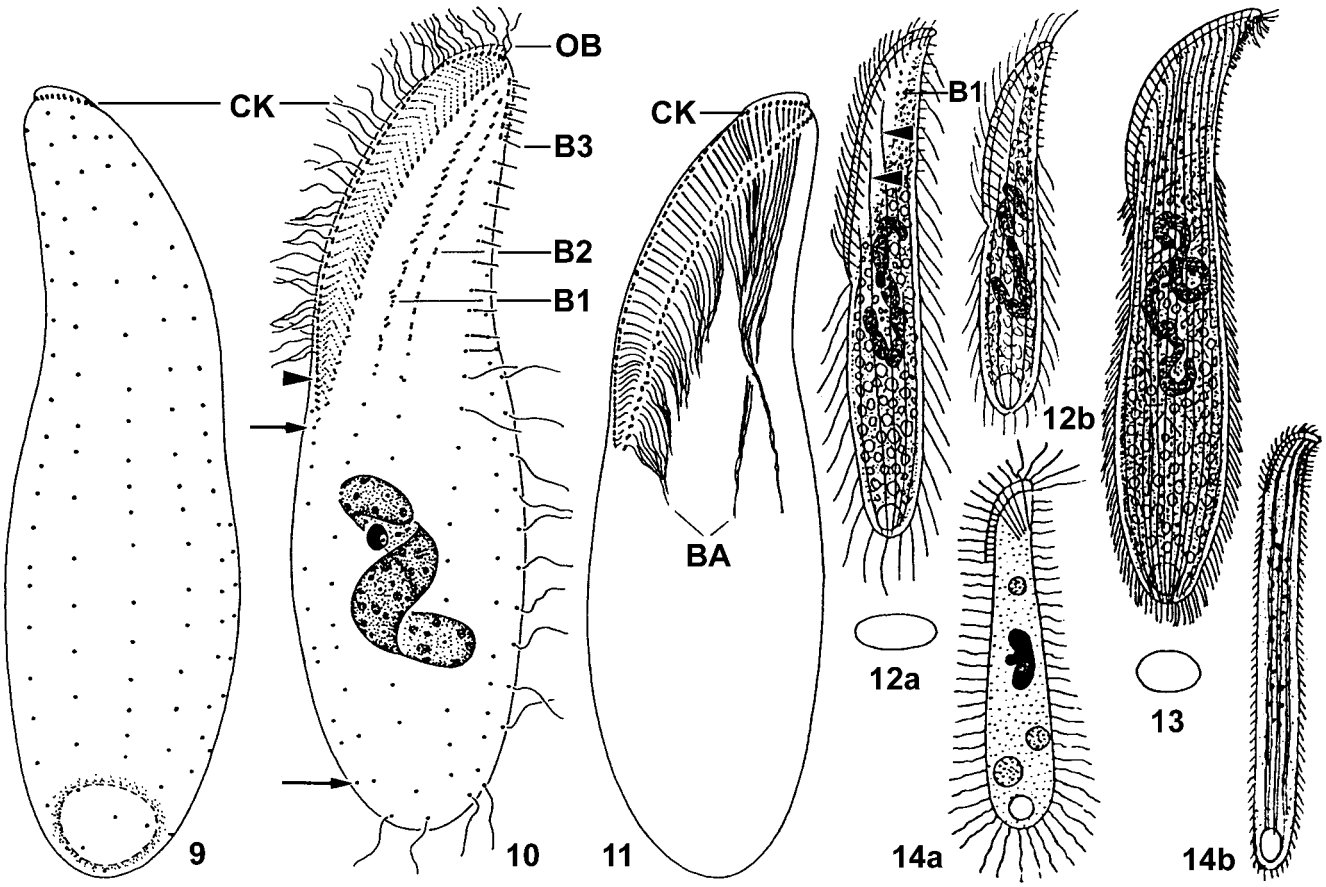

Figs 9-14. *Cultellothrix velhoi* sp. n. (9-11) and related species (12-14). **9-11 -** right and left side ciliary pattern (9, 10), nuclear apparatus (10), and oral basket (11) of a small (length 77 µm), stout specimen of *C. velhoi* after protargol impregnation. Note lack of cilia in proximal portion of circumoral kinety (arrowhead) and postoral basal body row (arrows). Dorsal brush row 3 (B3) has a monokinetidal bristle tail. The oral bulge (OB) is cuneate, hardly set off from body proper, and contains fibres originating from the circumoral dikinetids. Oral basket rods (nematodesmata) likely originate only from the right half of the circumoral kinety. Note lack of ordinary somatic ciliary rows between circumoral kinety and dorsal brush, a main difference to *C. lionotiformis*, which has at least two such rows (Figs 12a, b); **12a, b -** left side view and postoral transverse section of *Spathidium* (now *Cultellothrix*) *lionotiforme* from life, length 140-220 µm (from Kahl 1930a, b). Arrowheads mark two ordinary somatic ciliary rows, lacking in *C. velhoi* (Figs 7, 8, 10), between circumoral kinety and brush row 1 (B1); **13 -** left side view and postoral transverse section of *Spathidium* (now *Arcuospathidium*) *scalpriforme* from life, length 250-330 µm (from Kahl 1930a). Foissner (1984) misidentified this species as *Spathidium* (now *Cultellothrix*) *lionotiforme*; **14a -** left side view of *Cranotheridium stilleri* from life, length 80 µm (from Lepsi 1959); **14b -** left side view of *Litonotus dubius* from life, length 160 µm (from Vuxanovici 1962). B1, 2, 3 - dorsal brush rows; BA - oral basket; CK - circumoral kinety; OB - oral bulge.

tortuous. Extrusomes approximately 6 x 0.3 µm, form short, oblique rows in oral bulge and a long postoral row extending to dorsal side of cell. On average 12 ciliary rows, those left of circumoral kinety anteriorly modified to dorsal brush; brush row 3 distinctly shortened consisting of an average of 7 dikinetids.

Type location: floodplain soil of Paraná River in Brazil, near the town of Maringá, 53°15'W 22°40'S.

Dedication: dedicated to Dr. Luiz Felipe Machado Velho, Universidade Estadual de Maringá, Brazil, who provided the sample containing this and other new species.

Description: size 80-150 x 20-40 µm *in vivo*, laterally flattened up to 2:1, fragile and thus frequently more or less inflated in protargol preparations (Table 1). Slenderly to broadly knife-shaped with blade (oral portion), however, often indistinctly separated from cylindroidal handle; dorsal outline more or less distinctly sigmoidal, ventral slightly convex; anterior end bluntly pointed, posterior more or less broadly rounded (Figs 1, 2, 7, 9, 15). Nuclear apparatus slightly underneath midbody in postoral portion of cell. Macronucleus about 40 µm long, basically rod-shaped, usually, however, more or less tortuous and coiled; contains many small and

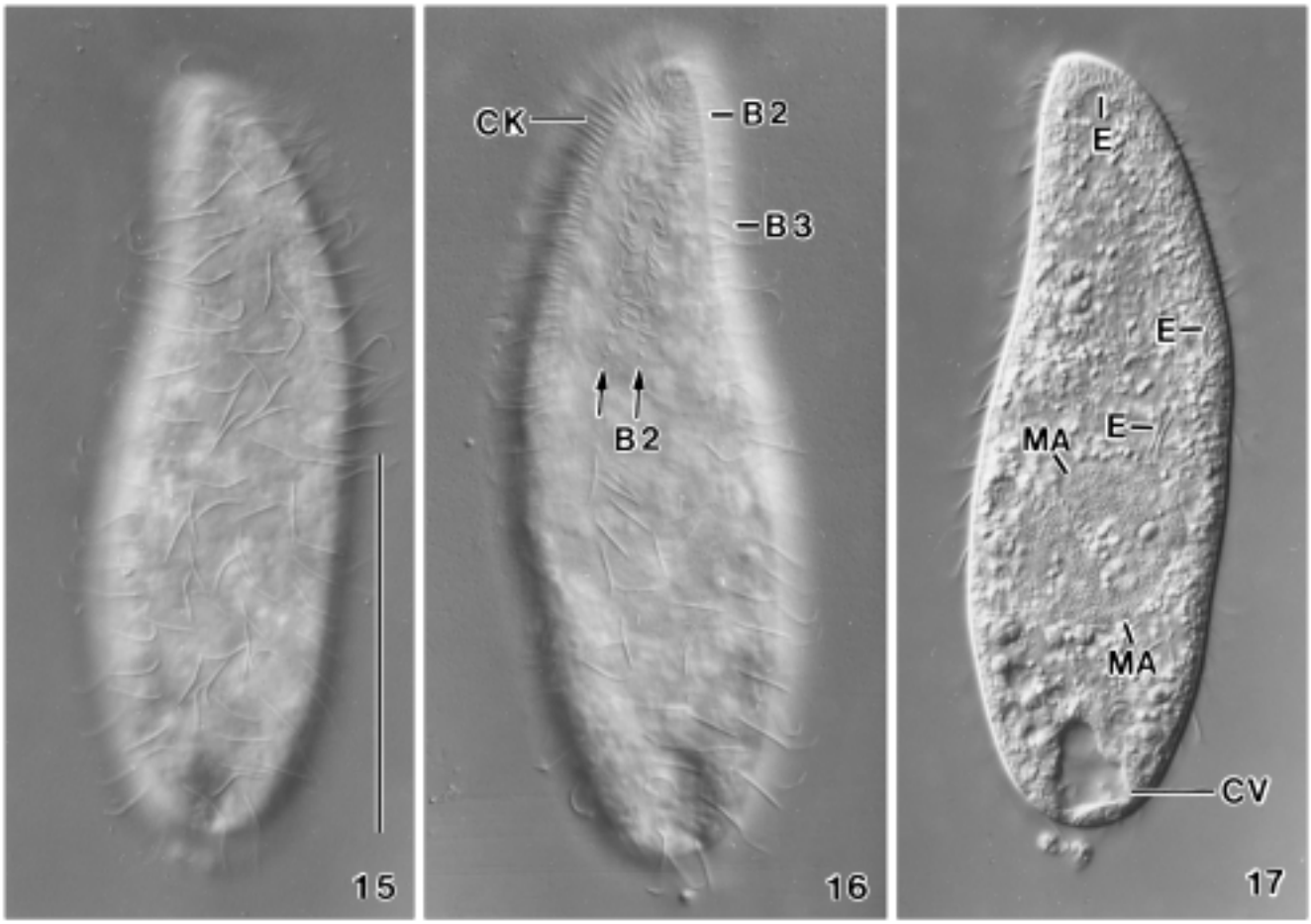

Figs 15-17. *Cultellothrix velhoi* sp. n., right side (15) and left side (16) surface view, and optical section (17) of a slightly squeezed and flattened (by cover glass pressure), live specimen under interference contrast optics. Note the loose ciliation and the dorsal brush rows (arrows) on the left side of the cell; row 3 (B3) is short, but has a monokinetidal bristle tail. The extrusomes are fine and thus inconspicuous in cells viewed laterally (17); the postoral extrusome row is out of focus. B2, 3 - dorsal brush rows; CK - circumoral kinety; CV - contractile vacuole; E - extrusomes; MA - macronucleus. Scale bar 50 µm.

medium-sized nucleoli. Micronucleus attached to middle third of macronucleus, broadly ellipsoidal, 3-4 µm *in vivo*. Contractile vacuole in posterior body end; excretory pore(s) not impregnated. Cortex thin, bright and very flexible; cortical granules and/or extrusomes not recognizable, not even with interference contrast optics. Extrusomes 6-7 x 0.3 µm and slightly curved *in vivo*, do not impregnate with the protargol method used, form many short, oblique rows in oral bulge and a single postoral row extending across posterior body end to dorsal side of cell; some scattered in cytoplasm (Figs 1, 2, 4, 5, 17-19, 21, 22). Oral area flat and hyaline, postoral portion, depending on state of nutrition, also flattened and hyaline or packed with lipid droplets 1-5 µm across and some large food vacuoles containing rotifers in various stages of digestion. Slowly glides on and between soil particles and the microscope slide showing great flexibility.

Somatic cilia 7-8 µm long *in vivo*, widely spaced, arranged in an average of 12 meridional rows commencing at and near curved anterior end of body and thus more or less distinctly curved dorsally at both sides of circumoral kinety (oral bulge), as in *Arcuospathidium* (Foissner 1984), except of a single or two, rather irregular postoral rows, which, interestingly, lack cilia; all kineties equidistantly spaced, except of more narrowly arranged postoral and dorsal brush rows 1 and 2 (Figs 1, 7, 9, 10, 15, 16; Table 1). Dorsal brush occupies left surface of anterior body third, produced by paired bristles at anterior end of first three ciliary rows left of circu-

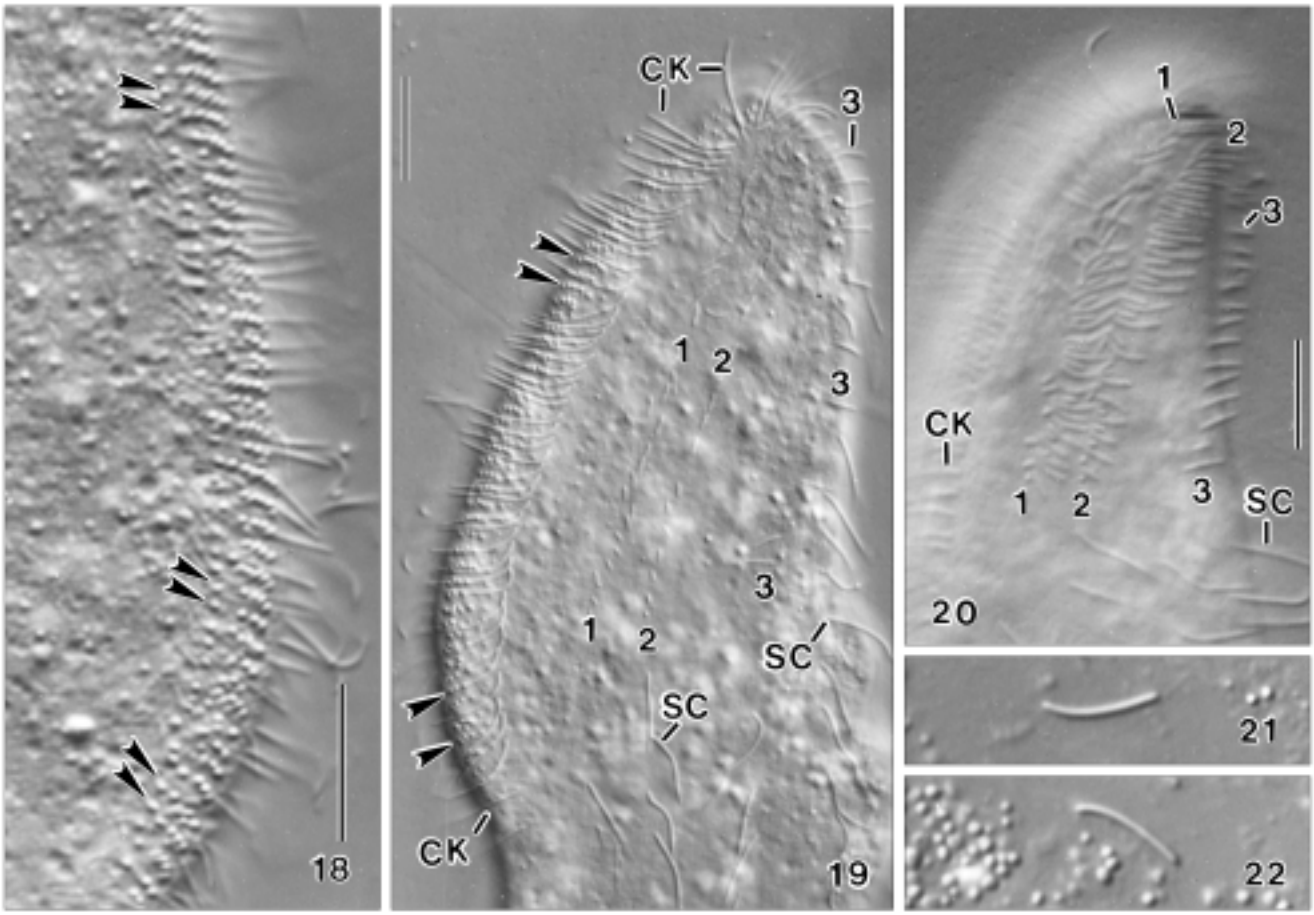

Figs 18-22. *Cultellothrix velhoi* sp. n. from life, interference contrast optics. **18 -** a heavily flattened (by cover glass pressure) specimen showing the oblique extrusome rows, some marked by arrowheads, in the oral bulge; **19 -** same specimen as depicted in figure 18, showing the up to 3 µm long dorsal bristles forming three rows (numbers 1-3) in the anterior portion of the cell's left side; brush row 3 mainly consists of 3 µm long, monokinetidal bristles. Arrowheads mark oblique extrusome rows in oral bulge, shown at higher magnification in figure 18. The cilia of the circumoral kinety (CK) are slightly longer (10 µm) than the ordinary somatic cilia (7 µm; SC); **20 -** left anterior portion of a specimen with about 5 µm long dorsal bristles, which are arranged in three rows (numbers 1-3); the posterior portion of row 3 consists of monokinetidal, 4 µm long bristles; **21, 22 -** extrusomes, length 6-7 µm. CK - circumoral kinety; SC - somatic cilia. Scale bars 10 µm.

moral kinety; posterior bristle of dikinetids 3-5 µm long and slightly inflated distally, anterior granule-like because only 1-2 µm long; bristle length gradually decreases in posterior third of rows 1 and 2 and is rather variable in individual cells; one or few monokinetids may occur at anterior end of one or all brush rows. Brush row 1 composed of an average of 29 narrowly spaced dikinetids, of similar length as row 2 consisting of only 23 dikinetids; row 3 extends along dorsal margin of cell, strongly shortened posteriorly, composed of only 7 dikinetids on average, has , however, a monokinetidal tail of 3-4 µm long bristles extending to second body third (Figs 1, 3, 6-8, 10, 16, 19, 20; Table 1).

Oral area more or less distinctly curved dorsally, bulge thus convex; hyaline because flattened about 2:1 and containing only few, small lipid droplets. Mouth occupies anterior body half on average, very steep because extending parallel to main body axis, conspicuous due to the oblique rows of refractive extrusomes contained. Oral bulge inconspicuous because less than 3 µm high and thus hardly set off from body proper, contains short, anteriorly directed fibres, originating from circumoral dikinetids, forming arrowhead-like pattern; in frontal view elongate cuneate to almost parallel-sided with proximal portion wedge-like narrowed, about 5 µm wide *in vivo*. Circumoral kinety of same shape as oral bulge, composed of comparatively widely spaced dikinetids each associated with a slightly elongated, about 10 µm long cilium lacking in proximal, wedge-shaped portion of kinety. Nematodesmata originate only from right side dikinetids of circumoral kinety, gradually decrease in length from anterior to posterior, the long

anterior rods form bundles extending to mid-body; I could not decide whether the left side basket rods are lacking or present, but not impregnated (Figs 1, 2, 6-11, 15-17, 18, 19; Table 1).

Occurrence and ecology: *Cultellothrix velhoi* sp. n. is a rare species because I did not find it in about 1000 other soil and moss samples, including approximately 100 samples from similar habitats, collected world-wide. Although looking fragile, *C. velhoi* is a rapacious predator feeding mainly on large rotifers, showing that the oral apparatus can open widely and the body is very flexible. The second species, *C. lionotiformis*, is obviously also rare because it has not yet been redescribed (see Discussion).

DISCUSSION

Spathidiid classification and the new genus *Cultellothrix*

Cultellothrix belongs to the gymnostomatous haptorids, as defined by Corliss (1979) and Foissner and Foissner (1988). Both live and protargol-impregnated specimens of *Cultellothrix* highly resemble pleurostomatid ciliates, such as *Litonotus* and *Amphileptus*, many of which have a similar body shape and basic ciliary pattern (Figs 1, 2, 7-11). However, pleurostomatids invariably have the left side ciliature reduced to short bristles, and many have a special nuclear pattern, viz., two globular macronuclear nodules and a micronucleus in between (Kahl 1931, Foissner and Leipe 1995, Foissner *et al.* 1995). *Cultellothrix* has ordinary cilia at both body sides and a tortuous macronucleus and thus does not belong to the Pleurostomatida.

The body plan and ciliary pattern show that *Cultellothrix* belongs to the Spathidiina, as defined by Foissner and Foissner (1988). Within this suborder, it resembles members of the family Spathidiidae. *Cultellothrix* is unique among the spathidiids in having the dorsal brush not dorsally or dorsolaterally located, as the other genera mentioned in the Introduction (for examples, see Foissner *et al.* 2002), but on the left side (Figs 1, 7, 10, 16). Admittedly, this is a rather inconspicuous difference; however, the two species known look quite unique, indicating that further characters, especially the curious body shape and the special arrangement of the extrusomes, can be added to the diagnosis when further species with the same features have been discovered. Generally, most spathidiid genera are separated by rather sophisticated features; nonetheless, their recognition greatly aids in recognizing species within this rich assemblage.

Within the spathidiids, *Arcuospathidium*, *Apertospathula*, and *Cultellothrix* form a special group characterized by the *Arcuospathidium* type somatic ciliature, that is, all lateral ciliary rows form acute angles with the circumoral kinety because they are directed dorsally at both sides of the oral bulge. This is an indication for a common ancestor and a (sub)familial split. The arrangement of the oral bulge extrusomes in short, transverse rows and the single postoral row in *C. velhoi* resemble several *Bryophyllum* species, whose oral bulge and circumoral kinety, however, extend along the whole body length and curve around the posterior body end to terminate on the dorsal side of the cell (for description of representative species, see Foissner *et al.* 2002). The oral bulge and circumoral kinety of *Cultellothrix*, in contrast, extend only to mid-body. Thus, it is more closely related to the spathidiid than bryophyllid evolutionary path.

Species assignable and comparison of *Cultellothrix velhoi* sp. n. with similar species

Spathidium lionotiforme Kahl, 1930a has the same generic features as *Cultellothrix velhoi* and is thus transferred to this genus: *Cultellothrix lionotiformis* (Kahl, 1930a) comb. n. (Figs 12a, b). This species, which Kahl (1930a, b) discovered in *Sphagnum* moss and in a pond among *Hottonia palustris* in the surroundings of Hamburg, differs from *C. velhoi* by body length (140-200 µm *vs.* 80-150 µm), the lack of a postoral extrusome row, and in having two ordinary ciliary rows between brush row 1 and circumoral kinety (none in *C. velhoi*). Kahl (1930a, b) recognized that *S. lionotiforme* is an "atypical species" showing "transistions to *Amphileptus*". Indeed, this kind of spathidiids is easily confused with pleurostomatids, as discussed above. Further, Kahl (1931) mentioned a single specimen of an *Amphileptus* sp., found among colonies of *Carchesium polypinum*, which might be a further distinct *Cultellothrix* species. *Cranotheridium stilleri* Lepsi, 1959 (Fig. 14a) and *Litonotus dubius* Vuxanovici, 1962 (Fig. 14b) might also belong to *Cultellothrix*. Unfortunately, data are too incomplete for a definite transfer; both need redescription with modern methods.

As concerns the redescription of *S. lionotiforme* Kahl (1930a, b) by Foissner (1984), see following chapter on *Arcuospathidium cultriforme scalpriforme*. Kahl

described *S. lionotiforme* as species nova two times, viz., in 1930a, b. I suggest Kahl (1930a) as correct date because he described also many other new species in this paper later referred to "Kahl, 1930a" by Kahl (1930b).

Arcuospathidium cultriforme scalpriforme (Kahl, 1930) comb. n., stat. n. (Fig. 13)

1930 *Spathidium scalpriforme* Kahl, *Arch. Protistenk*. 70: 381.1930 *Lionotus scalpriforme* Kahl,

1930 - Kahl, *Tierwelt Dtl*. 18: 165 (although seemingly transferred to *Lionotus*, described under the genus *Spathidium*).

1984 *Arcuospathidium lionotiforme* (Kahl, 1930) nov. comb. - Foissner, *Stapfia* 12: 78 (misidentification).

2002 *Arcuospathidium cultriforme lionotiforme* (Kahl, 1930) Foissner, 1984 nov. stat. - Foissner, Agatha and Berger, *Denisia* 5: 300 (ranked as a subspecies).

The present study shows that my former redescription of *S. lionotiforme* Kahl (1930a, b) is based on an unfortunate misidentification caused by insufficient experience and the widespread opinion that *Spathidium* is highly variable. The species I investigated in 1984 obviously belongs to the *Spathidium cultriforme* complex, specifically to *S. scalpriforme* Kahl, 1930a (Fig. 13), a species which I never found in soil and moss (Foissner 1998), although it lives there (Kahl 1930a, b), simply because I continuously misidentified it as *S. lionotiforme*.

Based on the investigations by Foissner *et al.* (2002), I here consider *S. scalpriforme* as a subspecies of *S. cultriforme* Penard, 1922. My published (Foissner 1984, Foissner *et al*. 2002) and unpublished notes on that type of *Spathidium* show that all belong to *Arcuospathidium* and have similar extrusomes, viz., moderately fine and sometimes slightly acicular rods with a size of 4-6 x 0.8-1 µm; when the extrusomes are partially exploded, as in some protargol preparations, they look like small knifes, just as depicted by Penard (1922) in *S. cultriforme*.

Acknowledgements. The technical assistance of Dr. B. Moser, Dr. E. Herzog and Mag. E. Strobl is gratefully acknowledged. Financial support was provided by the Austrian Science Foundation (FWF Project 15017).

REFERENCES

Corliss J. O. (1979) The Ciliated Protozoa. Characterization, Classification and Guide to the Literature. 2nd ed. Pergamon Press, Oxford, New York, Toronto, Sydney, Paris, Frankfurt

Dragesco J., Dragesco-Kernéis A. (1979) Cilies muscicoles nouveaux et peu connus. *Acta Protozool.* **18:** 401-416

Foissner W. (1984) Infraciliatur, Silberliniensystem und Biometrie einiger neuer und wenig bekannter terrestrischer, limnischer und mariner Ciliaten (Protozoa: Ciliophora) aus den Klassen Kinetofragminophora, Colpodea und Polyhymenophora. *Stapfia, Linz* **12:** 1-165

Foissner W. (1991) Basic light and scanning electron microscopic methods for taxonomic studies of ciliated protozoa. *Europ. J. Protistol.* **27:** 313-330

Foissner W. (1996) Terrestrial ciliates (Protozoa, Ciliophora) from two islands (Gough, Marion) in the southern oceans, with description of two new species, *Arcuospathidium cooperi* and *Oxytricha ottowi*. *Biol. Fertil. Soils* **23:** 282-291

Foissner W. (1998) An updated compilation of world soil ciliates (Protozoa, Ciliophora), with ecological notes, new records, and descriptions of new species. *Europ. J. Protistol*. **34:** 195-235

Foissner W. (1999) Notes on the soil ciliate biota (Protozoa, Ciliophora) from the Shimba Hills in Kenya (Africa): diversity and description of three new genera and ten new species. *Biodiv. Conserv*. **8:** 319-389

Foissner W. (2000) Two new terricolous spathidiids (Protozoa, Ciliophora) from tropical Africa : *Arcuospathidium vlassaki* and *Arcuospathidium bulli*. *Biol. Fertil. Soils* **30:** 469-477

Foissner W., Foissner I. (1988) The fine structure of *Fuscheria terricola* Berger *et al.*, 1983 and a proposed new classification of the subclass Haptoria Corliss, 1974 (Ciliophora, Litostomatea). *Arch. Protistenkd.* **135:** 213-235

Foissner W., Leipe D. (1995) Morphology and ecology of *Siroloxophyllum utriculariae* (Penard, 1922) n. g., n. comb. (Ciliophora, Pleurostomatida) and an improved classification of pleurostomatid ciliates. *J. Euk. Microbiol*. **42:** 476-490

Foissner W., Berger H., Blatterer H., Kohmann F. (1995) Taxonomische und ökologische Revision der Ciliaten des Saprobiensystems - Band IV: Gymnostomatea, *Loxodes*, Suctoria. *Informationsberichte des Bayer. Landesamtes für Wasserwirtschaft* **1/95:** 1-540

Foissner W., Agatha S., Berger H. (2002) Soil ciliates (Protozoa, Ciliophora) from Namibia (Southwest Africa), with emphasis on two contrasting environments, the Etosha region and the Namib Desert. *Denisia* **5:** 1-1459

Kahl A. (1930a) Neue und ergänzende Beobachtungen holotricher Infusorien. II. *Arch. Protistenkd.* **70:** 313-416

Kahl A. (1930b) Urtiere oder Protozoa I: Wimpertiere oder Ciliata (Infusoria) 1. Allgemeiner Teil und Prostomata. *Tierwelt Dtl.* **18:** 1-180

Kahl A. (1931) Urtiere oder Protozoa I: Wimpertiere oder Ciliata (Infusoria) 2. Holotricha außer den im 1. Teil behandelten Prostomata. *Tierwelt Dtl.* **21:** 181-398

Leitner A. R., Foissner W. (1997) Morphology and infraciliature of *Microthorax pusillus* Engelmann 1862 and *Spathidium deforme* Kahl 1928, two ciliates (Protozoa, Ciliophora) from activated sludge. *Linzer biol. Beitr*. **29:** 349-368

Lepsi J. (1959) Über einige neue holotriche Süßwasser-Ciliaten. *Arch. Protistenk.* **104:** 254-260

Penard P. (1922) Études sur les Infusoires d'Eau Douce. Georg & Cie, Genève

Vuxanovici A. (1962) Contributii la sistematica ciliatelor (Nota III). *Studii Cerc. Biol. (Biol. Anim.)* **14:** 549-573 (in Rumanian with Russian and French summaries)

Received on 14th May, 2002; accepted on 3rd September, 2002

Acta Protozool. (2003) 42: 55 - 70

ACTA
PROTOZOOLOGICA

Morphology and Ontogenesis of *Bromeliophrya brasiliensis* gen. n., sp. n., a New Ciliate (Protozoa: Ciliophora) from Brazilian Tank Bromeliads (Bromeliaceae)

Wilhelm FOISSNER

Universität Salzburg, Institut für Zoologie, Salzburg, Austria

Summary. This is the first of a series of papers describing the morphology and ontogenesis of new ciliates occurring in the cisterns of tank bromeliads, a group of rosette plants of tropical America, entrapping rainwater between the coalescing leaf axils. Likely, most of these new ciliates have a restricted (Gondwanan) geographic distribution, and some might even be specific inhabitants of tank bromeliads. *Bromeliophrya brasiliensis* gen. n., sp. n. was discovered in the tanks of ground bromeliads at the east coast (Mata Atlantica) of Brazil, South America. Its morphology and ontogenesis were investigated using live observation, silver impregnation, and scanning electron microscopy. *Bromeliophrya* belongs to the hymenostome ciliate order Tetrahymenida, where it represents a new family, Bromeliophryidae fam. n., unique by the partially reduced somatic ciliature and migrating somatic kinety fragments during ontogenesis. The oral apparatus, especially a patch ("X-group") of basal bodies originating from the anterior end of adoral membranelle 2, indicates the Glaucomidae as the nearest relatives of the Bromeliophryidae. Further main characteristics of *B. brasiliensis* are: (i) a metopid body shape and ciliary pattern; (ii) two large, unciliated areas: one left of the oral opening, the other with barren basal bodies occupies the right posterior half of the cell; (iii) elongated caudal cilia; (iv) silverlines projecting loop-like in the right side kineties; (v) a large, C-shaped adoral membranelle 3 forming a ring-like oral pattern with membranelle 1 at left margin of buccal cavity; and (vi) an unciliated paroral membrane.

Key words: biodiversity, biogeography, bromeliad tanks, *Bromeliophrya brasiliensis* gen. n., sp. n., Mata Atlantica, South America.

INTRODUCTION

Finlay *et al*. (1996) claim that the main biotopes of the Earth have already been sufficiently investigated for free-living ciliates and estimate a low total diversity of only 3000-4000 species. Both statements are contradicted by evidence discussed in Foissner (1999) and Foissner *et al*. (2002). For instance, ciliates have not been investigated in detail in South America and Australia, nor in the 25 world species diversity hotspots selected by Myers *et al*. (2000), except for the Mediterranean Basin. Likewise, soil ciliates are largely unknown, as shown by a recent study describing 130 new species from 73 soil samples of Namibia (Foissner *et al*. 2002).

Here, I present a new ciliate world discovered in the water cisterns (tanks) of bromeliads, which are well-known for inhabiting a rich, more or less specific fauna and flora, but whose protists, although obviously being common and abundant, were never studied in detail (Picado 1913, Laessle 1961, Maguire 1971, Janetzky and

Address for correspondence: Wilhelm Foissner, Universität Salzburg, Institut für Zoologie, Hellbrunnerstrasse 34, A-5020 Salzburg, Austria; Fax. ++43 (0) 662 8044 5698

Vareschi 1992, Esteves and da Silva Neto 1996, Little and Hebert 1996, Martinelli 2000). Only testate amoebae were investigated in some extent (Van Oye 1923), and recently three new species were described from Brazilian tank bromeliads, one even representing a new family (Torres-Stolzenberg 2000).

Bromeliads are rosette plants, the most famous of which is the pine-apple. The tanks are formed by the coalescing leaf axils, which collect the rain water, and the rosettes of the larger species may entrap up to 30 litres. During holidays in Brazil, I collected some of the entrapped, muddy water of a ground bromelia, just for fun, because I supposed that, if there were specific ciliates at all, they would either be killed by the putrefying water or eaten by the micrometazoans during the long transport to my Salzburg laboratory. Fortunately, this did not happen, likely because the water was surprisingly acidic (pH 5) and abundances were too high to be exhausted by rotifers, small crustaceans, and mosquito larvae. It was a great surprise to discover two new species, each even representing a new genus, in this sample. Thus, I asked a Brazilian colleague, who later visited me in Salzburg, for further samples. Unfortunately, he could collect only one small sample from an epiphytic bromeliad, but this again contained a new species and genus (Foissner and Cordeiro 2000). Finally, another new species, *Urosomoida reticulata*, was discovered in the dry mud from the tanks of a tree bromeliad in Costa Rica. Later, this species was found in soil from Venezuela and Namibia (Foissner *et al.* 2002). Five other new species and two new genera, I discovered recently in a few tank bromeliads from the Dominican Republic.

These data indicate that tank bromeliads contain many undescribed ciliate species. We do not know how many, but the number must be considerable, considering that there are more than 3000 bromelia species, many of which have special life styles and grow in peculiar environments; some or even most release specific substances into the tank water, whose chemical and physical properties show great local and temporal differences providing innumerable niches for the minute protists (Maguire 1971, Martinelli 2000).

MATERIALS AND METHODS

The sample, which contained *Bromeliophrya brasiliensis* sp. n., was collected in 1996 at the Atlantic Sea coast (Mata Atlantica) in the surroundings of the village of Praia do Forte (S14°33' W38°; 1500 mm annual precipitation), that is, about 81 km North of the town of Salvador, Bahia, Brazil. About 500 ml leaf axil water was collected from two specimens of a large ground bromelia and transported without special precautions to Salzburg. Unfortunately, I could not identify the bromelian species; possibly, it was *Aechmea* sp. The tank water contained partially decomposed leaf litter, mud, various small metazoans, and had a brownish colour and strongly acidic reaction (pH 5).

In the laboratory, the water was filtered through a 500 µm net to remove larger metazoa. Part of the sample was fixed for preparations, while the rest was used to set up cultures enriched with 1-3 squashed wheat grains. *Bromeliophrya brasiliensis* and some other ciliates occurred in the native tank water and grew well in the wheat grain cultures, where they fed on bacteria. Thus, ontogenesis could be studied as well; cultures set up mainly with Eau de Volvic (French table water) developed poorly, indicating that the tank water contained substances promoting growth of ciliates.

Cells were studied *in vivo* using a high-power, oil immersion objective and differential interference contrast optics. The infraciliature and various cytological structures were revealed by scanning electron microscopy and the silver impregnation techniques described in Foissner (1991). Counts and measurements on prepared specimens were performed at a magnification of x1000. *In vivo* measurements were conducted at magnifications of x100-1000. Although these provide only rough estimates, it is worth giving such data as specimens may change in preparations. Illustrations of live specimens were based on video-records and micrographs, while those of prepared cells were made with a camera lucida. Terminology is according to Peck (1974), Corliss (1952, 1979) , and Foissner (1996).

RESULTS

Bromeliophryidae fam. n.

Diagnosis: medium-sized Tetrahymenida with partially reduced somatic ciliature and a patch ("X-group") of basal bodies between the anterior ends of adoral membranelles 1 and 3. Stomatogenesis glaucomid, while somatogenesis is unique in that some left side ciliary rows split and the anterior fragments migrate to the left margin of the oral apparatus.

Type genus: *Bromeliophrya* gen. n.

Bromeliophrya gen. n.

Diagnosis: *Metopus*-shaped Bromeliophryidae with some right side ciliary rows rectangularly curved to abut on dorsal side rows preorally; two large, unciliated areas: one left of oral opening, the other with barren basal bodies occupies the right posterior half of the cell. Oral apparatus in second quarter of cell; adoral membranelle 1 short and concave, forms ring-like pattern with the large, C-shaped membranelle 3; membranelle 2 short and convex, extends along proximal part of membranelle

3. Paroral membrane unciliated. Silverlines projecting loop-like from kineties in second quarter of right side.

Type species: *Bromeliophrya brasiliensis* sp. n.

Etymology: composite of the plant generic name *Bromus* (Bromeliaceae) and the Greek noun *ophrya* (eyebrow ~ cilia ~ ciliate), meaning a "ciliate associated with bromeliads". Feminine gender.

Description of *Bromeliophrya brasiliensis* sp. n.

Diagnosis: size about 55 x 35 µm *in vivo*. One broadly ellipsoidal macronucleus and micronucleus in centre of cell. Contractile vacuole in posterior fifth of body. Extrusomes mainly left of ciliary rows, rod-shaped, about 2 x 0.8 µm. On average 32 ciliary rows, of which 16 are distinctly shortened postorally and left laterally; two left lateral kinety fragments at left margin of oral apparatus; about 5 elongated caudal cilia originating from right side kineties. Adoral membranelle 1 composed of one ciliated row; membranelle 2 four-rowed with anterior row shortened at right; membranelle 3 composed of three rows.

Type location: tanks of ground bromeliads in the surroundings of the village of Praia do Forte (S14°33' W38°), Atlantic Sea coast of Bahia, Brazil.

Type material: 1 holotype slide each of cultivated, protargol-impregnated, Chatton-Lwoff silver nitrate-impregnated, and Klein-Foissner silver nitrate-impregnated specimens and 10 paratype slides have been deposited in the Oberösterreichische Landesmuseum in Linz (LI). Specimens shown in Figures 16-34 and some other well-

Table 1. Morphometric data on *Bromeliophrya brasiliensis* sp. n.

Characteristics[a]	Method	x	M	SD	SE	CV	Min	Max	n
Body, length	CHL	50.6	51.0	4.5	1.0	8.9	42	58	21
Body, width in lateral view	CHL	34.9	34.0	3.1	0.7	8.8	30	40	21
Body, width in ventral view	CHL	30.3	30.0	2.5	0.5	8.2	26	35	21
Anterior end to upper mouth margin, distance	CHL	12.5	13.0	2.3	0.5	18.4	7	16	21
Anterior end to lower mouth margin, distance	CHL	24.6	25.0	2.5	0.6	10.3	18	28	21
Anterior end to adoral membranelle 3, distance	CHL	9.4	9.0	1.5	0.3	15.7	6	12	21
Anterior end to proximal summit of adoral membranelle 3, distance	CHL	27.0	27.0	1.7	0.4	6.0	25	30	21
Anterior end to macronucleus, distance	CHL	19.4	19.0	3.7	0.8	19.0	9	27	21
Anterior end to distal end of 1st preoral kinety (=K2), distance	CHL	13.9	14.0	1.6	0.4	11.5	12	18	21
Anterior end to last postoral kinety, distance[h]	CHL	29.2	29.0	2.1	0.5	7.3	25	34	21
Posterior end to excretory pore, distance	CHL	9.6	10.0	1.9	0.4	19.4	6	13	21
Macronucleus, length	CHL	14.4	15.0	2.9	0.6	20.3	10	20	21
Macronucleus, width	CHL	11.3	11.0	1.9	0.4	16.6	8	15	21
Micronucleus, length	CHL	2.7	2.5	0.7	0.1	23.7	2	4	21
Micronucleus, width	CHL	2.6	2.5	0.6	0.1	22.7	2	3.5	21
Oral opening, width[b]	CHL	9.5	10.0	0.8	0.2	7.9	8	11	21
Oral opening, width[c]	CHL	13.0	13.0	1.6	0.3	11.9	10	16	21
Buccal cavity, depth[d]	CHL	14.3	14.0	1.5	0.3	10.4	12	18	21
Somatic kineties, total number[e]	CHL	31.5	32.0	0.8	0.2	2.6	29	33	21
Postoral kineties, number[e,h]	CHL	15.8	16.0	0.7	0.2	4.3	14	17	21
Left lateral kinety fragments, number[f]	CHL	2.0	2.0	0.0	0.0	0.0	2	2	21
Kinetids in somatic kinety 2, number	P	77.0	80.0	11.2	2.5	14.6	49	94	21
Kinetids in postoral kinety 7, number[h]	CHL	12.4	12.0	2.3	0.5	18.2	7	16	21
Kinetids in left lateral fragment 1, number	P	7.4	7.0	1.1	0.2	15.1	5	10	21
Kinetids in left lateral fragment 2, number	P	12.1	12.0	1.4	0.3	11.4	9	14	21
Caudal cilia, number[g]	P	5.3	5.0	-	-	-	5	7	21

[a] Data based on cultivated, mounted, randomly selected, morphostatic specimens. [b] Distance from paroral membrane to first kinety left of oral opening (=kinety fragment 1). [c] Distance from outer margin of adoral membranelle 1 to outer margin of membranelle 3. [d] From laterally orientated specimens (Fig. 22). [e] Without the two kinety fragments left of oral opening. [f] Two kinety fragments left of oral opening, see ontogenesis. [g] Approximate values because often indistinctly separated from somatic kinetids. [h] Postoral kineties include left lateral kineties, which are also shortened and thus inseparable. All measurements in µm. CHL - Chatton-Lwoff silver nitrate impregnation, CV - coefficient of variation in %, M - median, Max - maximum, Min - minimum, n - number of individuals investigated, P - protargol impregnation (Wilbert's method), SD - standard deviation, SE - standard error of arithmetic mean, x - arithmetic mean.

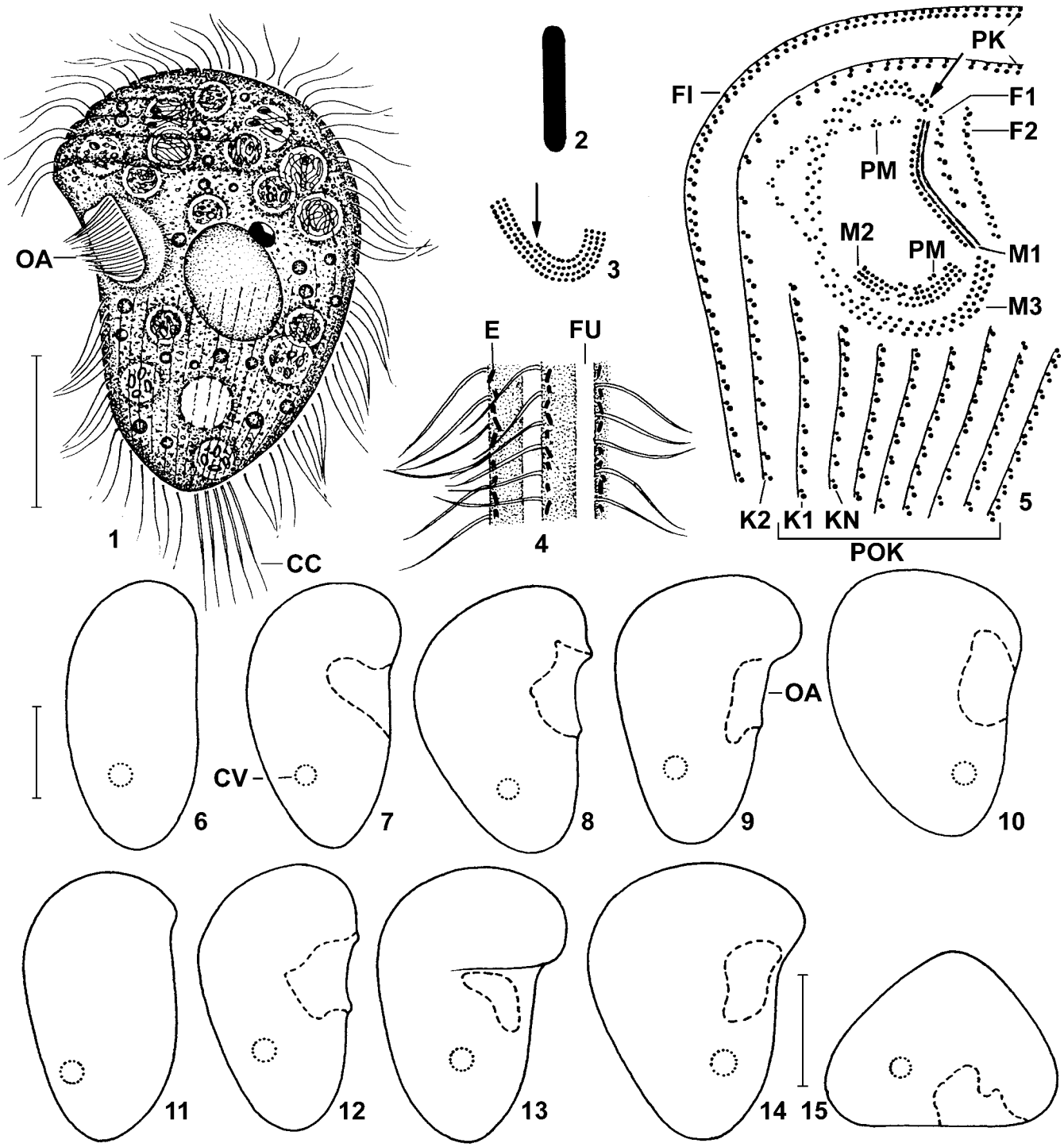

Figs 1-15. *Bromeliophrya brasiliensis* sp. n. from life (1, 2, 4, 6-15) and after silver carbonate impregnation (3, 5). **1** - left side view of a representative specimen; **2** - extrusome, 2 x 0.8 µm; **3** - adoral membranelle 2 consists of four basal body rows, of which the anterior row is distinctly shortened (arrow); **4** - the cortex of "wild" specimens is distinctly furrowed; **5** - slightly schematised ventral view of oral and circumoral ciliature. Arrow marks a patch ("X-group") of basal bodies between the anterior ends of adoral membranelles 1 and 3. The somatic kinetids are composed of two granules, of which the posterior one bears a cilium, while the anterior granule is likely a parasomal sac. Note that paroral kinetids are composed of three granules in the anterior half of the organelle; **6-14** - body shape-changes of two specimens rotating from dorsal (6, 11) to right side (10, 14), redrawn from video records; **15** - transverse view. CC - caudal cilia; CV - contractile vacuole; E - extrusomes; F1 - fibre; FU - furrow; F1, 2 - kinety fragments; K1, 2, N - kineties 1, 2, N; M1, 2, 3 - adoral membranelles; OA - oral apparatus; PK - preoral kineties; PM - paroral membrane; POK - postoral and left lateral kineties. Length of cells: 55 µm (1), 60 µm (6-10), 50 µm (11-14). Scale bars 20 µm.

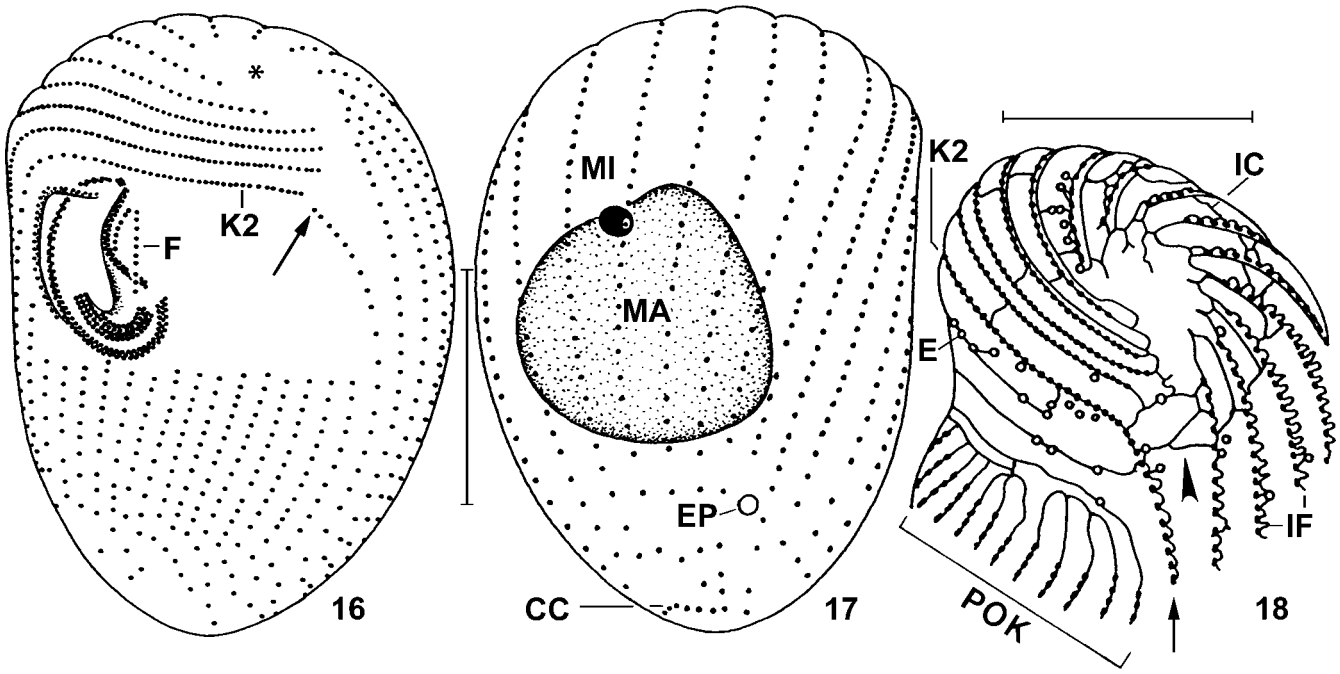

Figs 16-18. *Bromeliophrya brasiliensis* sp. n. after protargol (Wilbert's method; 16, 17) and silver nitrate (Chatton-Lwoff method; 18) impregnation. **16, 17** - ciliary pattern of left and right side of holotype specimen. Note the large, unciliated area left of the oral opening and that basal bodies are unciliated, except for the caudal cilia, in the right posterior half (cp. fig. 38). Arrow denotes the last dorsal kinety, which is so strongly curved that it abuts to the anterior end of right side kinety 2. Asterisk denotes the unciliated anterior pole field, which contacts the bare, obtriangular area between the last and penultimate dorsal kinety. For details on oral structures, see fig. 5; **18** - oblique left side view of anterior body portion showing lack of silverlines in the unciliated pole area. Arrow marks curved last dorsal kinety, which abuts to right side kinety 2. Arrowhead denotes silverlines connecting last and penultimate dorsal kinety. Resting extrusomes (E) are surrounded by a silverline. CC - caudal cilia; E - resting extrusome; EP - excretory pore of contractile vacuole; F - kinety fragments left of oral opening; IC - intermeridional connectives; IF - intrameridional cross-fibres; K2 - somatic kinety 2; MA - macronucleus; MI - micronucleus; POK - postoral and left lateral kineties. Length of left specimen - 54 µm. Scale bars 20 µm.

impregnated cells are individually marked by a black ink circle on the cover glass.

Etymology: named after the native country.

Description: size 45-65 x 30-40 µm *in vivo*, usually about 55 x 35 µm (Table 1). Shape rather constant, cells, however, distinctly asymmetrical and thus showing a variety of shapes, depending on side and angle viewed (Figs 1, 6-15, 35, 36, 38, 39); lateral view highly characteristic because similar to that of members of the genus *Metopus*, that is, with broad, projecting preoral dome and rounded obconical postoral portion. Anterior body end broadly rounded, posterior narrowly rounded to bluntly pointed; ventral body half more distinctly flattened than dorsal, producing more or less rounded triangular outline in ventral, dorsal, and transverse view. Nuclear apparatus in or near body centre. Macronucleus globular to ellipsoidal (2:1), on average broadly ellipsoidal (1.3:1); nucleoli scattered, inconspicuous. Micronucleus attached to macronucleus, globular. Contractile vacuole in posterior fifth of cell, that is, distinctly subterminal, invariably with a single excretory pore at end of a shortened ciliary row in or near midline of right side. Cytopyge extends between posteriorly shortened (stomatogenic) kinety 1 and posterior pole centre, appears as a thick silverline in silver nitrate preparations (Figs 1, 19, 22, 24-26, 38). Extrusomes numerous, slightly left of ciliary rows, left of kinety fragments, at both sides of adoral membranelle 3, and attached to silverlines traversing unciliated areas, about 2 x 0.5 µm in size and rod-shaped *in vivo*, do not impregnate; resting extrusomes surrounded by a heavily impregnated silverline ring, while minute argyrophilic granules mark sites of discharged extrusomes (Figs 4, 20, 23, 25, 51, 56). Cortex of "wild" specimens distinctly furrowed right of ciliary rows (Fig. 4), while almost smooth in cultivated specimens (Figs 35, 36, 38, 39, 57). Cytoplasm colourless, packed with food vacuoles, mainly in anterior body half, and some scattered, up to 5 µm-sized lipid droplets. In

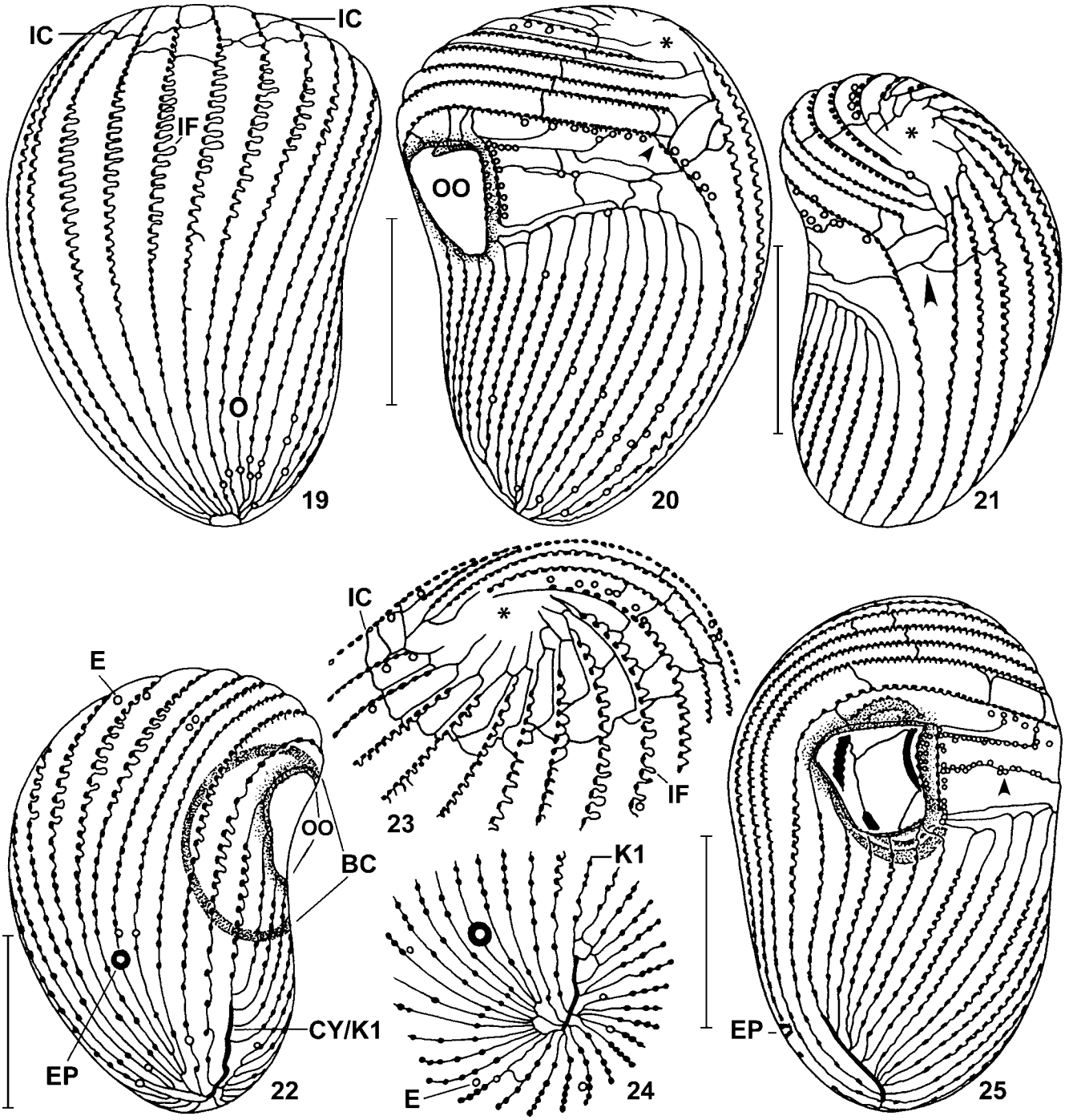

Figs 19-25. *Bromeliophrya brasiliensis* sp. n., silverline and ciliary pattern after Chatton-Lwoff silver nitrate impregnation. **19, 20** - right and left side view of same specimen. Note the conspicuous, loop-like outgrowths (IF) of the intrameridional silverlines in the second quarter of the right side and the wide-meshed silverline pattern in the large, unciliated area left of the oral apparatus. Right side kinety 2 extends to near dorsal side, where it abuts to the curved anterior end of the last dorsal kinety (arrowhead); **21** - dorsolateral view showing silverlines connecting last and penultimate dorsal kinety. Asterisk marks unciliated anterior pole area. Arrowhead denotes silverline connecting last lateral and first dorsal ciliary row; **22** - ventrolateral view showing deep buccal cavity; **23** - anterior portion showing the unciliated pole area (asterisk) partially occupied by the intermeridional connectives, which extend subapically; **24** - posterior polar view showing the thick cytopyge silverline in kinety 1; **25** - ventral view of a representative specimen showing many extrusomes (arrowhead), which are surrounded by minute silverline rings, attached to the silverlines in the unciliated area left of the oral apparatus. BC - buccal cavity; CY - cytopyge; E - extrusomes; EP - excretory pore of the contractile vacuole; IC - intermeridional connectives; IF - intrameridional cross-fibres; K1 - somatic kinety 1; OO - oral opening. Length of cells: 56 µm (19, 20), 48 µm (21), 52 µm (22), 57 µm (25). Scale bars 20 µm.

culture feeds exclusively on about 4 µm long bacterial rods digested in 4-6 µm-sized vacuoles, except the bacterial spores, which often impregnate with protargol and silver carbonate, making photographic documentation of the ciliary pattern difficult (Figs 1, 37, 62, 63). When undisturbed, cells dance conspicuously on bacterial flocks and accumulate at the dark side of the Petri dish; when transferred to the microscope slide, they swim rather rapidly, frequently changing direction by short jumps.

Ordinary somatic cilia about 10 µm long *in vivo*, single throughout; kinetids, however, composed of two obliquely arranged granules in silver carbonate and silver nitrate preparations, but only the larger posterior granule is ciliated, while the smaller anterior granule is likely a parasomal sac (Figs 1, 4, 5, 16, 17, 35, 38-40, 53, 57, 58). Caudal cilia in a roughly transverse array formed by last kinetids of some right side kineties, longer (15 µm) and stiffer than ordinary somatic cilia and thus well recognizable *in vivo* (Figs 1, 17, 38, 43). Ciliary pattern complicated by several unciliated areas and specializations (Figs 1, 5, 16-26, 35-39, 41-48; Table 1). On average 32 ciliary rows, those on right side slightly more widely spaced than those on left; distances between individual kinetids increase from anterior to posterior, especially in right side kineties, cells thus more densely ciliated anteriorly than posteriorly; accompanied by a fibre at right. Somatic kinety 1 is stomatogenic and distinctly shortened anteriorly, where it commences at right margin of oral opening, and posteriorly, where it abuts to the cytopyge. Right of kinety 1, six to eight, usually seven, very long ciliary rows, rectangularly curving around upper mouth margin and extending transversely as preoral kineties to near dorsal side of cell; kinety 2 loosely ciliated in oral area, abuts to curved end of last dorsal kinety; other preoral kineties do not abut, producing a rather large, elliptical, unciliated anterior pole area; transverse portion of all preoral rows very densely ciliated, while basal bodies lack cilia, except for caudal cilia, in kineties 3/4 to 8/9, that is, in posterior right half of cell, which is thus unciliated. Rest of right side and dorsal kineties extend longitudinally from anterior to posterior end of cell; last dorsal kinety anteriorly curved right to abut on kinety 2 as described above, producing an obtriangular, bare area, which contacts the unciliated anterior pole field, between last and penultimate dorsal kinety. Left side kineties strongly shortened and indistinguishable from postoral kineties (thus, all may be designated as postoral), producing large, bare area left of oral opening; bare area anteriorly bordered by kinety 2, at left by last dorsal kinety, and at right by two kinety fragments originating from leftmost postoral kineties (see ontogenesis). The silverline pattern shows that most of the postoral kineties abut to the cytopyge to form some kind of suture with kinety 1 (Figs 1, 5, 16-26, 35-39, 41-48; Table 1).

Oral opening in second quarter of cell, rounded triangular to broadly reniform due to a small convexity that bears membranelle 1 at left; margin slightly thickened; anteriorly and posteriorly smaller than buccal cavity, adoral membranelles thus only partially recognizable *in vivo* and scanning electron micrographs (Figs 1, 20, 22, 25, 35, 36, 39, 41, 57, 58, 60; Table 1). Buccal cavity about 14 µm deep and roughly hemispherical in silver nitrate preparations. Oral ciliature inconspicuous *in vivo* due to lack of paroral membrane and deep location of adoral membranelles, only cilia of membranelle 1 project distinctly from buccal cavity. Adoral membranelle 1 at left wall of buccal cavity, well recognizable *in vivo* and SEM micrographs because located on small convexity at margin of oral entrance, composed of a single row of cilia, at left accompanied by one or two argyrophilic lines in silver carbonate and protargol preparations, possibly unciliated kineties because at least two basal body rows are recognizable in early and middle dividers (Figs 28, 29). Adoral membranelle 2 extends on posterior bottom of buccal cavity and is thus concave and not recognizable in ordinary SEM preparations; ciliated *in vivo* and SEM of broken cells, composed of four ciliary rows, the upper row is distinctly shortened at right. Adoral membranelle 3 also deep in buccal cavity and thus only partially recognizable in SEM micrographs, extends along upper, right and posterior buccal wall and is thus large and C-shaped, composed of three ciliary rows with cilia more narrowly spaced in left than right and upper portion of organelle. "X-group", that is, a small array of about six basal bodies located between anterior ends of membranelles 1 and 3; likely, it originates from membranelle 2 (see ontogenesis). Paroral membrane extends along right and posterior half of oral entrance, unciliated and thus not recognizable *in vivo* and SEM micrographs; composed of single, weakly impregnated granules in protargol and silver nitrate preparations, while silver carbonate reveals groups of three granules in anterior half and paired granules in posterior half, or paired granules throughout. Pharyngeal fibres inconspicuous, recognizable only in protargol preparations, originate at left end of membranelles 1 and 3 and extend obliquely to anterior left quadrant of cell.

Silverline pattern complex, as shown by Figs 18-25 and 49-56, connects all main cortical organelles, such as

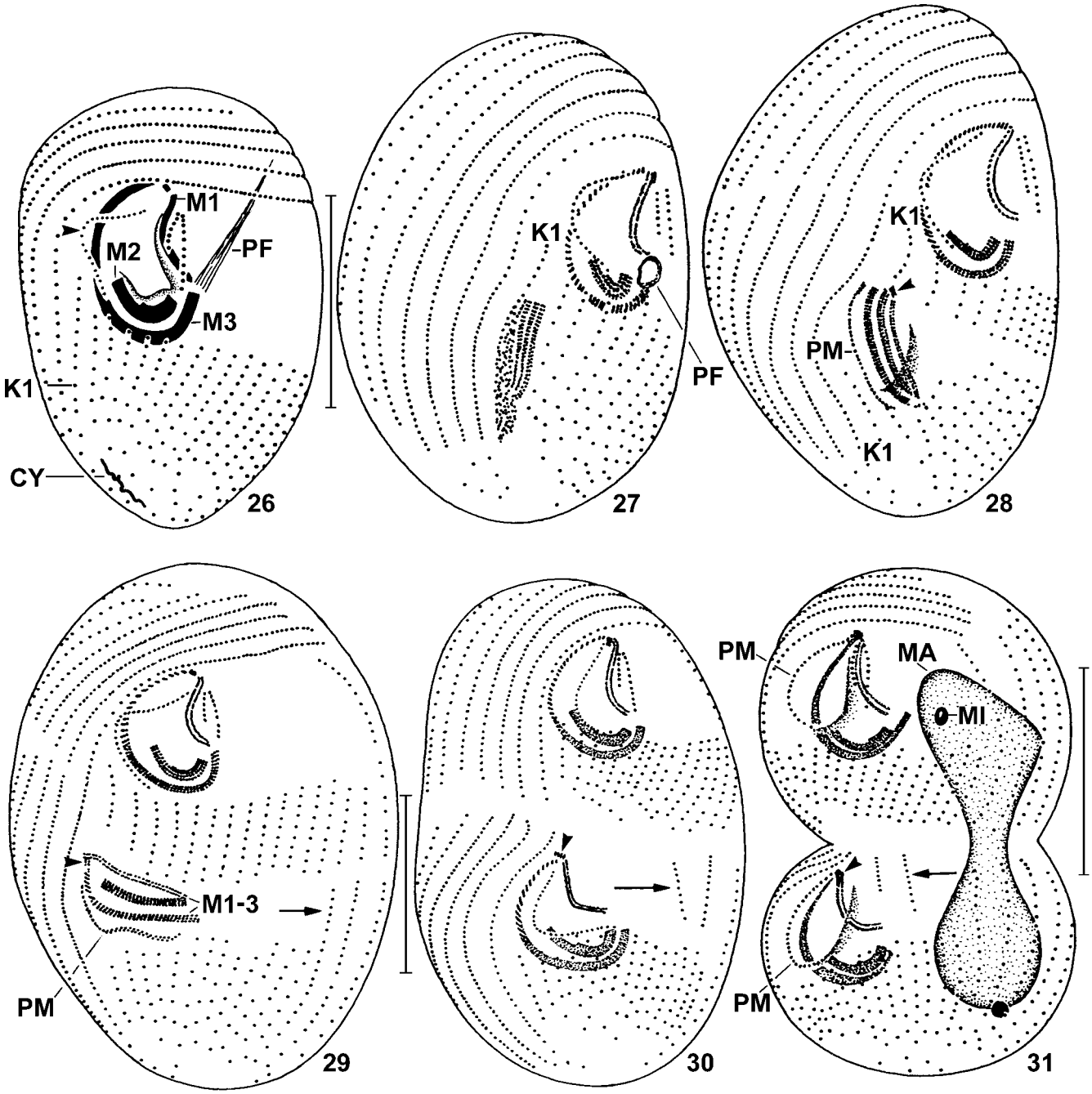

Figs 26-31. *Bromeliophrya brasiliensis* sp. n., ventral views of ciliary pattern of a morphostatic (26) and dividing (27-31) specimens after protargol impregnation with Wilbert's (26, 29, 30) and Foissner's (27, 28, 31) protocol. **26** - a representative, morphostatic specimen with pharyngeal fibres supplemented from another specimen. Note that the unciliated basal bodies of the paroral membrane (arrowhead) are smaller than those of the ciliated somatic kinetids; **27-31** - ontogenesis, especially stomatogenesis, occurs in the typical tetrahymenid manner. The parental oral apparatus is not involved and does not reorganize. Arrowheads mark a patch of basal bodies ("X-group"), likely separating from the anterior end of membranelle 2, which becomes four-rowed and distinctly shortens in middle and late dividers (29, 30). Arrows mark the two leftmost postoral kineties, which proliferate basal bodies anteriorly, producing kinetofragments which migrate to the left margin of the buccal cavity. Note that the shortened postoral and left lateral ciliary rows cause the division axis to become oblique in early dividers (28); however, the disparity is balanced by an increased growth of the left lateral area in middle dividers, generating the broad, blank area left of the buccal cavity and transverse cytokinesis in late dividers (29-31). CY - cytopyge; K1 - kinety 1; MA - macronucleus; MI - micronucleus; M1-3 - adoral membranelles; PF - pharyngeal fibres; PM - paroral membrane. Length of cells: 42 µm, 47 µm, 49 µm, 60 µm, 58 µm, 50 µm. Scale bars 20 µm.

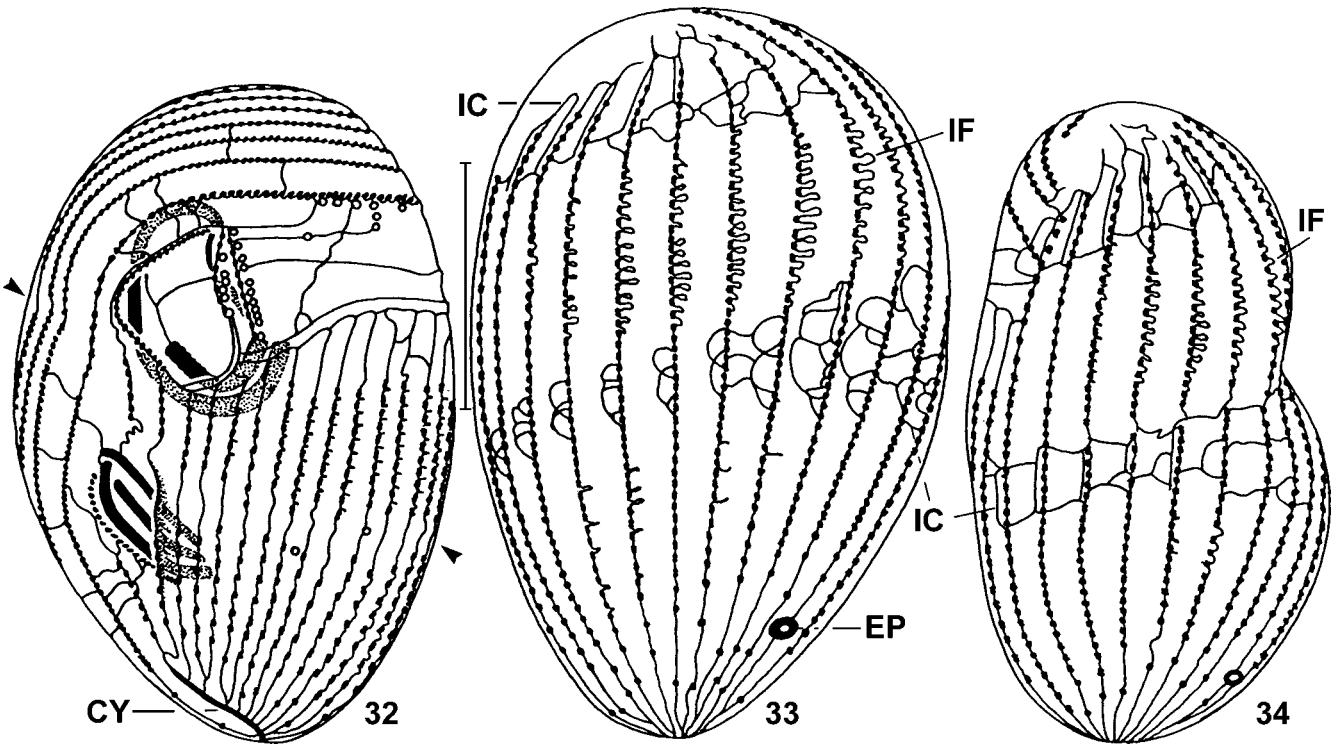

Figs 32-34. *Bromeliophrya brasiliensis* sp. n., ciliary and silverline pattern of middle (32, 33) and late (34) dividers after Chatton-Lwoff silver nitrate impregnation. **32** - ventral view of an early-middle divider showing the invaginating opisthe oral apparatus and the oblique division axis (arrowheads) produced by the strongly shortened left lateral ciliary rows (for details, see text and explanation to figures 27-31). Note that the dividing kineties remain connected by the intrameridional silverlines; **33, 34** - right side view of an early divider and left side view of a late divider showing the origin of the intermeridional connectives from foamy silverline arrays developing at the right margin of the left and right side and dorsal ciliary rows. The arrays develop underneath the prospective division furrow and are, likely, outgrowths of the intrameridional silverline connecting the basal bodies within a row. The proter (parental) connectives are not reorganized. Note that the loop-like intrameridional cross-fibres in the anterior portion of the right side ciliary rows develop very late and are thus not yet recognizable in the late divider shown in figure 34. CY - cytopyge; EP - excretory pore of contractile vacuole; IC - intermeridional connectives; IF - intrameridional cross-fibres; PM - paroral membrane. Length of cells: 56 µm, 61 µm, 54 µm. Scale bar 20 µm.

basal bodies, oral apparatus and excretory pore, and extends, left of oral apparatus, into the unciliated area, which is thus less conspicuous in silver nitrate than protargol preparations. Basal bodies of individual ciliary rows connected by an intrameridional silverline having conspicuous, loop-like outgrowths (intrameridional cross-fibres) in second quarter of right-side; silverlines of individual ciliary rows end in the unciliated anterior pole area or merge into the intermeridional connectives, posteriorly they merge into each other or abut to the cytopyge silverline. Intrameridional silverlines of shortened postoral and left lateral kineties extend into the unciliated area left of the oral apparatus to form a wide-meshed pattern with silverlines extending between oral apparatus, kinety 2, and last dorsal kinety. A wide-meshed silverline pattern occurs also in the buccal cavity and connects the adoral membranelles with each other and with some intrameridional somatic silverlines; short, longitudinal silverlines connect the preoral kineties. A single, narrow area with intermeridional connectives, probably originating from intrameridional silverlines, occurs subapically and extends via anteriorly directed, straight silverlines also into the unciliated anterior pole area. Resting extrusomes surrounded by a minute silverline, found mainly left of kineties in the intrameridional cross-fibres and attached to the silverlines crossing the unciliated area left of oral apparatus.

Ontogenesis (for terminology, see Foissner 1996) of *B. brasiliensis* is homothetogenic and occurs in freely-motile (non-encysted) condition. Stomatogenesis is monoparakinetal, as in most members of the group, and the parental oral apparatus is transmitted to the next generation without distinct signs of reorganization, which must be very rare in interphase specimens because I did

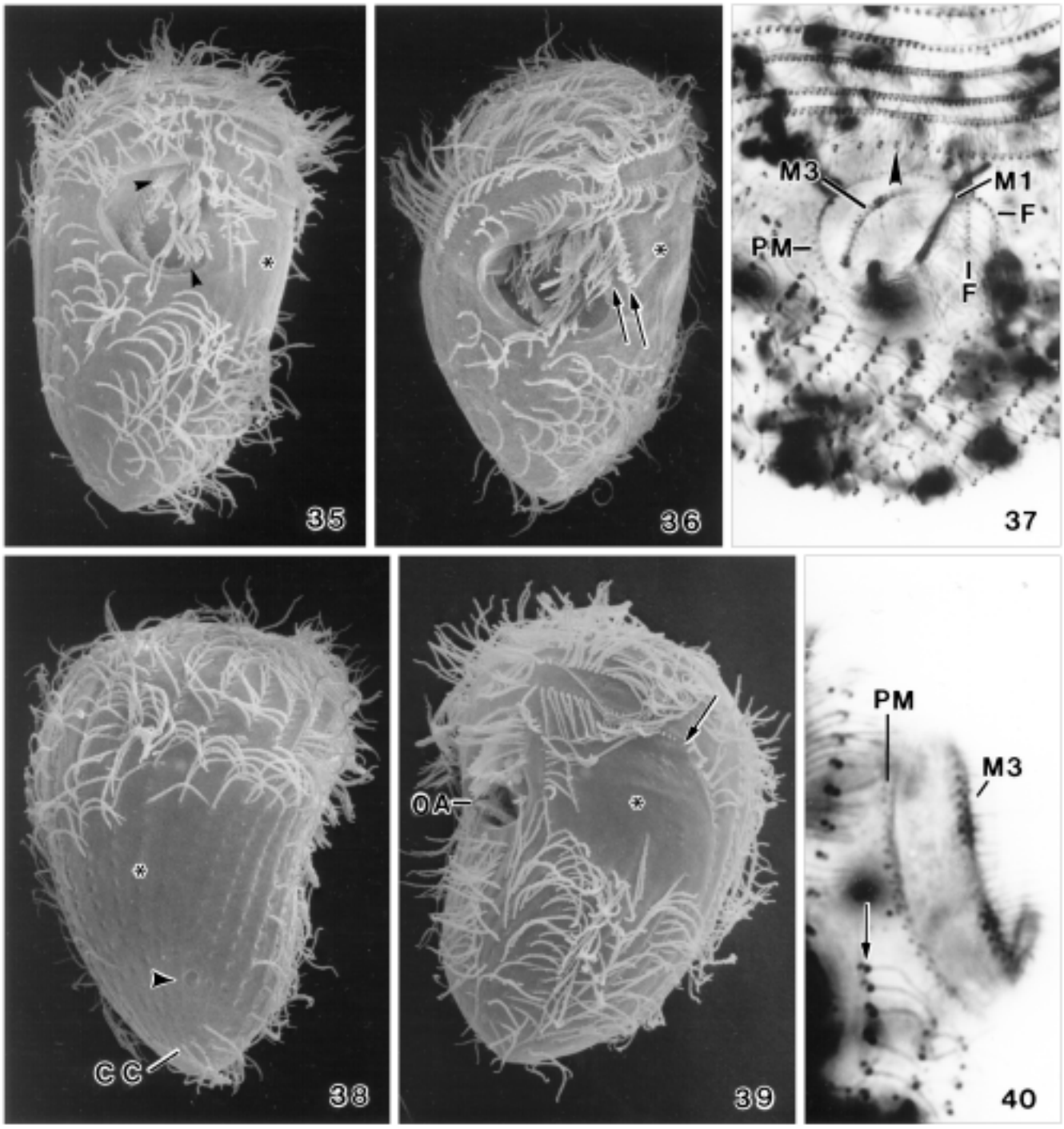

Figs 35-40. *Bromeliophrya brasiliensis* sp. n. in the scanning electron microscope (35, 36, 38, 39) and after silver carbonate impregnation (37, 40). **35, 36** - ventral views showing oral apparatus in second quarter of cell and metopid arrangement of ciliary rows. Asterisks denote barren area left of oral opening. Arrows mark two short ciliary rows, which migrate from dorsolateral to the oral opening, a main family character. Arrowheads denote the large, C-shaped adoral membranelle 3; **38, 39** - right and left side view showing a main feature of the Bromeliophryidae family, viz., the two large, unciliated areas (asterisks): the right posterior half of the cell, where, however, basal bodies are present (Figs 42, 43); and a quadrangular field left of the oral opening, where even basal bodies are lacking. Arrowhead marks excretory pore of contractile vacuole. Arrow denotes site where right side ciliary row 2, which extends preorally and left laterally, abuts to the last dorsal kinety; **37, 40** - oral area of strongly squashed specimens, showing the inconspicuous, unciliated paroral membrane. Note that, in silver carbonate preparations, the kinetids consist of oblique pairs of granules (arrow): the smaller anterior granule is barren and likely a parasomal sac, while the larger posterior granule bears a cilium. Arrowhead in figure 37 marks kinety 2, which is loosely ciliated right of the oral opening. CC - caudal cilia; F - kinety fragments; M1, 3 - adoral membranelles; OA - oral apparatus; PM - paroral membrane.

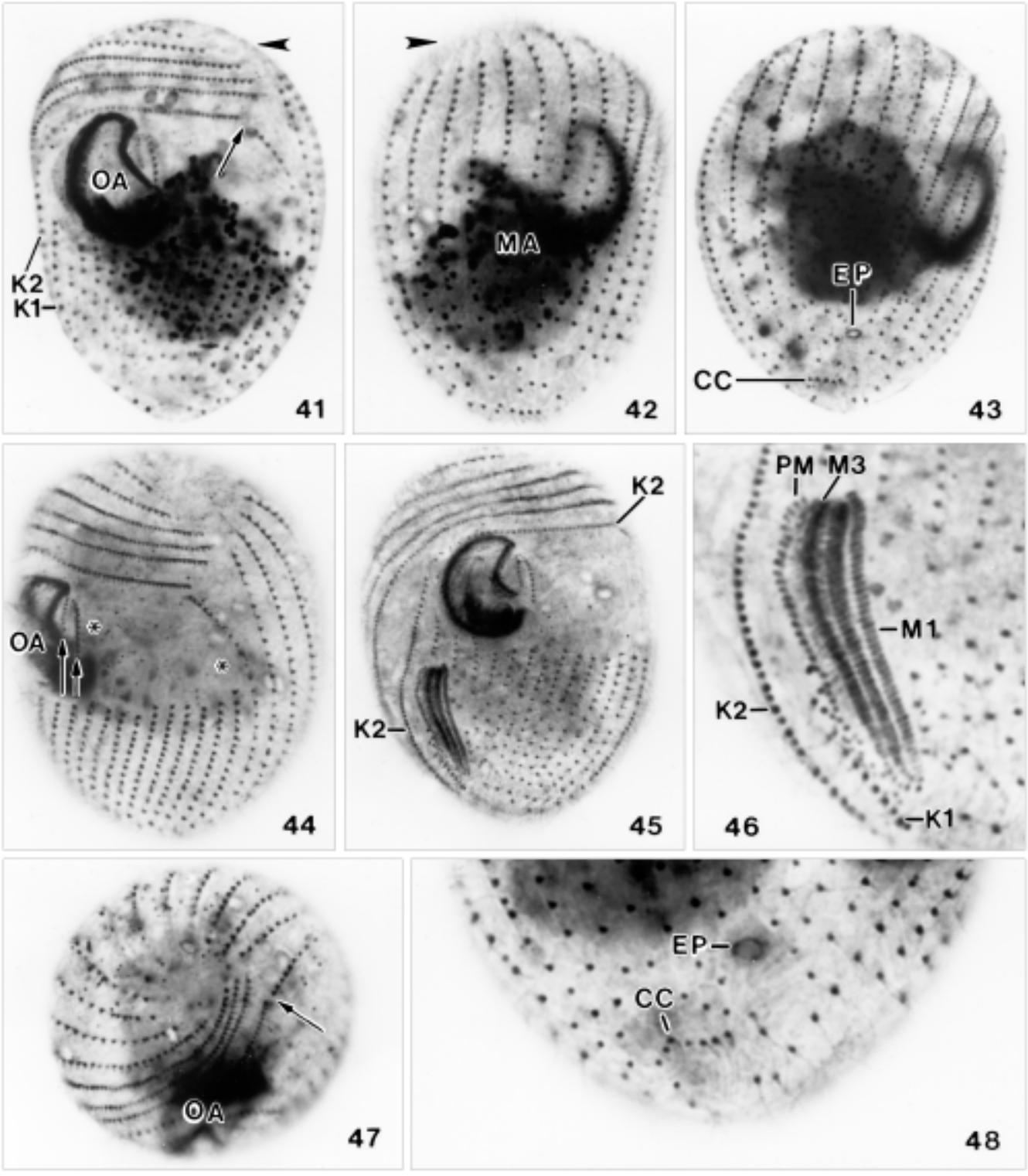

Figs 41-48. *Bromeliophrya brasiliensis* sp. n., somatic ciliary pattern (41- 44, 47, 48) and ontogenesis (45, 46) after protargol impregnation (Wilbert's method). **41, 42, 47** - ventro-and dorsolateral view of same specimen and anterior polar view of another cell. Note the elliptical, unciliated anterior pole area (arrowheads) and kinety 2, which abuts on the last dorsal kinety (arrows); **43, 48** - dorsal views showing the transverse row of caudal cilia and the unciliated basal bodies of the right side (cp. figure 38); **44** - left side view showing the large, unciliated area left of the oral opening (asterisks), posteriorly bordered by the shortened postoral and left lateral kineties. Arrows mark kinety fragments left of oral opening; **45, 46** - ventral view of an early divider with a conspicuous, dikinetidal paroral membrane. CC - caudal cilia; EP - excretory pore; K1, 2 - somatic kineties; M1, 3 - adoral membranelles; MA - macronucleus; OA - oral apparatus; PM - paroral membrane.

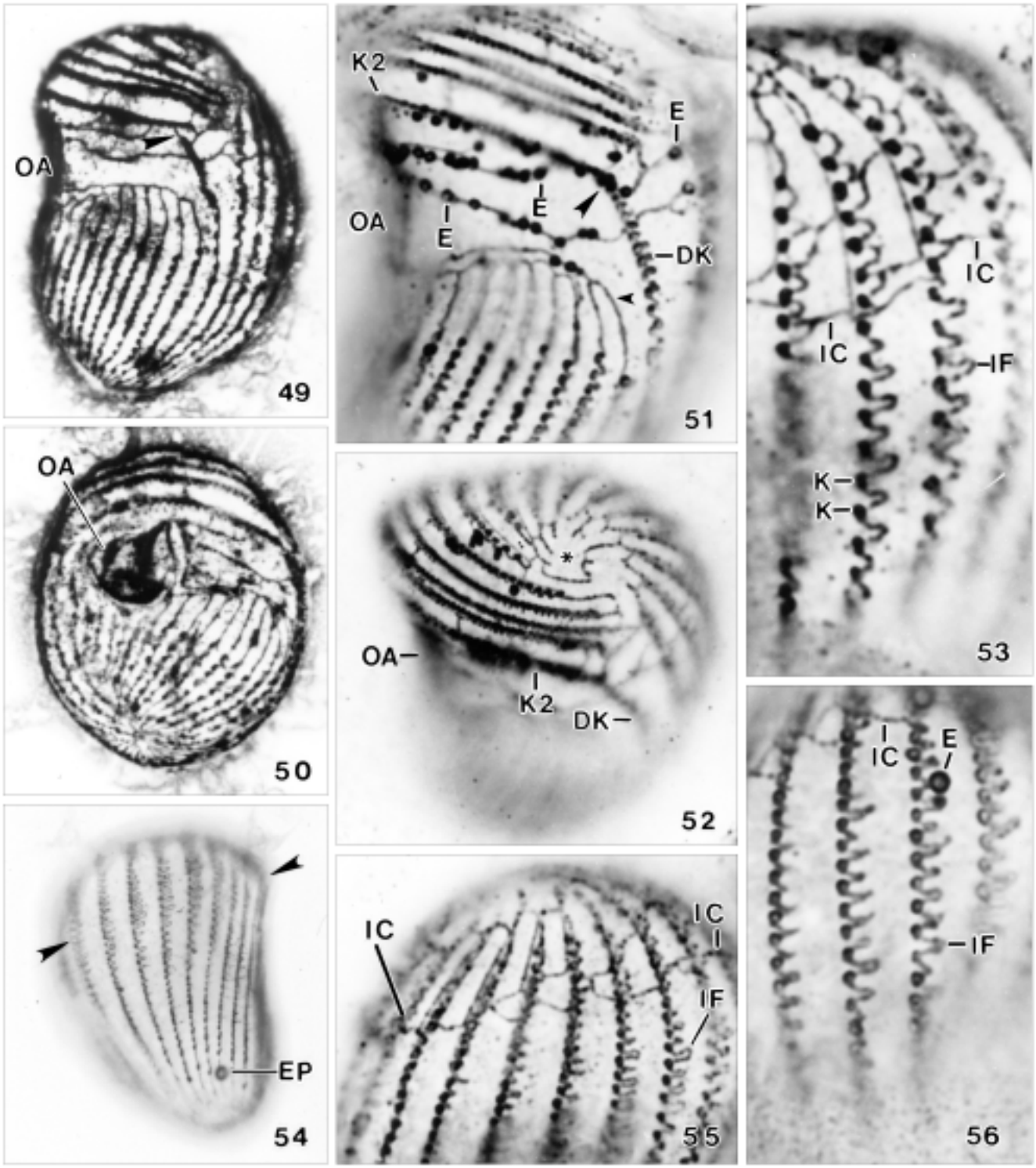

Figs 49-56. *Bromeliophrya brasiliensis* sp. n., silverline and ciliary pattern after Klein-Foissner (49, 50) and Chatton-Lwoff (51-56) silver nitrate impregnation. **49, 51** - left side views showing site where right side kinety 2 abuts on the last dorsal kinety (large arrowheads). Small arrowhead denotes intrameridional silverlines extending into the unciliated area left of oral opening. **50** - ventral view; **52** - the anterior pole (asterisk) is unciliated; **53-56** - right side views showing the loop-like projecting intrameridional cross-fibres (arrowheads in 54) and the subapical intermeridional connectives (IC). DK - last dorsal kinety; E - extrusomes; EP - excretory pore; K - kinetids; K2 - kinety 2; IC - intermeridional connectives; IF - intrameridional cross-fibres; OA - oral apparatus.

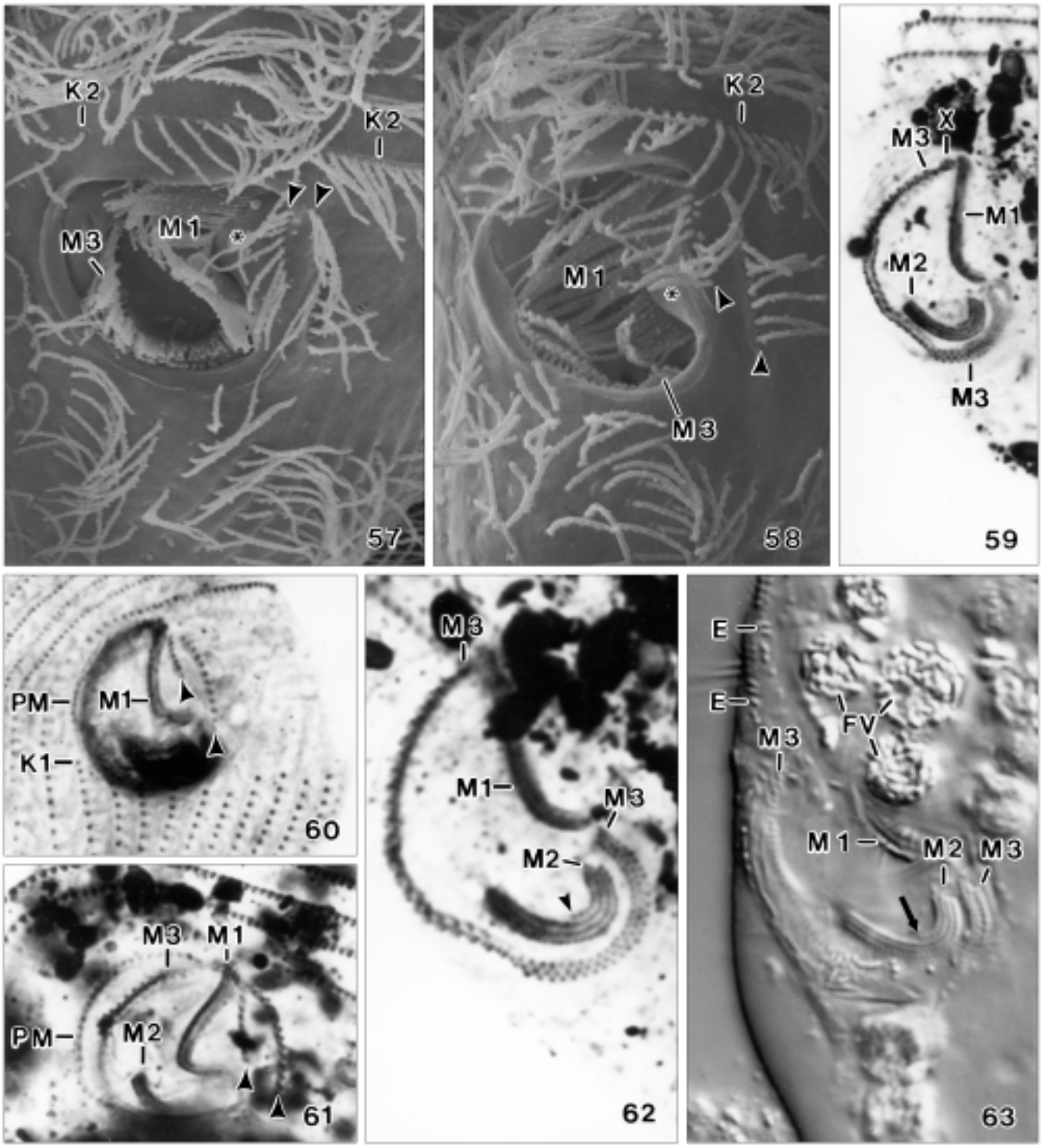

Figs 57-63. *Bromeliophrya brasiliensis* sp. n., oral apparatus in the SEM (57, 58), after silver carbonate (59, 61, 62) and protargol (60) impregnation, and *in vivo* (63). Arrowheads in figures (57, 58, 60, 61) mark two kinety fragments at left margin of oral opening. These fragments have a special origin described in the ontogenesis section. Arrow in figure (63) marks shortened kinety in membranelle 2. Asterisks in figures (57, 58) denote convex left margin of oral opening. Basically, the oral apparatus is in the second quarter of the cell (Figs 35, 36) and has a broadly reniform opening (Figs 57, 58). The buccal cavity is rather deep (Fig. 22) and contains three membranelles of different shape and structure (Figs 57-63) described in the results section and diagramatically shown in figure (5). A small patch of basal bodies ("X-group") is between the anterior ends of membranelles 1 and 3 (Fig. 59). The paroral membrane consists of single, unciliated basal bodies (Figs 60, 61) and is thus not recognizable in scanning micrographs (Figs 57, 58). E - extrusomes; FV - food vacuoles; K1, 2, - somatic kineties; M1-3 - adoral membranelles; PM - paroral membrane; X - "X-group" (patch) of basal bodies.

not find a single reorganizer among more than a thousand specimens investigated. Nuclear division and cytokinesis occur as is usual.

Stomatogenesis commences with the formation of an oral primordium in or very near to kinety 1, that is, the posterior half of the rightmost postoral ciliary row, with an intense proliferation of basal bodies, soon forming three axially oriented protomembranelles each consisting of two basal body rows; at right, scattered basal bodies remain and later form the paroral membrane; the anterior portion of kinety 1 is not involved in stomatogenesis and later reorganizes to a new proter kinety 1 (Figs 27, 28). I could not clarify whether basal bodies of kinety 1 are included in the oral primordium. Figures 28 and 45, 46 indicate that this is not the case because a posterior fragment with an ordinary number of basal bodies becomes recognizable after the paroral has formed. Next, protomembranelles 2 and 3 become three-rowed, a patch of basal bodies ("X-group") separates from the anterior end of membranelle 2, and the posterior portion of the membranelles begins to invaginate and rotate clockwise. At right, the paroral is formed from the scattered basal bodies of the oral primordium, leaving back a short (parental?) row of basal bodies forming opisthe's kinety 1 (Figs 28, 32, 45, 46). In middle dividers (Fig. 29), the newly formed oral structures arrange transversely to the main body axis, membranelle 2 becomes four-rowed and begins to shorten, and the paroral membrane is distinctly dikinetidal. I could not clarify whether the fourth row of membranelle 2 originates de novo or by a re-arrangement of existing basal bodies; the latter is more likely, considering that the membranelle becomes shorter. When cytokinesis commences, the newly formed oral structures invaginate and obtain their specific shape and arrangement; further, the dikinetidal structure of the paroral becomes indistinct (Figs 30, 31).

Somatogenesis commences in early dividers with the intrakinetal proliferation of basal bodies and a rather early split of the ciliary rows in the prospective division furrow (Figs 27-29), except row 2, which splits only in late dividers, that is, when cytokinesis commences (Fig. 30). The rows split in the middle, even the strongly shortened postoral and left lateral kineties, producing an oblique division axis in early dividers (Figs 28, 29, 34). However, the disparity is balanced by an increased growth of the left side in middle dividers, generating the blank area left of the buccal cavity and transverse cytokinesis in late dividers (Figs 29-31). At the left margin of the blank area, two opisthe ciliary rows generate additional basal bodies forming two projecting kinetofragments (Fig. 29, arrow), which separate (Fig. 30) and migrate (Fig. 31) to the left margin of the buccal cavity (Fig. 26).

The silverlines connect all parental and newly-formed structures, including the separating ciliary rows (Fig. 32). The parental silverline system is not reorganized. The intermeridional connectives originate from foamy silverline arrays developing at the right margin of the right side and dorsal ciliary rows. The arrays are generated underneath the prospective division furrow and are, likely, outgrowths of the intrameridional silverline connecting the basal bodies within a row (Figs 33, 34). The loop-like intrameridional cross-fibres in the anterior portion of the right side ciliary rows develop in very late dividers.

DISCUSSION

Ordinal and familiar classification

Bromeliophrya has all main features of a tetrahymenide ciliate (Corliss 1979, Lynn 1994), specifically, it has a paroral membrane and three adoral membranelles in a deep buccal cavity and in tetrahymenid position (subapical) and arrangement (Figs 1, 5, 22, 35, 57-62). Further, it has a monoparakinetal stomatogenesis (Fig. 27) and a striated silverline pattern (Figs 19, 20, 49, 53, 54), as all "good" tetrahymenids have (Foissner 1996). Thus, *Bromeliophrya* belongs to the order Tetrahymenida Fauré-Fremiet in Corliss (1956).

Familiar classification is more difficult, although the "X-group" of basal bodies between the anterior ends of adoral membranelles 1 and 3 (Figs 5, 30, 59), the curved anterior portion of some right side somatic kineties (Figs 16, 20, 25, 35, 39, 41, 49), and ontogenesis (transverse orientation of oral anlagen in middle dividers; Fig. 29) suggest the Glaucomidae Corliss, 1971 as nearest relatives (Corliss 1971, Peck 1974, McCoy 1975, Foissner *et al*. 1994, Lynn 1994). In contrast, the somatic ciliature with the two large, unciliated areas and the migrating kinety fragments is unique for the whole order, suggesting separation of *Bromeliophrya* at family level (Figs 16, 29-31, 38, 39). This is emphasized by the unique, metopid body plan (shape) and the silverline pattern, which lacks the secondary meridians so prominent in many tetrahymenids, especially *Glaucoma* and *Colpidium* (Foissner *et al*. 1994). Note that the kineties at the left margin of the buccal cavity of, e.g., *Colpidium*

and *Turaniella*, are also fragments of somatic kineties, however, they do not migrate, as in *Bromeliophrya*, but originate by a simple split of kineties during buccal shaping (Foissner 1970, Iftode *et al*. 1984).

The high (family) rating of the somatic peculiarities of *Bromeliophrya* is based on the Structural Conservatism Hypothesis of Lynn (1976, 1981), which suggests that somatic cortical features are more strongly conserved than oral ones because they are subjected to less selective pressures. Accordingly, the particularities of the oral structures define the new genus *Bromeliophrya*, while those of the body define the new family Bromeliophryidae.

Bromeliophrya brasiliensis as a new genus and species

As mentioned above, the new genus *Bromeliophrya* is defined by its oral structures which are unique in that membranelles 1 and 3 extend along the buccal wall and thus form a ring-like pattern (Figs 5, 25, 26, 57-63), similar to that found in another curious genus, *Bursostoma*, which belongs either to the tetrahymenids or the ophryoglenids (Ganner *et al*. 1988, Lynn *et al*. 1991). Basically, however, the oral apparatus of *Bromeliophrya* resembles that of *Glaucoma*, not only by the X-group of basal bodies at the anterior end of membranelle 2, but also due to the loosened ciliary rows composing the anterior half of membranelle 3; membranelle 2, in contrast, is much more conspicuous in *Glaucoma* than *Bromeliophrya* (Corliss 1971, McCoy 1975, Foissner *et al*. 1994).

Another remarkable feature of *Bromeliophrya* is the unciliated paroral membrane (Figs 5, 26-31, 57-62). In this respect, *Bromeliophrya* resembles *Turaniella* (Iftode *et al*. 1984), which Lynn (1994) classifies in the family Turaniellidae, together with *Colpidium*, which has the paroral ciliated, like *Tetrahymena* in the family Tetrahymenidae. In *Glaucoma*, only the anterior portion of the paroral is ciliated. See Foissner *et al*. (1994) for SEM-micrographs of the paroral of *Tetrahymena*, *Glaucoma*, and *Colpidium*. Obviously, this feature is too progressive to be useful for family classification, but useful for defining genera.

To the best of my knowledge, there is no ciliate described in the literature resembling *B. brasiliensis*. Thus, it is a new species. Both the metopid body shape and the unique somatic ciliary pattern make it easily recognizable *in vivo* and silver preparations (Figs 1, 16, 39, 41-44).

Biogeographic considerations

As mentioned in the Introduction, I found several new ciliates in the tank of Brazilian bromeliads. Most are rather small (~ 100 µm) and thus comparatively inconspicuous. Accordingly, it can not be excluded that they occur also in ordinary freshwaters of South America, but were overlooked up to now. Unfortunately, reliable studies on free-living ciliates of South America are practically non-existant. Most of the literature is outdated, and even the few recent studies did not use modern methods, for instance, Cairns (1966) and Hardoim and Heckman (1996). But there is evidence that the South American ciliate biota contain a large number of undescribed species. Foissner (1997) reported 20 new species in two soil samples from the Amazon flood plain, and Steffens and Wilbert (2002) found several undescribed species in ephemeral flushs of Brazilian inselbergs.

However, we can be rather sure that *Bromeliophrya brasiliensis* and the other new species from tank bromeliads are absent in the much better investigated central Europe, suggesting that they have a restricted geographical distribution, like some other ciliates and testate amoebae (Foissner 1999). There is even some probability that they are restricted to bromelian tanks because one of them has a special life cycle (Foissner and Cordeiro 2000).

Acknowledgements. The technical assistance of Dr. B. Moser, Dr. E. Herzog, and Mag. E. Strobl is gratefully acknowledged. Financial support was provided by the Austrian Science Foundation (FWF Project P-15017).

REFERENCES

Cairns J., Jr. (1966) The Catherwood Foundation Peruvian-Amazon Expedition III - Protozoa. *Monogr. Acad. nat. Sci. Philad.* **14:** 53-61

Corliss J. O. (1952) Comparative studies on holotrichous ciliates in the *Colpidium-Glaucoma-Leucophrys-Tetrahymena* group I. General considerations and history of strains in pure culture. *Trans. Am. microsc. Soc.* **71:** 159-184

Corliss J. O. (1956) On the evolution and systematics of ciliated protozoa. *Syst. Zool.* **5:** 68-91, 121-140

Corliss J. O. (1971) Establishment of a new family (Glaucomidae n. fam.) in the holotrich hymenostome ciliate suborder Tetrahymenina, and description of a new genus (*Epenardia* n. g.) and a new species (*Glaucoma dragescui* n. sp.) contained therein. *Trans. Am. microsc. Soc.* **90:** 344-362

Corliss J. O. (1979) The Ciliated Protozoa. Characterization, Classification and Guide to the Literature. 2 ed. Pergamon Press, Oxford, New York, Toronto, Sydney, Paris, Frankfurt

Esteves C. B., da Silva Neto I. D. (1996) Study of Hymenostomatida ciliates found in water tanks of Bromeliaceae from Bracuhy Port, Angra dos Reis, Rio de Janeiro. *Mem. Inst. Osw. Cruz* **91 (Suppl.):** 63 (abstract)

Finlay B. J., Corliss, J. O., Esteban G., Fenchel T. (1996) Biodiversity at the microbial level: the number of free-living ciliates in the biosphere. *Quart. Rev. Biol.* **71:** 221-237

Foissner W. (1970) Corticale Morphogenese bei *Colpidium kleini* (Ciliata, Holotricha). *Acta Protozool.* **8:** 129-142

Foissner W. (1991) Basic light and scanning electron microscopic methods for taxonomic studies of ciliated protozoa. *Europ. J. Protistol*. **27:** 313-330

Foissner W. (1996) Ontogenesis in ciliated protozoa, with emphasis on stomatogenesis. In: Ciliates. Cells as Organisms (Eds. K. Hausmann, P. C. Bradbury). Fischer, Stuttgart, Jena, Lübeck, Ulm, 95-177

Foissner W. (1997) Soil ciliates (Protozoa: Ciliophora) from evergreen rain forests of Australia, South America and Costa Rica: diversity and description of new species. *Biol. Fertil. Soils* **25:** 317-339

Foissner W. (1999) Protist diversity: estimates of the near-imponderable. *Protist* **150:** 363-368

Foissner W., Cordeiro T. (2000) A new, peculiar colpodid ciliate from the tanks of a Brasilian bromeliad. *J. Eukaryot. Microbiol*. **47(Suppl.):** 9A, abstract 69

Foissner W., Berger H., Kohmann F. (1994) Taxonomische und ökologische Revision der Ciliaten des Saprobiensystems - Band III: Hymenostomata, Prostomatida, Nassulida. *Informationsberichte des Bayer. Landesamtes für Wasserwirtschaft* **1/94:** 1-548

Foissner W., Agatha S., Berger H. (2002) Soil ciliates (Protozoa, Ciliophora) from Namibia (Southwest Africa), with emphasis on two contrasting environments, the Etosha region and the Namib Desert. *Denisia* **5:** 1-1459

Ganner B., Foissner W., Adam H. (1988) Morphology and morphogenesis of *Bursostoma bursaria* Vörösváry, 1950 (Ciliophora, Ophryoglenina). *Annls Sci. nat. (Zool.)* **9:** 3-11

Hardoim E. L., Heckman C. W. (1996) The seasonal succession of biotic communities in wetlands of the tropical wet-and-dry climatic zone: IV. The free-living sarcodines and ciliates of the Pantanal of Mato Grosso, Brazil. *Int. Revue ges. Hydrobiol.* **81:** 367-384

Iftode F., Fryd-Versavel G., Lynn D. H. (1984) New details of the oral structures of *Colpidium* and *Turaniella* and transfer of the genus *Colpidium* to the Turaniellidae Didier, 1971 (Tetrahymenina, Hymenostomatida). *Protistologica* **20:** 463-474

Janetzky W., Vareschi E. (1992) Phytotelmata in bromeliads as microhabitats for limnetic organisms. In: Animal-Plant Interactions in Tropical Environments (Eds. W. Barthlott, C. M. Naumann, K. Schmidt-Loske, K. L. Schuchmann). Results of the Annual Meeting of the German Society for Tropical Ecology, Bonn 1992. Zoologisches Forschungsinstitut und Museum Alexander Koenig, 199-209

Laessle A. M. (1961) A micro-limnological study of Jamaican bromeliads. *Ecology* **42:** 499-517

Little T. J., Hebert P. D. N. (1996) Endemism and ecological islands: the ostracods from Jamaican bromeliads. *Freshwat. Biol.* **36:** 327-338

Lynn D. H. (1976) Comparative ultrastructure and systematics of the Colpodida. Structural conservatism hypothesis and a description of *Colpoda steinii* Maupas. *J. Protozool.* **23:** 302-314

Lynn D. H. (1981) The organization and evolution of microtubular organelles in ciliated Protozoa. *Biol. Rev.* **56:** 243-292

Lynn D. H. (1994) Ordre des Tetrahymenida Fauré-Fremiet in Corliss, 1956. *Traite Zool.* **2(2):** 791-812

Lynn D. H., Frombach S., Ewing M. S., Kocan K. M. (1991) The organelle of Lieberkühn as a synapomorphy for the Ophryoglenina (Ciliophora: Hymenostomatida). *Trans. Am. microsc. Soc.* **110:** 1-11

Maguire B., Jr. (1971) Phytotelmata: biota and community structure determination in plant-held waters. *Ann. Rev. Ecol. Syst.* **2:** 439-464

Martinelli G. (2000) Gefährdete Raritäten. Bromelien im atlantischen Regenwald. *Spektrum der Wissenschaft* **6/2000:** 66-73

McCoy J. W. (1975) Updating the tetrahymenids IV. Cortical properties of *Glaucoma*. *Protistologica* **11:** 149-158

Myers N., Mittermeier R. A., Mittermeier C. G., da Fonseca G. A. B., Kent J. (2000) Biodiversity hotspots for conservation priorities. *Nature* **403:** 853-858

Peck R. K. (1974) Morphology and morphogenesis of *Pseudomicrothorax, Glaucoma* and *Dexiotricha*, with emphasis on the types of stomatogenesis in holotrichous ciliates. *Protistologica* **10:** 333-369

Picado C. (1913) Les broméliacees épiphytes. Considérées comme milieu biologique (1). *Bull. scient. Fr. Belg.* **47:** 215-360

Steffens S., Wilbert N. (2002) Ciliates (Protozoa: Ciliophora) of selected ephemeral flushs on tropical inselbergs. *Int. Revue ges. Hydrobiol.* **27:** 401-410

Torres-Stolzenberg V. (2000) Procta em associacao com *Vriesea* sp. (Bromeliaceae): tres novos taxa de amebas testaceas (Protoctista: Rhizopoda, Testacealobosea). *Not. Faun. Gembloux* **41:** 105-113.

Van Oye P. (1923) De mikrofauna en flora der bladtrechters van Bromeliacea. *Natuurwet. Tijdschr.* **5:** 179-182

Received on 14th May, 2002; accepted on 5th September, 2002

Acta Protozool. (2003) 42: 71 - 73

ACTA
PROTOZOOLOGICA

A New Species of *Eimeria* from the Eared Dove *Zenaida auriculata* (Aves: Columbidae) in Brazil

Edson A. ADRIANO, Patrícia J. THYSSEN and Nelson S. CORDEIRO

Departamento de Parasitologia, Instituto de Biologia, Universidade Estadual de Campinas (UNICAMP), Campinas, São Paulo, Brasil

Summary. Thirty-four out of 142 (23.9%) eared doves, *Zenaida auriculata* Des Murs, 1847 had oocysts of an *Eimeria* species described here as a new species. Sporulation is exogenous and fully developed oocysts are spheroid to subspheroid, 23.8 µm (22.1-26.4) x 20.3 µm (19.2-22.1); the shape index (length/width ratio) is 1.2. The oocyst wall is bilayered, with a slightly pitted outer layer and a brown inner layer. There is no micropyle or oocyst residuum, but a prominent elongated polar granule is present. Sporocysts are elongated, 13.1 µm (12.0-14.4) x 7.4 µm (7.2-7.7); the shape index is 1.8 µm with a smooth, thin wall. A large Stieda body is present, but there is no sub-Stieda body. The sporocyst residuum consists of numerous, nearly uniform granules scattered randomly. Sporozoites are elongate with a large, clear refractile body in the posterior end and a smaller refractile body in the anterior region.

Key words: birds parasite, Brazil, coccidia, *Eimeria zenaidae* sp. n.

INTRODUCTION

The Columbidae consists of about 300 species of primarily granivorous and fructivorous birds with a cosmopolitan distribution (Bennett and Peirce 1990). In the neotropical region, 65 species are present (Stotz *et al*. 1996), 21 of which have been recorded in Brazil (Sick 1984).

Columbids of the genus *Zenaida* Bonaparte, 1838 are widely distributed in the New World (American Ornithologists' Union 1983). The eared dove, *Zenaida auriculata* Des Murs, 1847, is common in the neotropics and occurs from the Antilles to Tierra del Fuego (Sick 1984) in arid scrub areas, in open areas such as fields and farms and around human dwellings (Donatelli *et al*. 1994). In some regions of Brazil, *Z. auriculata* is an important agricultural pest because of its large numbers (Donatelli *et al*. 1994), while in other regions, such as in areas of arid scrub, this dove is an important food source (Aguirre 1976).

During a survey of Columbiformes parasites, carried out in the municipality of Junqueirópolis, São Paulo State, Brazil, we found a new species of *Eimeria* in the faeces of *Z. auriculata*. This is described below.

Address for correspondence: Edson A. Adriano, Departamento de Parasitologia, Instituto de Biologia, Universidade Estadual de Campinas (UNICAMP), C. P. 6109 Campinas, São Paulo, CEP. 13083-970, Brasil; Fax: +55-19-3788.6282; E-mail: andrian@unicamp.br

This work is part of a Masters thesis by E. A. Adriano

MATERIALS AND METHODS

One hundred and forty-two adult specimens of *Z. auriculata* were captured using gauze-traps (IBAMA 1994) in the municipality of Junqueirópolis, State of São Paulo, Brazil, from February to October,

1998. The doves were housed individually in cages for 2 h to obtain fecal samples, and then tagged and released. The fecal samples were examined microscopically after flotation, using Sheather's sugar solution. To determine the time to sporulation, fecal samples were placed in 2.5% potassium dichromate ($K_2Cr_2O_7$) at 23-28ºC. Photomicrographs were obtained using a Zeiss microscope and Kodak TMAX 100 film. Thirty-four oocysts and sporocysts were measured and compared to those of *Eimeria* spp. previously reported in Columbiformes. All measurements and means are in µm with the range given in parentheses followed by the shape index (length/width ratio).

RESULTS

Of 142 adult specimens of *Z. auriculata* examined, 34 (23.9%) had coccidian oocysts. A morphological comparison of these oocysts revealed differences between them and those of other *Eimeria* spp. from Columbiformes, as described below.

Eimeria zenaidae sp. n. (Figs 1-3)

Oocysts spheroid to subspheroid (Figs 1, 3), length 23.8 (22.1-26.4), width 20.3 (19.2-22.1), shape index (length/width) 1.2, wall of uniform thickness (1.7) and bilayered, composed of a slightly pitted outer layer, 1.2 thick, and brown inner layer 0.5 thick. One prominent elongated polar granule is present, but a micropyle and oocyst residuum are absent (Fig. 1). Sporocysts elongated (Figs 2, 3), length 13.1 (12.0-14.4), width 7.4 (7.2-7.7), shape index 1.8 (1.7-1.9), with smooth, thin, single-layered wall. A large Stieda body is present, but there is no sub-Stieda body. Sporocyst residuum composed of numerous, nearly uniform granules scattered randomly (Fig. 1). Sporozoites elongate with a large, clear refractile body in the posterior end and a smaller refractile body in the anterior region (Figs 1-3).

Type-host: eared dove, *Zenaida auriculata* Des Murs, 1847 (Aves: Columbidae).

Type location: municipality of Junqueirópolis, State of São Paulo, Brazil (21º 31' S, 51º 27' W).

Prevalence: 34/142 (23.9%) *Z. auriculata* examined were infected.

Site of infection: unknown, oocysts collected directly from host feces.

Time of sporulation: most oocysts sporulated within 38 h at 23-28ºC.

Type specimens: phototypes of oocysts are deposited in the collection of the Museum of Natural History of the Institute of Biology, State University of Campinas (UNICAMP), Campinas, State of São Paulo, Brazil (accession numbers ZUEC 08 and 09).

Etymology: the specific name is derived from the generic name of the host.

DISCUSSION

There have been so far recorded only two coccidian species parasitising columbids of the genus *Zenaida*: an unnamed *Eimeria* sp., reported by Conti and Forrester (1981) infecting *Zenaida asiatica* and *Zenaida macroura* in Florida, USA and *Eimeria palumbi*, described by McQuistion (1991) parasitising

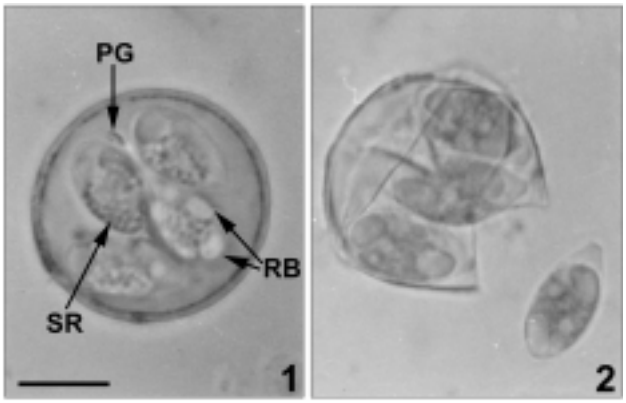

Figs 1, 2. Photomicrographs of sporulated oocysts of *Eimeria zenaidae* sp. n. **1** - typical oocyst showing the polar granule (PG), sporocyst residuum (SR) and refractile bodies (RB); **2** - broken oocyst with a free sporocyst; note the large Stieda body. Scale bar 10µm.

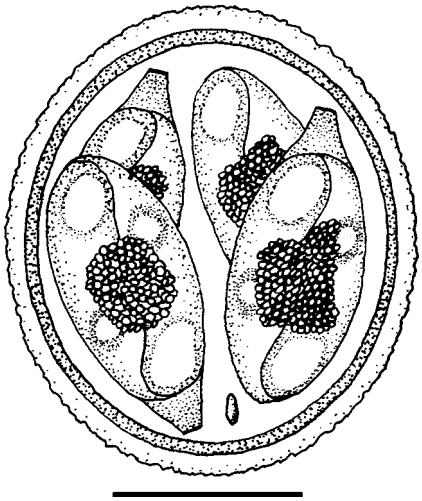

Fig. 3. Composite line drawing of a sporulated oocyst of *Eimeria zenaidae* sp. n. Scale bar 10 µm.

Zenaida galapagoensis in the Galapagos Archipelago, Equator.

This is the fisrt report of an *Eimeria* species in *Z. auriculata*. The morphological characteristics of *E. zenaidae* sporulated oocysts were compared to those of other *Eimeria* spp. previously described in Columbiformes. Only *Eimeria palumbi* McQuistion, 1991, found parasitising *Zenaida galapagoensis* from the Galapagos Archipelago, resembled the species described here in the size of its oocysts and sporocysts. However, the oocysts of *E. zenaidae* can be easily distinguished from those of *E. palumbi* by the absence of the residuum, the presence of a conspicuous elongated polar granule and by the slightly pitted aspect of the outer wall. The sporocysts of *E. zenaidae* differ from those of *E. palumbi* by the presence of an extremely large Stieda body and the presence of two refractile bodies, a large, clear one in the posterior end and a smaller one in the anterior region. Based on these characteristics, we consider the species described here to be a new coccidian for which the name *E. zenaidae* is proposed.

Acknowledgments. This work was supported in part by CAPES. The authors thank Elizeu Adriano and Evair Adriano for collaboration in the field work and Dr. Stephen Hyslop for correction of the English.

REFERENCES

Aguirre A. C. (1976) Distribuição, costumes e extermínio da "avoante" *Zenaida auriculata noronha* Chubb. Academia Brasileira de Ciências, Rio de Janeiro, RJ

American Ornithologist's Union. (1983) Check-list of North American Birds. 6th ed. Allen Press, Lawrence, Kansas

Bennett G. F., Peirce M. A. (1990) The haemoproteid parasites of the pigeons and doves (family Columbidae). *J. Nat. Hist.* **24:** 311-325

Conti J. A., Forrester D. J. (1981) Interrelationships of parasites of white-winged doves and mourning doves in Florida. *J. Wild. Dis.* **17:** 529-536

Donatelli R. J., Gezzeta C., Silva M. C., Serra M. A. S., Pezzutto N. L., Andrela S., Leonel W. (1994) Aspectos da biologia reprodutiva de *Zenaida auriculata* Des Murs, 1847 (Aves: Colubiformes). *Salusvita* **13:** 71-85

IBAMA (1994) Manual de anilhamento de aves silvestres. 2nd ed. Instituto Brasileiro do Meio Ambiente e dos Recursos Naturais Renováveis, Brasília

McQuistion T. E. (1991) *Eimeria palumbi*, a new coccidian parasite (Apicomplexa: Eimeriidae) from the galapagos dove (*Zenaida galapagoensis*). *Trans. Am. Microsc. Soc.* **110:** 178-181

Sick H. (1984) Ornitologia brasileira, uma introdução. Vol. I. 3rd ed. Editora Universidade de Brasília, Brasília

Stotz D. F., Fitzpatrick J. W., Parker T. A., Moskovits D. V. (1996) Neotropical Birds. Ecology and Conservation. The University of Chicago Press, Chicago

Received on 26th June, 2002; accepted on 16th October, 2002

Acta Protozool. (2003) 42: 75 - 80

ACTA
PROTOZOOLOGICA

Corythionella golemanskyi sp. n.: a New Freshwater, Filose, Testate Rhizopod

Kenneth H. Nicholls

S-15 Concession 1, RR #1, Sunderland Ontario, Canada L0C 1H0

Summary. A previously undescribed species of *Corythionella* was discovered in three widely separated freshwater lakes in Ontario, Canada. A formal description of this species (*Corythionella golemanskyi* sp. n.) is given, together with comments on related taxa in the Testaceafilosia. Tightly packed elliptical (and occasionally circular) scales, a small, flared oral collar and a rounded-triangular cross-sectional shape of the test set *C. golemanskyi* apart from all other *Corythionella* species.

Key words: *Corythionella golemanskyi* sp. n., Cyphoderiidae, Euglyphida, Filosea, Psammonobiotidae, Pseudocorythionidea, Testaceafilosia.

INTRODUCTION

Over the past three decades, a rich and diverse assemblage of testate amoebae inhabiting the supralittoral zones of marine beaches has been described (Golemansky 1974, 1998a; Chardez 1977). Comparable freshwater communities are not known, perhaps because these habitats have been largely ignored in limnological and biotic surveys of freshwater lakes. Beginning in 1997 (Nicholls 1998), the supralittoral of some freshwater beaches and nearshore littoral sands were sampled as part of a broader investigation of testate rhizopods in freshwater habitats in Ontario, Canada. The purpose of this paper is to describe *Corythionella golemanskyi* sp. n., a previously undescribed filose testacean discovered in three widely separated freshwater lakes in Ontario, Canada.

Address for correspondence: Kenneth H. Nicholls, S-15 Concession 1, RR #1, Sunderland Ontario, Canada L0C 1H0; E-mail: khnicholls@interhop.net

MATERIALS AND METHODS

Samples of nearshore (submerged) and supralittoral sand (100-1000 cm^3) were collected with a garden trowel and placed in a clean pail with about 1 l of lake water. After thorough mixing to dislodge and suspend any organisms attached to sand grains, the supernatant was poured off into 500 ml polycarbonate screw-capped bottles for transportation on ice to the laboratory. Another portion (25 ml) was immediately preserved with formalin (about 1.5 % formaldehyde).

Living and preserved samples were examined with an inverted microscope using a 10x objective under dark-field illumination for initial detection and high power (40x and 100x oil immersion objectives) with Zernike phase-contrast for critical measurements and examination of scale structure of rhizopod tests. Isolation of single specimens was done with a micro-pipette (drawn out in a flame); manipulation of single specimens to facilitate measurements in two dimensions was by hand with a single-hair brush. Specimens were

mounted in Styrax® or Canada Balsam to aid in measurement of scales and for permanent preservation of type material. Test dimensions and terminology were as portrayed in Figs 1 and 2. Statistical data describing test morphology (mean, standard deviation, median, minimum, maximum, coefficient of variation) and Mann-Whitney *U*-tests of significant difference between populations were done in *CoStat* (CoHort Software 1995).

RESULTS

Corythionella golemanskyi sp. n.

Phylum, Rhizopoda; Class, Filosea; Subclass, Testaceafilosia; Family, Cyphoderiidae

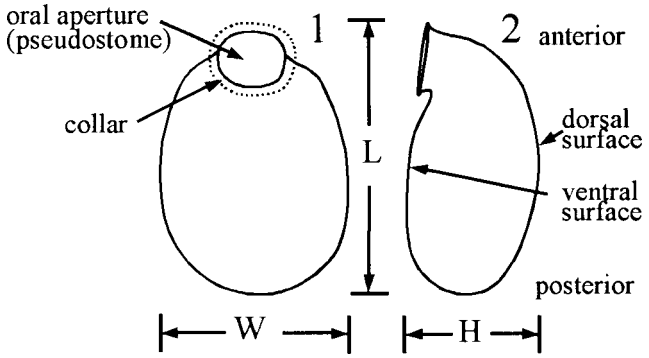

Figs 1, 2. Diagrammatic representation of the, **1** - ventral and **2** - left lateral views of *Corythionella golemanskyi* sp. n. illustrating the main test dimensions for which descriptive statistics were compiled (Table 2); keyed as follows: L - total test length; W - test width; H - test height.

Diagnosis: test, translucent, pale yellow in colour, elongate-elliptical to nearly circular in outline (ventral and dorsal views); wider than high, rounded-triangular in cross-section. Oral aperture not invaginated, but separated from the main body of the test by a short neck and surrounded by a flared collar about 2 µm wide. Diameter of the oral aperture 15-22 µm, including the flared collar. Test length, 45-62 µm; width, 31-49 µm; height, 23-30 µm. Test covered with small elliptical (occasionally circular) silica scales, 1.5-2.7 µm. Scales are densely arranged, sometimes overlapping at their margins. Protoplast with long, sometimes branching filose pseudopodia.

Etymology: the specific epithet is in honour of Prof. Dr. Vassil Golemansky, who pioneered the study of marine sand-dwelling rhizopods over the past 35 years and who has provided much help with reprints and other information during the course of my investigations.

Type specimen: the type specimen mounted in Canada Balsam on a glass slide, was deposited with the Invertebrate Zoology Division, Canadian Museum of Nature, Catalogue No. CMNI-2002-0001.

Holotype material: retained by the author in sample No. V-1321, collected 12 October, 1999.

Type Locality: littoral zone sands of Sibbald Point Provincial Park, Lake Simcoe, Ontario, Canada (44° 18' N; 79°18' W).

Specimens of *C. golemanskyi* were first found in samples collected 12 October, 1999 at Sibbald Point Provincial Park, Lake Simcoe, but others were later discovered in collections of submerged beach sand made September 5, 2001 at Dorcas Bay, Lake Huron (45°11'30"N; 81°35' W), and January 23, 2002 from the littoral zone of Mazinaw Lake, Ontario (44°50'N; 77°15' W). These three lakes range widely in size and depth, but all have generally excellent water quality with low concentrations of N and P (Table 1). The Lake Simcoe and Lake Huron collections contained specimens in adequate abundance for statistical comparisons of the test dimensions of the two populations (Table 2).

There was no significant difference in test length between the Lake Simcoe and Lake Huron populations (medians of 55.5 and 55 µm, respectively); although in all

Table 1. Comparative morphometric and water quality data for the three Ontario lakes from which *Corythionella golemanskyi* sp. n. was collected. Data are summer average values from OWRC (1971), Nicholls (1995) and the Ontario Ministry of the Environment (unpublished).

	Lake Huron	Lake Simcoe	Mazinaw Lake
Lake area (km^2)	59500	722	16
Maximum depth (m)	230	40	145
Total alkalinity (mg/l)	80	125	20
Conductivity (µmhos/cm)	220	350	100
Total phosphorus (µg P/l)	8	11	6
Total inorganic N (µg N/l)	550	20	50
Total organic N (µg N/l)	310	380	250
Total chlorophyll *a* (µg/l)	4	5	1.2

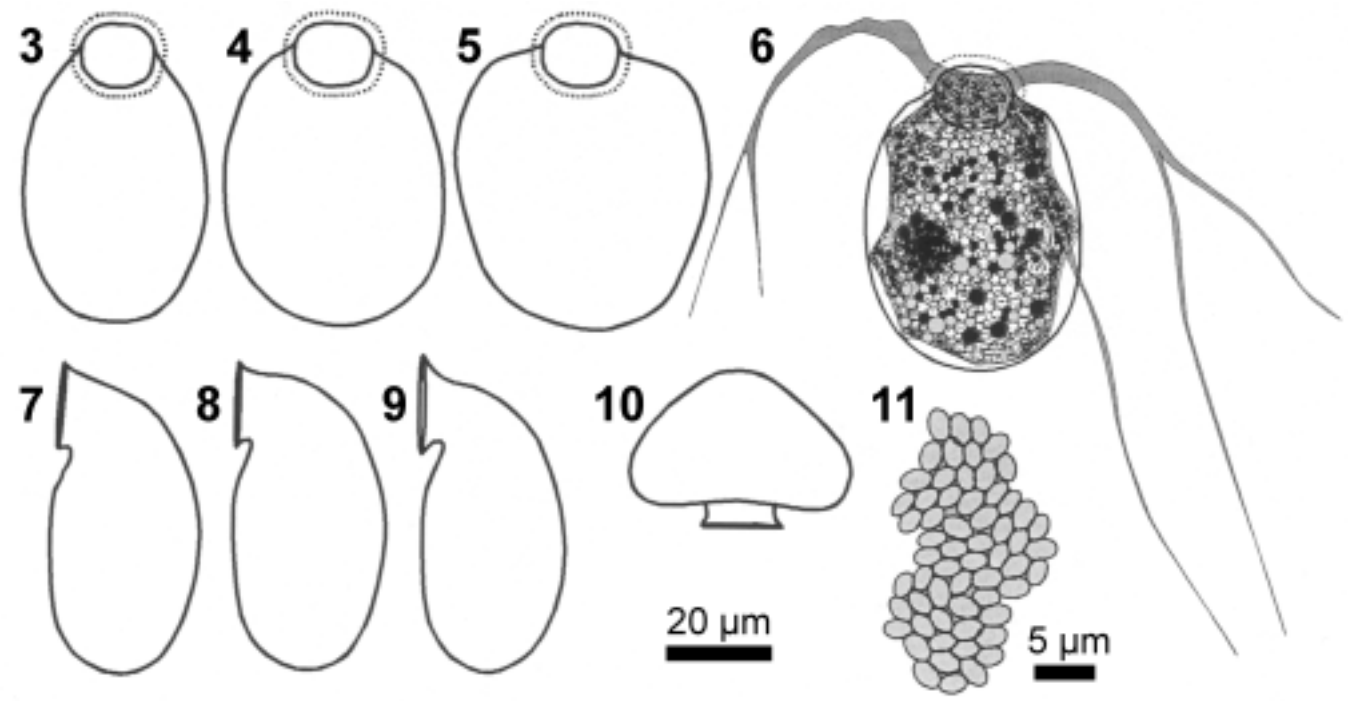

Figs 3-11. Some examples of form variation in test, pseudopod and test scales of *Corythionella golemanskyi* sp. n.; **3-5** - test shapes in ventral views; **6** - representation of a living cell with extended pseudopodia; **7-9** - test shapes in left lateral views; **10** - optical cross-section of the test showing rounded triangular form; **11** - scales covering the test.

Table 2. Descriptive statistics for critical test dimensions of *Corythionella golemanskyi* sp. n. from Lake Huron and Lake Simcoe. Units of measurement are µm; L = length; W = width; H = height; PS = oral aperture excluding collar; CO = outer diameter of oral collar (see Figs 1 and 2). Mann-Whitney *U*-test probabilities greater than 0.05 are considered indicative of a strong likelihood of no significant difference between the two populations.

Lake Simcoe		L	W	H	PS	CO
	Mean	55.2	34.3	27.4	13.4	17.6
	Median	55.5	33.5	28	13	17
	Minimum	45	31	24	12	15
	Maximum	62	42	30	16	22
	SD	4.6	3.0	1.9	1.3	1.9
	CV (%)	8.5	8.7	6.9	9.7	10.7
	N	22	22	21	21	21
Lake Huron		L	W	H	PS	CO
	Mean	54.9	38.2	25.2	14.6	18.8
	Median	55	39	25	15	19
	Minimum	47	33	23	13	16
	Maximum	59	49	30	16	21
	SD	3.0	3.8	1.4	0.8	1.5
	CV (%)	5.5	10.2	5.5	5.6	8.0
	N	21	21	21	21	21
Mann-Whitney *U*-test probability		0.751	0.0008	0.0002	0.001	0.031

other dimensions, the tests from Lake Huron were significantly larger (Mann-Whitney U-test probabilities all < 0.05; Table 2). Despite some variability in overall test shape in both populations (Figs 3-5, 7-9, 12-16), test width was greater than test height in all 42 specimens measured. The ratio W:H was significantly greater in the Lake Huron population. Test cross-section had the appearance of a very rounded isosceles triangle with a

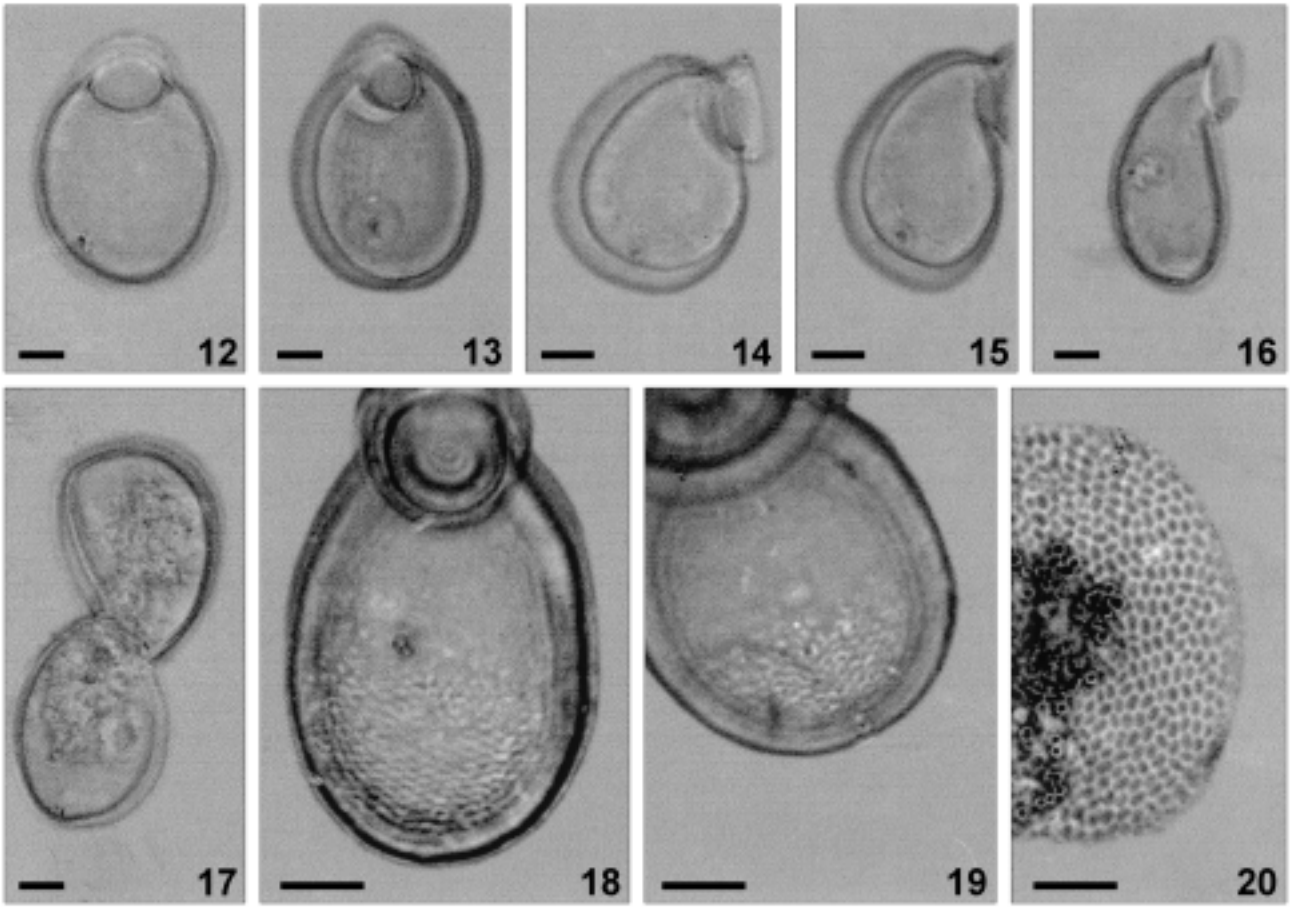

Figs 12-20. Photographs of *Corythionella golemanskyi* sp. n. tests. **12, 13** - ventral views; **14** - oblique lateral view; **15, 16** - lateral views; **17** - reproduction (tests are joined at their oral apertures); **18, 19** - scales covering the test are faintly visible in the posterior regions of the tests (mounted in water); **20** - Scales covering test (dried and mounted in Canada Balsam). Scale bars 10 µm.

slightly concave base that was greater in length than height (Fig. 10). In optimum optical cross-sectional views (most easily achieved after the specimen was transferred to a viscous medium (e.g. glycerol) and manipulated with a single hair brush), the collar surrounding the oral aperture could be seen as a projection from the base of the test (Fig. 10).

Scales on the test surface (Figs 11, 18, 19) were difficult to see, even with oil immersion, phase contrast optics. Visualization improved after drying and mounting in media with a high refractive index (Fig. 20), but this method tended to obscure the slight marginal overlap of many of the scales seen in specimens mounted in water. Most scales on the main body of the test were elliptical, measuring 1-1.5 µm wide x 1.5-2.7 µm long. Occasional circular scales were also present. Scales in the anterior region of the test in the area surrounding the oral aperture were smaller than those on the main body of the test.

Protoplasts observed in living specimens of this species appeared to be typical of the family; for example, pseudopodia were very *Cyphoderia*-like (Fig. 6). Another typical characteristic of living cells was the occurrence of multiple attachment points of the plasma membrane with the interior of the test, separated by concavities in regions of the protoplast where there was no contact with the test wall (Fig. 6).

DISCUSSION

The genus *Corythionella* was erected by Golemansky (1970) to include *Pseudocorythion*-like taxa with tests covered with endogenously produced elliptical or oval

(*Corythion*-like) scales *(Pseudocorythion* tests have circular imbricated scales). *Corythionella* differs from *Corythion* in the structure of the pseudostome which, in *Corythion,* is invaginated and surrounded by a series of specialized toothed scales; *Corythionella* lacks these toothed scales and its pseudostome is not invaginated. In all but one species (*C. acolla* Gol.) the pseudostome is surrounded by a flared collar, which, like the rest of the test, is covered with scales. There are six known species of *Corythionella*: *C. pontica* Gol., *C. acolla* Gol. *C. minima* Gol., *C. anteroplanata* Chardez, *C. sudzukii* Chardez, and *C. minima* var. *nipponica* Sudzuki [I presume that Sudzuki (1979a) intended this latter taxon to be a subspecies, not a variety, as defined by Article 45 (g) of the Int. Code Zool. Nomenclature (ICZN 1985). There is, however, considerable confusion surrounding the nomenclature for this taxon. In Sudzuki (1979a, bottom of p. 288) he refers to it as "*P. minima* var. *nipponica"* (implying *Pseudocorythion*?) in a section of the paper headed *Corythionella*; but, in the same paper the caption of his Fig. 12 clearly states "*Corythionella minima* var. *nipponica*". In a companion publication (Sudzuki 1979b), he referred to this taxon as "*C. minima* f. *nipponica* Sud. '79"].

The flared collar in *C. golemanskyi* is only slightly greater than the pseudostome diameter. *C. minima, C. minima* var. *nipponica,* and *C. pontica* all have flared pseudostome collars that are much greater in size, being about equal in diameter to the main body of the test. *C. acolla* lacks a pseudostome collar. Other differences between *C. golemanskyi* and *C. acolla* include the apparently large inter-scale spaces in the investiture of test scales [e.g. see figure 5 in Golemansky (1973)] and the smaller size of *C. acolla*. Chardez (1977) reports sizes for *C. acolla* that are about one-half those measured for *C. golemanskyi*.

Corythionella sudzukii Chardez (1977) is closest to *C. golemanskyi* in the proportional sizes of the pseudostome and flared collar, but overall test size in *C. sudzukii* is much smaller (L = 26-30 µm; W = 10-15 µm; H = 8-10 µm; PS = 4-7 µm; CO = 6-11 µm). Also, Chardez's (1977) figure 6 suggests that test scales in *C. sudzukii* are large and much more elongate than in *C. golemanskyi*. The main feature separating *C. anteroplanata* (Chardez 1977) from all other species of this genus is its highly compressed anterior (marked dorso-ventral flattening). The tightly packed elliptical (occasionally circular) scales, the small flared oral collar and the rounded triangular cross-sectional shape of the test set *C. golemanskyi* apart from all other *Corythionella* species.

The only critical study of *Corythionella* scales has been done by Ogden and Coûteaux (1989). They showed that the SEM structure of the scales on the collar of *C. pontica* were smaller than those covering the main body of the test; they also differed in shape, being more elongate with nearly parallel sides (their figure 11). There is, however, some question about whether or not their specimen is really *C. pontica*; the collar (though damaged - see their figure 9) is very narrow relative to the test body width, and the total test length, estimated at about 40 µm from their figure 9, is much too short for *C. pontica*. Test lengths for *C. pontica* given by Golemansky (1970, 1998b) are 77-96 µm. Ogden and Coûteaux (1989) may have described the scales on *C. minima,* or some other (perhaps undescribed) species.

The taxonomy of the genus *Corythionella* and the related genera *Pseudocorythion* and *Messemvriella* is not clearly defined at the family level. All three were placed in the family Psammonobiontidae along with other marine psammonobionts like *Psammonobiotus* and *Chardezia* by Golemansky (1974); but Sudzuki (1979b) proposed a new family (Pseudocorythionidae) for *Pseudocorythion* (and others) and that a new sub-family, Corythionellinae, be erected for *Corythionella* and another taxon he described as "*Pseudowailesella*". Unfortunately, several of the new taxa described by Sudzuki (1979b) were inadequately described, so the logic of his proposed family and sub-family taxonomy is not entirely convincing at this point in time. Taxa like Sudzuki's "*Corythionelloides*", *Micropsammelloides*", and "*Pseudowailesella*" await rediscovery and critical examination before Sudzuki's taxonomy can be accepted. In the interim, Meisterfeld (2002) has suggested an appropriate (but perhaps temporary) solution to the taxonomy of this group, whereby both *Pseudocorythion* and *Corythionella* were placed in the family Cyphoderiidea de Saedeleer, 1934. This proposal is attractive because it groups together at the family level all taxa having (i) a test covered in endogenously produced scales, and (ii) a non-invaginated pseudostome at the anterior terminus of a curved neck. The revised family Psammonobiotidae continues to include genera with pseudostome morphology like those in the Cyphoderiidae, but their tests consist of an uncovered organic matrix or are covered in particles of exogenous, not endogenous, origin.

Although it has a test structure that would otherwise qualify it for membership in the Cyphoderiidae, *Corythion* must remain in the separate family Trinematidae, because it has an invaginated pseudostome with a surrounding row of specialized toothed scales (like its sister genera *Trinema*, *Pileolus* and *Puytoracea*, in the same family).

It was not without considerable vacillation that I assigned *C. golemanskyi* to the genus *Corythionella*. Some characteristics of this species (the occasional presence of circular, overlapping scales) suggest affinities with the genera *Pseudocorythion* and *Messemvriella*. The scale structure of *C. golemanskyi* is intermediate between that generally typical of *Corythionella* (ellipsoidal, or oval and non-imbricate) and that of *Pseudocorythion* and *Messemvriella* (circular, imbricate). The dorsal-ventral compression (width>height), the cross-sectional rounded-triangular shape and rounded posterior, together with its predominantly elliptical scales is justification for assignment of *C. golemanskyi* to the genus *Corythionella*, in my view. Still, the distinguishing features of the three genera *Corythionella*, *Pseudocorythion* (test with a pointed posterior) and *Messemvriella* (tests with a rounded posterior) relating to minor differences in scale structure and test shape might be better ascribed to species differences within a single genus rather than generic differences. For example, Chardez (1979) has shown that the posteriors of specimens of *Pseudocorythion undulacollis* Chardez & Thomas from Corsica are highly variable and include some with rounded as well as pointed posteriors. It is possible that further study of these and related taxa will result in some new taxonomic combinations.

REFERENCES

Chardez D. (1977) Théamoebiens du mésopsammon des plages de la Mer du Nord. *Rev. Verviétoise d'Histoire naturelle*. **34:** 3-19

Chardez D. (1979) Étude cytologique et variations morphologiques chez *Pseudocorythion undulacollis* Chardez et Thomas, thecamoebien psammophile. *Ronéo chez l'auteur*

CoHort Software (1995) *CoStat*. Minneapolis, Minnesota, 55419, U.S.A.

Golemansky V. (1970) Rhizopodes nouveaux du psammon littoral de la mer Noire. *Protistologica* **6:** 365-371

Golemansky V. (1973) Deuxième contribution à la connaissance des théamoebiens (Rhizopoda, Testacea), du psammal littoral de la Mer Baltique. *Bull. Inst. Zool. Mus. (Bulgaria)* **38:** 49-60

Golemansky V. (1974) Psammonobiotidae fam. nov. - une nouvelle famille de thécamoebiens (Rhizopoda, Testacea) du psammal supralittoral des mers. *Acta Protozool*. **13:** 137-141

Golemansky V. (1998a) Interstitial testate amoebae (Rhizopoda: Arcellinida and Gromida) from the Finnish coast of the Baltic Sea and summary check list of the interstitial amoebae in the Baltic Sea. *Acta Protozool*. **37:** 133-137

Golemansky V. (1998b) Interstitial testate amoebae (Rhizopoda: Testacea) from the sand supralittoral of the eastern Marmorean coast (Turkey). *Acta Zool. Bul.* **50:** 3-7

ICZN (1985) International Code of Zoological Nomenclature adopted by the XX General Assembly of the International Union of Biological Sciences. International Commission on Zoological Nomenclature. University of California Press, Berkeley

Meisterfeld R. (2002) Testate amoebae with filopodia. In: An Illustrated Guide to the Protozoa, (Eds. J. J. Lee, G. F. Leedale and P. Bradbury). 2 ed., Society of Protozoologists, Lawrence, Kansas, **2:** 1054-1084

Nicholls K. H. (1995) Some recent water quality trends in Lake Simcoe, Ontario: implications for basin planning and limnological research. *Can. Water Res. J.* **20:** 213-226

Nicholls K. H. (1998) *Amphidiniopsis sibbaldii* sp. nov. (Thecadiniaceae, Dinophyceae), a new freshwater sand-dwelling dinoflagellate. *Phycologia* **37:** 334-339

Ogden C.G., Coûteaux M-M. (1989) Interstitial marine rhizopods (Protozoa) from the littoral sands on the east coast of England. *Europ. J. Protistol.* **24:** 281-290

OWRC (1971) Report on water quality in Mazinaw and Mackavoy Lakes, 1971. Recreational Lakes Program. Ontario water Resources Commission. Toronto

Sudzuki M. (1979a) Psammobiont Rhizopoda and Actinopoda from marine beaches of Japan. *Acta Protozool*. **18:** 293-304

Sudzuki M. (1979b) Marine Testacea of Japan. *Sesoko Mar. Sci. Lab., Tech. Rep.* **6:** 51-61

Received on 7th October, 2002; accepted on 29th November, 2002

Acta Protozool. (2003) 42: 81 - 82

ACTA
PROTOZOOLOGICA

Book Review

Soil Ciliates (Protozoa, Ciliophora) from Namibia (Southwest Africa), with Emphasis on Two Contrasting Environments, the Etosha Region and the Namib Desert. Part I. Text and Line Drawings. Part II. Photographs. W. Foissner, S. Agatha and H. Berger. Denisia, Vol. 5. Linz, Austria. 2002. ISSN 1608-8700. 1459 pp., 443 figures, 203 tables, hard covers. 150 € (*ca* $150 U.S.)

Once again, Wilhelm Foissner (and colleagues) have produced a monumental profusely illustrated taxonomic work on the ciliated Protozoa, this time requiring two volumes. Emphasis is on generic and species uniquenesses and on diversity and community structure within restricted habitats (collections were taken from some 73 specific sites) located in the Namibian area of Southwest Africa. It is to be noted that most "classical" types of fresh-, estuarine, and salt-water habitats, although present in Namibia, were deliberately excluded from the present (time-limited and already massive!) research project on principally soil forms. The monograph is in English!

As typical of the experienced Foissner teams, taxonomic study techniques included observations on living material, TEM and (mostly) SEM ultrastructural methods, and wide employment of silver impregnation for examination by light microscopy of carefully fixed specimens. Type material (preserved on *ca* 800 slides) has been deposited in the Museum of Upper Austria in Linz. Rules from the latest edition of the International Code of Zoological Nomenclature have been followed rigorously.

The fine illustrations merit special comment. Actual figures number far more than the "443" mentioned in the heading of this review. Typically, one "Figure" alone contains multiple drawings or photographs of a given species, including different body views and highlighting different organelles or particular structures or stages in the life cycle of the organism. For admittedly perhaps an extreme example of such multiplicity, 13(!) plates/pages of Vol. II are devoted to such figures of the single colpodid species *Exocolpoda augustini* (for which a new genus has been created). The entire 395 pages of Vol. II are filled with 2500 excellent photographs! The first 79 of them are in color, the remaining black-and-white ones average over half-dozen to a "Figure" and are mainly of living organisms, silver impregnated specimens, or SEM images. A few collection sites have also been photographed.

In the 1063 pages of Part I (Vol. I of the set), we find another 221 Figures (with multiple line drawings per "Figure") of the same - and sometimes different - species as those displayed so beautifully in the much slimmer Part II (Vol. II). But here, of course, we also find the text of the whole monograph and the full taxonomic (and nomenclatural) identifications or descriptions of some 365 species, new (*ca* 40%) and/or old, included in the overall study. Involved as well are descriptions of a new order and suborder, three new families, and 33 new genera and subgenera. And there is a 100-page section on ecology with emphasis on species distribution and their community structure. The great majority of the 203 Tables in this monograph is devoted to detailed morphometric data on the individual species studied.

In addition to the helpful "summarizing" tables near the beginning of Vol. I, where all species involved are listed and very briefly identified, the volume concludes with an extensive Systematic Index of 16 pages. Here, bonafide (valid, acceptable, "good") species, genera, etc. and their names are helpfully differentiated by type of print from the non-acceptable (in the authors' opinion). Multiple page numbers supplied refer only to locations in Vol. I; however, when one consults such pages, one discovers references to pages of Vol. II where photographic figures are found for many species.

A special word should also be said about the 21-page References section (located in Vol. I, just preceding the Systematic Index). It is a treasure trove indeed of ciliate literature relevant to the topics treated in the monograph, including older as well as very recent papers of significance. Out of the total of some 525 titles given, well over 20% represent publications - *not* inappropriately - from the Foissner school (with 86 of them sole- or senior-authored by Wilhelm Foissner himself). They offer evidence not only of Foissner's experience in taxonomic ciliatology built up over the past 25 years but also of his leadership ability. Incidentally, there are still additional (non-cited) papers by the prolific Austrian, and another big monograph is currently in press.

This review is not the place for a discussion of some of the controversial matters in modern ciliate biology, taxonomy, and ecology; for example, those involving the definition of a "true" species or endemism *versus* ubiquity of diverse species around the world. The Foissner school's view on such topics is generally the opposite to that of what we may call the Finlay-Fenchel-Esteban school's view. The latter group has offered data in support of its contention that most, probably all, free-living species are, or potentially are, cosmopolitan in nature. Thus only a few, generally the so-called cryptic species, may remain largely undescribed. Foissner, on the other hand, feels strongly that *his* researches prove beyond doubt that new species, many considered "endemics" geographically, exist in abundance awaiting proper taxonomic description. It is true that numerous general biologists, apparently plus many phycologists and some other protistologists, have an "intuitive feeling," at least, that protistan species yet-to-be-described (free-living and parasitic) may number in the tens of thousands. So the controversies mentioned briefly above probably require further studies for clearer resolution.

John O. Corliss
P.O. Box 2729
Bala Cynwyd, PA 19004, U.S.A.

INSTRUCTIONS FOR AUTHORS

ACTA PROTOZOOLOGICA publishes original papers on experimental or theoretical research in all fields of protistology with the exception of faunistic notices of local character and purely clinical reports. Short communications, as well as longer review articles may also be submitted. Contributions should be written in English. Submission of a manuscript to ACTA PROTOZOOLOGICA implies that the contents are original and have not been published previously, and are not under consideration or accepted for publication elsewhere. There are no page charges except colour illustration. Names and addresses of suggested reviewers will be appreciated. In case of any question please do not hesitate to contact Editor. Authors should submit papers to:

Mrs Małgorzata Woronowicz-Rymaszewska
Managing Editor of ACTA PROTOZOOLOGICA
Nencki Institute of Experimental Biology,
ul. Pasteura 3
02-093 Warszawa, Poland
Fax: (4822) 822 53 42
E-mail: jurek@ameba.nencki.gov.pl

Extensive information on ACTA PROTOZOOLOGICA is now available *via* internet. The address is: **http://www.nencki.gov.pl/ap.htm**

Organization of Manuscripts

Submissions

Please enclose three copies of the text, one set of original of line drawings (without lettering!) and three sets of copies with lettering, four sets of photographs (one without lettering). In case of photographs arranged in the form of plate, please submit one set of original photographs unmounted and without lettering, and three sets of plates with lettering.

The ACTA PROTOZOOLOGICA prefers to use the author's word-processor disks (format IBM or IBM compatible, and MacIntosh 6 or 7 system on 3.5" 1.44 MB disk only) of the manuscripts instead of rekeying articles. If available, please send a copy of the disk with your manuscript. Preferable programs are Word or WordPerfect for Windows. Disks will be returned with galley proof of accepted article at the same time. Please observe the following instructions:

1. Label the disk with your name: the word processor/computer used, e.g. IBM; the printer used, e.g. Laserwriter; the name of the program, e.g. Word for Windows.
2. Send the manuscript as a single file; do not split it into smaller files.
3. Give the file a name which is no longer than 8 characters.
4. If necessary, use only italic, bold, underline, subscript and superscript. Multiple font, style or ruler changes, or graphics inserted the text, reduce the usefulness of the disc.
5. Do not right-justify and use of hyphen at the end of line.
6. Avoid the use of footnotes.
7. Distinguish the numerals 0 and 1 from the letters O and l.

Text (three copies)

The text must be typewritten, double-spaced, with numbered pages. The manuscript should be organized into Summary, Key words, Abbreviations used, Introduction, Materials and Methods, Results, Discussion, Acknowledgements, References, Tables and Figure Legends. The Title Page should include the full title of the article, first name(s) in full and surname(s) of author(s), the address(es) where the work was carried out, page heading of up to 40 characters. The present address for correspondence, Fax, and E-mail should also be given.

Each table must be on a separate page. Figure legends must be in a single series at the end of the manuscript. References must be listed alphabetically, abbreviated according to the World List of Scientific Periodicals, 4th ed. (1963). Nomenclature of genera and species names must agree with the International Code of Zoological Nomenclature, third edition, London (1985) or International Code of Botanical Nomenclature, adopted by XIV International Botanical Congress, Berlin, 1987. SI units are preferred.

Examples for bibliographic arrangement of references:

Journals:

Häder D-P., Reinecke E. (1991) Phototactic and polarotactic responses of the photosynthetic flagellate, *Euglena gracilis*. *Acta Protozool.* **30:** 13-18

Books:

Wichterman R. (1986) The Biology of *Paramecium*. 2 ed. Plenum Press, New York

Articles from books:

Allen R. D. (1988) Cytology. In: *Paramecium*, (Ed. H.-D. Görtz). Springer-Verlag, Berlin, Heidelberg, 4-40

Zeuthen E., Rasmussen L. (1972) Synchronized cell division in protozoa. In: Research in Protozoology, (Ed. T. T. Chen). Pergamon Press, Oxford, **4:** 9-145

Illustrations

All line drawings and photographs should be labelled, with the first author's name written on the back. The figures should be numbered in the text as Arabic numerals (e.g. Fig. 1). Illustrations must fit within either one column (86 x 231 mm) or the full width and length of the page (177 x 231 mm). Figures and legends should fit on the same page. Lettering will be inserted by the printers and should be indicated on a tracing-paper overlay or a duplicate copy.

Line drawings (three copies + one copy without lettering)

Line drawings should preferably be drawn about twice in size, suitable for reproduction in the form of well-defined line drawings and should have a white background. Avoid fine stippling or shading. Computer printouts of laser printer quality may be accepted, however *.TIF, *.PSD, *.CDR graphic formats **(Grayscale and Color - 600 dpi, Art line - 1200 dpi)** on CD are preferred.

Photographs (three copies + one copy without lettering)

Photographs at final size should be sharp, with a glossy finish, bromide prints. Photographs grouped as plates (in size not exceeding 177 x 231 mm including legend) must be trimmed at right angles accurately mounted and with edges touching and mounted on firm board. The engraver will then cut a fine line of separation between figures. Magnification should be indicated. Colour illustration (charged) on positive media (slides 60 x 45 mm, 60 x 60 mm, transparency or photographs) is preferred.

Proof sheets and offprints

Authors will receive one set of page proofs for correction and are asked to return these to the Editor within 48-hours. Fifty reprints will be furnished free of charge. Orders for additional reprints have to be submitted with the proofs.

Indexed in Biosis, Current Contents (Agriculture, Biology and Environmental Sciences), Elsevier BIOBASE/Current Awareness in Biological Sciences, Protozoological Abstracts, Science Citation Index, Chemical Abstracts Service, Librex-Agen, Polish Scientific Journals Contents - Agric. & Biol. Sci. Data base are available in INTERNET under URL (Uniform Resource Locator) address: http://psjc.icm.edu.pl any WWW browser; Abstracts and Whole Articles Free in http://www.nencki.gov.pl/ap.htm; in graphical operating systems: MS Windows, Mac OS, X Windows - mosaic and Netscape programs and OS/2 - Web Explorer program; in text operating systems: DOS, UNIX, VM - Lynx and WWW programs.

ACTA
PROTOZOOLOGICA

ORIGINAL ARTICLES

S. L. Cameron, A.-D. G. Wright and P. J. O'Donoghue: An expanded phylogeny of the entodiniomorphida (Ciliophora: Litostomatea) 1

T. Suzaki, M. Arikawa, A. Saito, G. Omura, S. M. Mostafa Kamal Khan, M. Sakaguchi and K. Hausmann: Organelle movement in *Actinophrys sol* and its inhibition by cytochalasin B 7

M. Keedy, N. Yorgey, J. Hilty, A. Price, D. Hassenzahl and H. Kuruvilla: Pharmacological evidence suggests that the lysozyme/PACAP receptor of *Tetrahymena thermophila* is a polycation receptor 11

J. R. Nilsson: How cytotoxic is zinc? A study on effects of zinc on cell proliferation, endocytosis, and fine structure of the ciliate *Tetrahymena* 19

S. I. Fokin, L. Giamberini, D. P. Molloy and A. bij de Vaate: Bacterial endocytobionts within endosymbiotic ciliates in *Dreissena polymorpha* (Lamellibranchia: Mollusca) 31

A. Özer: The occurrence of *Trichodina domerguei* Wallengren, 1897 and *Trichodina tenuidens* Fauré-Fremiet, 1944 (Peritrichia) on three-spined stickleback, *Gasterosteus aculeatus* L., 1758 found in a brackish and freshwater environment 41

W. Foissner: *Cultellothrix velhoi* gen. n., sp. n., a new Spathidiid ciliate (Ciliophora: Haptorida) from a Brazilian floodplain soil 47

W. Foissner: Morphology and ontogenesis of *Bromeliophrya brasiliensis* gen. n., sp. n., a new ciliate (Protozoa: Ciliophora) from Brazilian tank bromeliads (Bromeliaceae) 55

E. A. Adriano, P. J. Thyssen and N. S. Cordeiro: A new species of *Eimeria* from the eared dove *Zenaida auriculata* (Aves: Columbidae) in Brazil 71

K. H. Nicholls: *Corythionella golemanskyi* sp. n.: a new freshwater, filose, testate rhizopod 75

BOOK REVIEW 81

2003 FEBRUARY
VOLUME 42 NUMBER 1